ESTIMATION OF TREE BIOMASS, MEASUREMENT UNCERTAINTIES, AND MORPHOLOGICAL TOPOLOGY OF *ANDROSTACHYS JOHNSONNII* PRAIN

By

Tarquinio Mateus Magalhães

Dissertation presented for the degree of Doctor of Phylosophy (Forestry) at the University of Stellenbosch

Supervisor: Prof. Thomas Seifert

Faculty of AgriSciences

Department of Forest and Wood Science
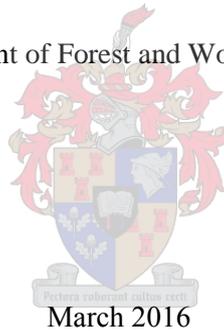
March 2016

DECLARATION

I declare that the research reported in this thesis, submitted for the degree of Doctor of Philosophy at the University of Stellenbosch, is the result of my own original research, except where otherwise indicated. This thesis has not been submitted for any degree or examination at any other university.

March 2016, Tarquinio Mateus Magalhães

2

AKNOWLEDGEMENTS

The research that has gone into this thesis has been thoroughly enjoyable. That enjoyment is largely a result of the interaction that I have had with my supervisor, colleagues and friends.

After receiving funds from Swedish International Development Cooperation Agency (SIDA) to pursue with research and studies towards a Ph.D in any Swedish or South African University, I first thought of Stellenbosch University. After an internet search, I found the e-mail address of Mr. Cori Ham to whom I sent an e-mail presenting my research proposal. Then, gently, he forwarded my proposal to an expert in my field of interest who promptly agreed to work with me as my supervisor. I address my huge and warm thanks to Mr. Cori Ham.

The expert that Mr. Ham introduced to me was Professor Thomas Seifert. I feel very privileged to have worked with Professor Thomas Seifert. To him I owe a great debt of gratitude for his patience, inspiration, friendship and wonderful lessons.

Stellenbosch City and University would not be the same when I arrived there if Mrs Ursula Petersen had not introduced me to Benedict Odhiambo. Odhiambo would be my only friend in Stellenbosch with whom I shared confidences and I received advices on how to deal with our supervisor (Professor Seifert), in order to get the highest scientific profits from him. Benedict Odhiambo showed me around, and YES, I will miss those nights with glasses of wine and beer celebrating our friendship. Odhiambo has always been there for me. Thank you Odhiambo for being my friend and thank you Ursula for introducing me to him. Thanks are extended to Professor Ben Du Toit for translating the English summary into Afrikaans opsomming.

However, to be here writing this thesis there were invisible hands that helped me unconditionally in most difficult moments, without those hands perhaps this thesis would have failed to materialize. Those invisible hands are from Professor Mário Paulo Falcão and Professor Agnelo Fernandes, both from Universidade Eduardo Mondlane. The first took my classes so that I could have time to study and helped me a lot when my scholarship was cancelled. The second helped me finacially for editing and publishing the papers that are part of this thesis. There are no words that I can use to express how I feel, because THANK YOU is not good enough.

I also want to thank my relatives, especially Mateus Magalhães (my father), Basiliana Patrício (my mother) and all my brothers and sisters for being there for me. Thanks are also extended to my friends, especially Jeremias Sacuze (Grande Impala). Warm thanks to all of you.

Stellenbosch, November 2015

Tarquinio Mateus Magalhães

3

ABSTRACT

This research was aimed at estimating biomass stocks separated in above- and belowground tree components, and studying the topology of the shoot and root systems of *Androstachys johnsonnii* Prain in woodlands in Mozambique. A two-phase sampling design was used to determine above- and belowground biomass. In the first phase 3574 trees were measured in 23 randomly located circular plots (20-m radius). In the second phase, 93 trees were randomly selected as a subsample from the first phase sample for destructive measurement of biomass and stem volume, along with the variables of the first phase and for topological analysis of the shoot and root systems. Estimates of biomass stocks and quantification of the errors associated with those estimates were obtained using Phase-1 data and regression models. Additionally, biomass expansion factors (BEFs) were fitted based on the 93 trees harvested in the second phase.

The estimated total tree forest biomass was 167.05 Mg ha^{-1} using biomass models and 150.74 Mg ha^{-1} using BEFs. The percent error resulting from plot selection and biomass regression equations for whole tree biomass stock was 4.55% and 1.53%, respectively, yielding a total error of 4.80%. Among individual variables in the first sampling phase, diameter at breast height (DBH) measurement was the largest source of error. Tree-height estimates contributed substantially to the error as well. For the second sampling phase, DBH measurements were the largest source of error, followed by height measurements and stem-wood density estimates. Of the total error (total variance) of the sampling process, 90% was attributed to plot selection and 10% to the biomass model. The BEF values of tree components were unrelated or weakly related to tree size, and root-to-shoot ratio (R/S) was independent of tree size; therefore, for *A. johnsonii*, constant component BEF and R/S values can be applied within the interval of sampled tree sizes.

Visual analysis indicated herringbone-like branching pattern for both the root and shoot systems. However, the topological index (TI) and topological trend (TT) suggested otherwise. This discrepancy was attributed to the fact that *A. johnsonii* has multiple laterals per stem/taproot node, suggesting that the topological indexes (TI and TT) might yield biased conclusions regarding the branching pattern when the main axis has multiple laterals per node. Hence, a modified topological index (TIM) was developed that could be applied in the cases of multiple laterals per node while conserving the values of TI for cases with one lateral per node; the modified index was more efficient and realistic than TI. The area preserving branching was confirmed for each stem node confirming the self-similar branching. For the root system, the area-preserving branching was only confirmed for the first node; therefore, self-similarity was not confirmed.

4

OPSOMMING

Hierdie navorsing was daarop gemik om die biomassa van *Androstachys johnsonnii* Prain (geskei in bo- en ondergrondse boom komponente) te skat en om die topologie van die loot- en wortelstelsels van hierdie boom in die bosland van Mosambiek te bestudeer. Twee-fase steekproefneming is gebruik om bo- en ondergrondse biomassa te bepaal. In die eerste fase is 3574 bome gemeet in 23 lukraak geleë sirkelvormige persele (20 m radius). In die tweede fase is 'n stel van 93 bome lukraak gekies vanuit die Fase 1 monster, en hierdie stel is gebruik vir destruktiewe meting van biomassa en stamvolume. Die gekose stel het ook die inligting bevat van alle veranderlikes wat in Fase 1 bemoster is plus topologiese ontledings van die loot- en wortelstelsels. Fase 1 data en regressie modelle is gebruik om die biomassa van die bos te skat en om die statistiese foute van hierdie beramings te bepaal. Verder is 'n biomassa opskalings faktore (BOFe) bepaal vanaf die data van die 93 bome wat in Fase 2 ingeoes is.

Die totale biomassa van die bos is geskat op 167,05 Mg ha^{-1} met behulp van biomassa modelle en op 150,74 Mg ha^{-1} met behulp die BOFe. Die persentasie fout as gevolg van perseel seleksie en biomassa regressievergelykings vir die totale boom biomassa was onderskeidelik 4,55% en 1,53%, wat gelei het tot 'n totale fout van 4,80%. Onder individuele veranderlikes in Fase 1, was deursnee op bors hoogte (DBH) metings die grootste bron van statistiese foute. Boomhoogte metings het ook aansienlik bygedra tot die fout. Vir die tweede bemonsteringsfase was DBH metings die grootste bron van statistiese foute, gevolg deur hoogte metings en digtheidsbepalings van die stamhout. Van die totale variansie van die monsternemingsproses is 90% toegeskryf aan monsterperseel seleksie en 10% aan die biomassa modelle. Die BOF waardes van boom komponente hou glad nie verband nie (of hou swak verband) met boomgrootte, en die ondergrondse:bogrondse biomassa (O/B) waarde was ook onafhanklik van boomgrootte. Vir hierdie rede kan BOF en O/B waardes vir *A. johnsonii,* as 'n konstante komponent toegepas word binne die interval van bemonsterde boomgroottes.

Visuele analise het 'n visgraatagtige vertakkingspatroon vir beide die wortel- en takstelsels aangetoon. Die topologiese indeks (TI) en topologiese tendens (TT) dui egter op 'n ander patroon. Die verskil word toegeskryf aan die feit dat *A. johnsonii* verskeie laterale vertakkings het vir elke knoop (nodus) van beide die stam en die penwortel. Die moontlikheid bestaan dat die TI en TT resultate bevooroordeelde gevolgtrekkings met betrekking tot die vertakkingspatroon kan oplewer onder hierdie omstandighede. 'n Aangepaste topologiese indeks (ATI) is ontwikkel wat in die geval van veelvuldige vertakkings per knoop toegepas kan word, met behoud van die waardes van die TI vir gevalle met net een tak per knoop. Hierdie gewysigde indeks was meer doeltreffend en realisties as die TI. Die beginsel van behoud van oppervlakte vir elke vertakking is bevestig vir elke knoop in die stam, wat aandui dat hierdie vertakkingspatroon konstant bly. Vir die wortelstelsel is die beginsel van behoud van oppervlakte slegs bevestig vir die eerste knoop, en daarom kon konstante vertakkingspatrone nie vir die wortelstelsel bevestig word nie.

5

LIST OF ORIGINAL ARTICLES

This thesis consists of an introdutory review followed by four published original articles. The articles are referred to by their Roman numerals (I, II, III and IV). The articles are reprinted with the kind permission of the publishers.

I.   Magalhães TM, Seifert T (2015) Biomass modelling of *Androstachys johnsonii* Prain – a comparison of three methods to enforce additivity. International Journal of Forestry Research 2015: 1–17. http://dx.doi.org/10.1155/2015/878402

II.   Magalhães TM, Seifert T (2015) Estimation of tree biomass, carbon stocks, and error propagation in Mecrusse woodlands. Open Journal of Forestry 5: 471–488. http://dx.doi.org/10.4236/ojf.2015.54041

III. Magalhães TM, Seifert T (2015) Tree component biomass expansion factors and root-to-shoot ratio of Lebombo ironwood: measurement uncertainty. Carbon Balance and Management 10: 9. http://www.cbmjournal.com/content/pdf/s13021-015-0019-4.pdf

IV.   Magalhães TM, Seifert T (2015) Below- and aboveground architecture of *Androstachys johnsonii* Prain: Topological analysis of the root and shoot systems. Plant and Soil 394: 257–269. DOI 10.1007/s11104-015-2527-0. http://link.springer.com/article/10.1007%2Fs11104-015-2527-0.

AUTHOR´S CONTRIBUTION

Tarquinio Mateus Magalhães and Thomas Seifert jointly designed the methodology. Tarquinio Mateus Magalhães collected and analysed the data and wrote all manuscripts with editorial support of Thomas Seifert.

TABLE OF CONTENTS

8

1 INTRODUCTION

1.1 Background

1.1.1 Concepts

Biomass is an essential variable in forestry and ecological research. It is defined as fresh mass (Levy et al. 2004) or oven-dry mass (Brown 1997; Lehtonen et al. 2004) of live or dead organic matter, both above- and belowground (IPCC 2003; GTOS 2009); and biomass density (also referred to as biomass stock) is the biomass per unit area (Brown 1997; IPCC 2003; GTOS 2009). Forest biomass density is defined either as aboveground biomass (AGB) per unit area (Brown 1997; Brown 2002a; Levy et al. 2004) or as total tree (above- and belowground) biomass per unit area (Soares and Tomé 2012). In this study, biomass refers to oven-dry mass of the total tree, as fresh mass is affected by both density and moisture content (de Gier 1992; Husch et al. 2003; Seifert and Seifert 2014) and therefore an unsuitable variable for comparison.

In this study, the term weight will commonly be used synonymous to mass, although they are distinct concepts. Mass is the quantity of matter present in a body (Simpson 2014) regardless of any force acting on it, is always constant at any time and place, and is expressed in grams (g) or multiples; whereas weight of a body is the force exerted on its mass by gravity (Parresol 1999; Simpson 2014), depends on the gravity at that place, and is expressed in Newton (N). Since gravity is only varying insubstantially on earth this synonymous use is justified.

1.1.2 Importance

Forest biomass is a crucial ecological variable for understanding the evolution and potential future changes of the climate system (GTOS 2009). Therefore, a global assessment of biomass and its dynamics is an essential input to climate change projection models and mitigation and adaptation strategies (GTOS 2009). Forest biomass is a key variable to make estimates of carbon pools in forests, and for studying other biochemical cycles (Husch et al. 2003; Rötzer et al. 2009). Further it is necessary to gauge the true production (Rötzer et al. 2012). The importance of biomass estimation has increased since the Kyoto Protocol was adopted in 1997 (Repola 2013).

Carbon dioxide sequestration, reduction, and storage associated with forest ecosystems is an important mechanism for mitigation of global warming (Husch el al. 2003). The estimation of carbon stock in forest ecosystems must include measurements in all relevant carbon pools (Brown 1999; Brown 2002b; IPCC 2006; Pearson et al. 2007, Wiese et al. 2015): live aboveground biomass (AGB) (trees and non-tree vegetation), belowground biomass (BGB), dead organic matter (dead wood and litter biomass), and soil organic matter (mineral and organic soils).

This study is focused on forest tree biomass; therefore, it includes only two carbon pools: AGB (excluding non-tree vegetation), and BGB.

1.2 Problem Statement and Research Objectives

The estimation of tree biomass is important to predict the amount of carbon that is sequestered (Parresol 1999; Brandeis et al. 2006; Goicoa et al. 2011), to assess nutrient cycling and fluxes and energy wood potentials (Parresol 1999; Repola 2013; Kunneke et al. 2014; Seifert and Seifert 2014), and to provide estimates for the different tree components (Seifert et al. 2006, Seifert and Müller-Starck 2009, Goicoa et al. 2011). Estimating biomass differentiated in tree components is important for several reasons: (i) stem wood biomass is an important variable because this component is the only one used in the forest and wood processing industry, and the carbon therefore remains stored for a long time in the products and is not released into the atmosphere; (ii) in many species, especially in tropical natural forests, branches and foliage are left in the forest and decompose, releasing CO_2 and nutrients; (iii) in some species, especially broadleaf species, the branches are collected by members of local communities for use as firewood, which will result in release of CO_2; (iv) the stump and root system are left in the forest, allowing the stump to either resprout (regrow), continuing the sequestration process, or decompose along with the roots, releasing CO_2 and nutrients. Hence, it is critical to estimate the biomass of all tree components separately as well as the total tree biomass in order to assess the carbon balance.

However, the biomass estimates of the considered tree components often do not sum up to the estimate of the total tree biomass, and a desired and logical feature of the tree component regression equation is that the predictions of the components sum up to the prediction for the total tree. This feature is called additivity. Various authors, such as, Kozak (1970), Cunia (1979), Jacobs and Cunia (1980), Cunia and Briggs (1984, 1985), Parresol (1999, 2001), Carvalho and Parresol (2003), Goicoa et al. (2011), and Seifert and Seifert (2014) have proposed and/or discussed various methods to ensure the property of additivity.

Notwithstanding, the errors associated with biomass estimates must be known for the derived biomass predictions to be reliable. However, the error is rarely evaluated carefully in biomass studies (Chave et al. 2004). Many studies that estimate biomass stock employ a two-phase sampling design. The error of estimates from two-phase sampling has two main components, one associated with each phase (Cunia 1986a; Cunia 1990). Moreover, each variable measured in each sampling phase contributes to the error of that phase.

On the other hand, besides the fact that biomass regression equations yield most accurate estimates (IPCC 2003; Jalkanen et al. 2005; Zianis et al. 2005; António et al. 2007; Soares and Tomé 2012), national and regional AGB estimates are typically calculated based on estimates of standing stem volume from forest inventories and from default biomass expansion factors (BEFs). The AGB estimates are then converted into BGB using default root-to-shoot ratio (R/S) values; the ratio of the oven-dry weight of the roots to that of the top (shoot) of a plant. This method is commonly used to estimate carbon stocks for national greenhouse gas (GHG) inventories (IPCC 2006).

However, BEF and R/S values can vary according to vegetation type, precipitation regime, mean annual temperature (Mokany et al. 2006), and tree age and size (Brown et al. 1989; Lehtonen et al. 2004; Cháidez 2009; Dutca et al. 2010; Sanquetta et al. 2011); thus, the use of default values for national- or regional-scale estimates might result in unreliable assessments of biomass, carbon, and GHGs. In addition, because BEF

10

and R/S values are not estimated during ordinary forest inventories, uncertainty in estimates of AGB and BGB is mainly attributed to BEF and R/S (Levy et al. 2004), and it thus represents a major gap in carbon accounting at regional and national levels (Lehtonen et al. 2007).

Root architecture determines the ability of plants to exploit soil resources (Lynch 1995), thereby affecting water and nutrient acquisition, carbon metabolism, and environmental stress resistance (Trubat et al. 2012). Shoot architecture, on the other hand, affects the allocation of light to leaf area and the manner in which leaves are arranged and displayed (Valladares 1999), thereby playing an important role in plant growth and survival (Valladares and Pearcy 2000).When modeling tree biomass, the use of species-specific equations are preferred because trees of different species may differ greatly in architecture (of the shoot and root systems) as shown by Ketterings et al. (2001). The architecture can influence biomass allocation and allometry (Coll et al. 2008; Trubat 2012). Aware of that van Noordwijk et al. (1994) proposed proximal root diameter as predictor of total root size for fractal branching models. This approach uses branching characteristics of the roots (root architecture) for estimating root length (Ong et al. 1999) and root biomass (Ozier-Lafontaine et al. 1999).

Asessing the current body of knowledge the following apparent gaps were identified:

    i.   Many biomass studies include only AGB not breakdown in further components (e.g. Overman et al. 1994; Grundy 1995; Eshete and Ståhl 1998; Pilli et al. 2006; Salis et al. 2006; Návar-Cháidez 2010; Suganuma et al. 2012; Sitoe et al. 2014; Mason et al. 2014), ignoring the fact that different tree components have distinguished uses and decomposition rates, affecting differently the storage time of carbon and nutrients (Magalhães and Seifert 2015b).

    ii.   Few studies have provided estimates of BEF and R/S with measures of uncertainty, and although R/S values for specific forest and woodland types have not been widely studied, these values facilitate more accurate estimates of BGB (Mokany et al. 2006) when compared to default ones. Therefore, estimates of BEF and R/S with uncertainty are needed for different types of woodlands.

    iii.   Despite the recent advances in examining root distribution and biomass with modern technology such as ground-penetrating radar (Butnor et al. 2001; Butnor et al. 2003; Cui et al. 2010; Raz-Yaseef et al. 2013; and Zhu et al. 2013), the belowground component of trees is still poorly known because, traditionally, it requires labour- and time-intensive in situ measurements (GTOS 2009). Yet, BGB constitutes a major share of total forest biomass. Cairns et al. (1997) and Litton et al. (2003) have stated that BGB may represent up to 40% of the total biomass.

    iv.   In most studies that considered BGB, the root system was not fully excavated (Green et al. 2007; Ryan et al. 2011; Ruiz-Peinado et al. 2011; Kuyah et al. 2012; and Paul et al. 2014), the excavation was done to a certain predefined depth or the fine roots were not considered; or a sort of sampling procedure was used (Kuyah et al. 2012; Mugasha et al. 2013). These procedures of estimating BGB are known to lead to an underestimation or to less accurate estimation of BGB (Mokany et al. 2006; Mugasha et al. 2013).

11

v.   Besides the importance of studying root and shoot architecture, such studies are relatively scarce in Africa (Oppelt et al. 2000 and Oppelt et al. 2001). To the knowledge of the author, similar studies in Mozambique and, especially, on *Androstachys johnsonii* are lacking.

vi.   The majority of the existing studies on root system architecture focus on seedlings (Martínez-Sánchez et al. 2003; Trubat et al. 2012; Chiatante et al. 2004; Berntson 1997; Fitter and Stickland 1991; Larkin et al. 1995; Nicotra et al. 2002; Tworkoski and Scorza 2001; Cortina et al. 2008; Riccardo 2007) and saplings (Coll et al. 2008; Spanos et al. 2008; Salas et al. 2004; van Noordwijk and Purnomosidhi 1995; Oppelt et al. 2001); this is probably because of the difficulty in excavating the root system of adult trees. Further, if the architecture of the root system of an adult tree is studied, often the root system is not totally removed and is therefore only partially analysed (Kalliokoski 2011; Kalliokoski et al. 2008; Soethe et al. 2007), which may lead to biased conclusions.

In order to address the knowledge gaps mentioned before, the objectives of this thesis were to:

1. fit independent linear and nonlinear tree component and total tree biomass models and compare three methods of enforcing the property of additivity for *Androstachys johnsonii* (Article I);

2. estimate the above and belowground biomass and carbon stocks of Mecrusse woodlands and quantify the errors in those estimates (Article II);

3. develop tree component BEF and R/S values with known uncertainty (Article III); and

4. investigate the branching behaviour and determine the application of the Leonardo da Vinci rule and fractal branching pattern (self-similarity) of the root and shoot systems (Article IV).

Thus, the starting hyphoteses to be tested were that:

i.   the multivariate methods of enforcing additivity achieve more efficient estimates, as found by various authors (Parresol 1999; Parresol 2001; Carvalho and Parresol 2003; Goicoa et al. 2011; Carvalho 2003; and Návar-Cháidez et al. 2004);

ii.   because biomass estimation is labour- and time intensive and then susceptible to errors, the error due to biomass model is larger than that due to plot selection and variability;

iii.   BEF and R/S vary with tree size as verified in various studies (Brown et al. 1989; Lehtonen et al. 2004; Cháidez 2009; Dutca et al. 2010; Sanquetta et al. 2011);

iv.   the area-preserving branching is observed in each stem and taproot node; and

v.   self-similarity is observed for both the root and shoot systems.

12

1.3 Literature review

1.2.1 Measurement and estimation methods for tree biomass

1.2.1.1 Aboveground Biomass

AGB can be measured or estimated by in situ sampling or remote sensing (Lu 2006; Ravindranath 2008; GTOS 2009; Vashum and Jayakumar 2012). The in situ sampling, in turn, is divided into destructive direct biomass measurement and non-destructive biomass estimation (GTOS 2009; Vashum and Jayakumar 2012). This study is focused in in situ sampling; therefore, the remote sensing biomass estimation is not discussed.

The in situ destructive direct biomass measurement is further devided in bulk sampling and biomass component sampling (Seifert and Seifert 2014). The first method entails harvesting trees or shrubs, herbs, etc., on a individual tree-basis or on plot area basis, drying them, and then weighting the biomass (GTOS 2009; Gibbs et al. 2007; Seifert and Seifert 2014). In the first case (on individual tree-basis), the biomass of each individual or the aboveground part of it is measured (GTOS 2009; Seifert and Seifert 2014). In the second case (on plot area basis), the total biomass of a specific sample plot is measured (GTOS 2009); it is usually based on in-field chipping and is a more industrial than scientific practice (Seifert and Seifert 2014), thus it is usually applied to invasive woody vegetation with a high proportion of multi-stemmed trees and bushes, where only a biomass value per area is required (Kitenge 2011).

The in situ destructive direct biomass measurement on single tree-basis is mostly used for developing biomass equations (Parresol 1999; Parresol 2001; Carvalho and Parresol 2003; Husch et al. 2003; Brandeis et al. 2006; Goicoa et al. 2011; Repola 2013) to be applied for estimating biomass on large scales (Segura and Kanninem 2005; GTOS 2009; Navar 2009).

The non-destructive biomass estimation does not require harvesting trees; therefore, it uses exsiting biomass equations or biomass expansion factors (BEF) to extrapolate biomass to unit areas (Pearson et al. 2007; GTOS 2009; Soares and Tomé 2012). However, the biomass equation and BEF values are fitted or determined from destructively sampled trees (Carvalho and Parresol 2003; Carvalho 2003; Dutca et al. 2010; Marková and Pokorný 2010; Sanquetta et al. 2011; Mate et al. 2014; Magalhães and Seifert 2015a-c). Biomass regression equations yield most accurate estimates (IPCC 2003; Jalkanen et al. 2005; Zianis et al. 2005; António et al. 2007; Soares and Tomé 2012, Petersson et al. 2012) as long as they are derived from a large enough and representative number of trees (Husch et al. 2003; GTOS 2009). Nonetheless, national and regional AGB estimates are often calculated based on BEFs (Magalhães and Seifert 2015c), especially when using national forest inventory data (Schroeder et al. 1997; Tobin and Nieuwenhuis 2007).

1.2.1.2 Belowground Biomass

The belowground component of tree biomass is still poorly understood because it can not be easily detected by remote observations and it needs labour- and time-intensive in situ measurements as pointed out before (GTOS 2009). However, BGB can represent up to 40% of total biomass (Cairns et al. 1997; Brown 1999;

Brown 2002b); nonetheless, no pratical standardized field tecniques yet exist for its determination (Körner 1994; Kurz et al. 1996; Cairns et al. 1997; Brown 2002a; Brown 2002b).

BGB is often estimated indirectly with different methodological approaches:

(i) root-to-shoot ratios (R/S) (Brown 2002a; Green et al. 2005; Mokany et al.2006; Carreiras et al. 2013; Magalhães and Seifert 2015c),

(ii) root BEFs (Magalhães and Seifert 2015c), or

(iii) regression equations of BGB on AGB (Brown 2002a; Pearson et al. 2007; Kuyah et al. 2012) or on easily measured variables such as diameter at breast height (DBH) and tree-height (Komiyama et al. 2005; Kuyah et al. 2012).

Whatever method is used to estimate BGB (R/S, BEFs, equations) it requires that the root system is measured directly to develop those methods.

Since measuring BGB is time consuming and cost intensive, the root system is often partially removed from the soil (Kalliokoski 2001; Levy et al. 2004; Soethe et al. 2007; Kalliokoski et al. 2008; Ruiz-Peinado et al. 2011; Sanquetta et al. 2011), depths of excavation are predefined (Sanquetta et al. 2011; Ruiz-Peinado et al. 2011; Paul et al. 2014), and fine roots are often excluded (Green et al. 2007; Bolte et al. 2004; Ryan et al. 2011). However, the depths of excavation and the definition of fine roots are not standardized (Brown 2002a, Miranda et al. 2014). In other cases, a root sampling procedure is applied, for example, where only a number of roots from each root system is fully excavated, and then the information from the sampled excavated roots is used to estimate biomass for the roots not excavated (Niiyama et al. 2010; Kuyah et al. 2012; Mugasha et al. 2013). Other direct methods that exist include cores and pits for fine roots (Yanai et al. 2007). However, these approaches are only providing a stand level fine root biomass estimates biomass values for individual trees.

To the best of the knowledge of the author, the only studies undertaken with complete root system excavation of adult trees, including fine roots, and without subsampling, conducted in Mecrusse woodland in Mozambique are those by Magalhães and Seifert (2015a-d) and Magalhães (2015).

2 MATERIAL AND METHODS

2.1 Study area and species description

Mecrusse is a forest type where the main species, and occasionally, the only one in the upper canopy, is *Androstachys johnsonii* Prain (Figure 1). It is the dominant and co-dominant species with a relative cover varying from 80 to 100% (Mantilla and Timane 2005).

Figure 1. *Androstachys johnsonii* Prain tree species

A. johnsonii (family *Euphorbiaceae*) is native to Africa and Madagascar and is the sole member of genus *Androstachys*; today, Mecrusse forest is primarily found in Mozambique (Cardoso 1963).

A. johnsonii trees can grow up to 20 m (Molotja et al. 2011). It is an evergreen tree. The crowns are long and slender, the trunks are long, bare and straight when in dense stands, but in open stands, crowns are moderately spreading, irregular round and sparse with lateral branches fairly low down. The young twigs are covered by a white villose layer (Molotja et al. 2011). The stems of trees that grow on sunny sides are grayish-white but stems of those growing under shade are nearly black. Barks are grooved longitudinally, resembling that of *Colophospermum mopane* (Molotja et al. 2011). Allelopathy is mediated by release of certain secondary metabolites by plant roots and plays an important role in the establishment and maintenance of terrestrial plant communities (Molotja et al. 2011).

A. johnsonii forms a yellow-pale heartwood, sometimes slightly pink. Distinct and wavy growth rings causing a fine streaked pattern. Medium lustrum, wavy and irregular grain, sometimes straight and a very

15

fine texture are characteristics of the wood (Bunster 2006), which is rather resistant to fungal and insect attack, including termites. However, standing trees are often attacked by fungi, which damage the structure of the wood (Bunster 2006). The wood of *A. johnsonii* is used for flooring, marine uses, turnery, furniture and interiors; although these uses are limited by the limited availability of large sizes (Bunster 2006).

In Mozambique, Mecrusse-dominated woodlands are mainly found in Inhambane and Gaza Provinces and in Massangena, Chicualacuala, Mabalane, Chigubo, Guijá, Mabote, Funhalouro, Panda, Mandlakaze, and Chibuto Districts. In this study, the east-most Mecrusse forest patches, covering the last five districts, were defined as the study area (Figure 2). The study area has an extension of 4,502,828 ha (Dinageca 1997), of which 226,013 ha (5%) were covered by Mecrusse woodlands.

In the study area, the climate is dry tropical except in the west part of Panda district and south-west part of Mandlakaze district where the climate is humid tropical (Dinageca 1997; Mae 2005a-e). The climate is divided into two seasons: warm or rainy season from October to March and cool or dry season from March to September (Mae 2005a-e).

The mean annual temperature is generally above 24°C, and the mean annual precipitation varies from 400 to 950 mm (Dinageca 1997; Mae 2005a-e). According to the FAO classification (FAO 2003), the soils in the study area are mainly Ferralic Arenosols covering more than 70% of the study area (Dinageca 1997). Arenosols, Umbric Fluvisols, and Stagnic soils are also found in the north-most part of the study area (Dinageca 1997).

The study area is characterised by shortage of water resources as well as precipitation; of the five districts comprising the study area, only Chibuto and Mandlakaze districts have water resources (Dinageca 1997; Mae 2005a-e).

2.2 Data collection

Two-phase sampling design was used to determine stem volume, and tree component biomass. In the first phase, DBH, total tree-height (H), crown height (CH), and live crown length (LCL) were measured in 3574 trees (m_1) in 23 randomly located circular plots of 20-m radius (Figure 2); only trees with DBH $\geq$ 5 cm were considered. In the second phase, 93 trees (m_2) were randomly selected from those analysed during the first phase (within the 23 plots, 2 to 6 trees per plot, in proportion to the frequency of five diameter classes) for destructive measurement of stem length, biomass and stem volume, along with the variables of the first phase. The felled trees were divided into the following components: (1) taproot + stump; (2) lateral roots; (3) root system (1 + 2); (4) stem wood; (5) stem bark; (6) stem (4 + 5); (7) branches; (8) foliage; (9) crown (7 + 8); (10) shoot system (6 + 9); and (11) whole tree (3 + 10). Tree components were sampled and the dry weights estimated as described in the following sections.

16
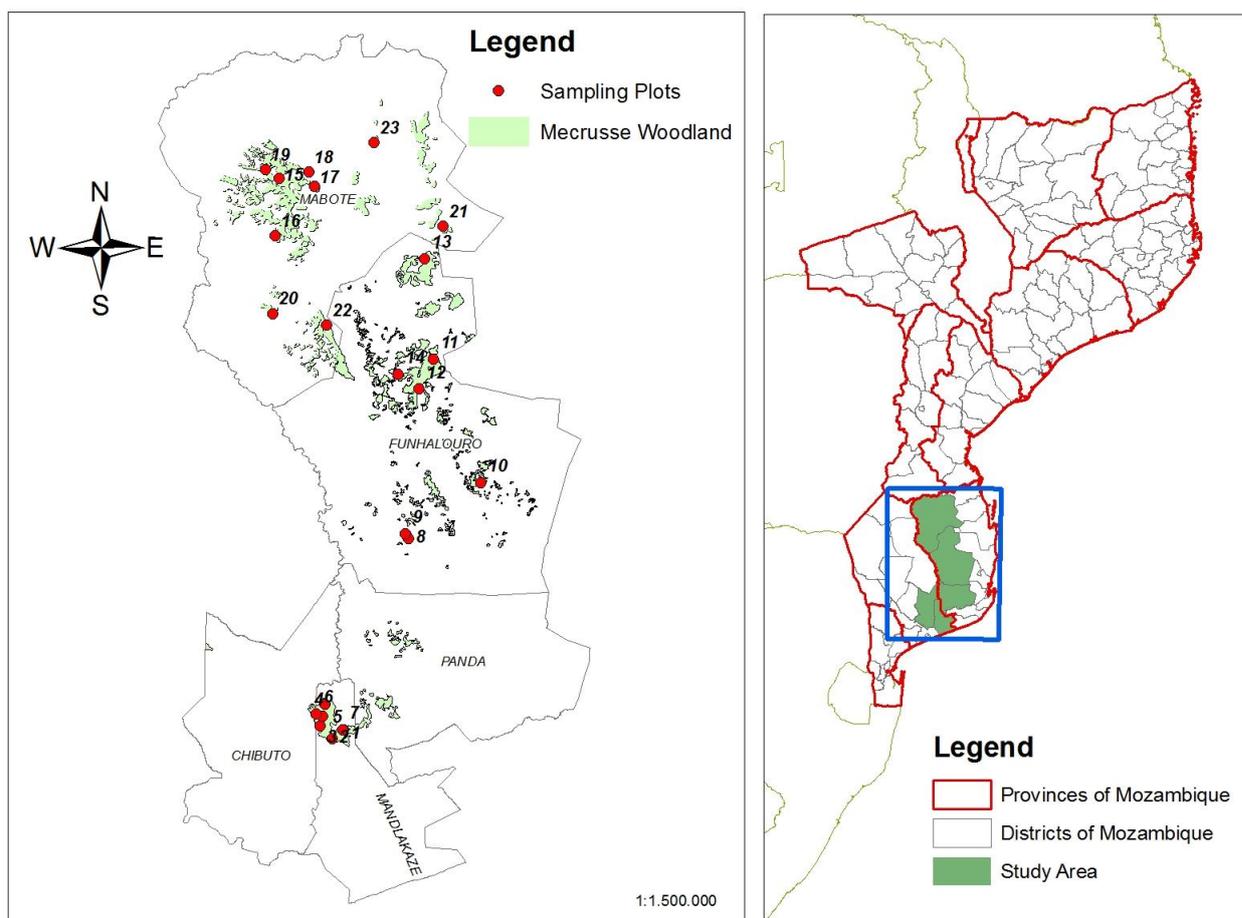
Figure 2. Distribution of sampling plots in Mecrusse forest patches

2.2.1 Root system

The stump height was predefined as being 20 cm from the ground level for all trees and the stump below was considered as part of the taproot, as recommended by Parresol (2001) and because in larger *A. johnsonii* trees this height (20 cm) is affected by root buttress; therefore, the root collar was also considered part of the taproot. The root system was divided into 3 sub-components: fine lateral roots, coarse lateral roots, and taproot. Lateral roots with diameters at insertion point on the taproot < 5 cm were considered as fine roots and those with diameters ≥ 5 cm were considered as coarse roots.

First, the root system was partially excavated to the first node, using hoes, shovels, and picks; to expose the primary lateral roots (Figure 3a, b). The primary lateral roots were numbered and separated from the taproot with a chainsaw (Figure 3a, b) and removed from the soil, one by one. This procedure was repeated in the subsequent nodes until all primary roots were removed from the taproot and the soil. Finally, the taproot was excavated and removed (Figure 3 c–f). The complete removal of the root system was relatively easy because 90% of the lateral roots of *A. johnsonii* are located in the first node, which is located close to ground level (Figure 3 a–c); the lateral roots grow horizontally to the ground level, do not grow downwards; and because the taproots had, at most, only 4 nodes and at least 1 node (at ground level). The root system was removed completely, so the depth of excavation depended on the vertical length of the taproot.

17

Additionally, the distal diameters before branching and the proximal diameters after branching were measured at each node by using a calliper or calliper rule. Similarly, the shoot system was measured. Only the primary laterals (lateral roots or branches), those originating from the main axis (taproot or stem), were considered. The link length (internode distance: internal link; distance from the last node to the apex (meristem): external link) was measured using a tape.
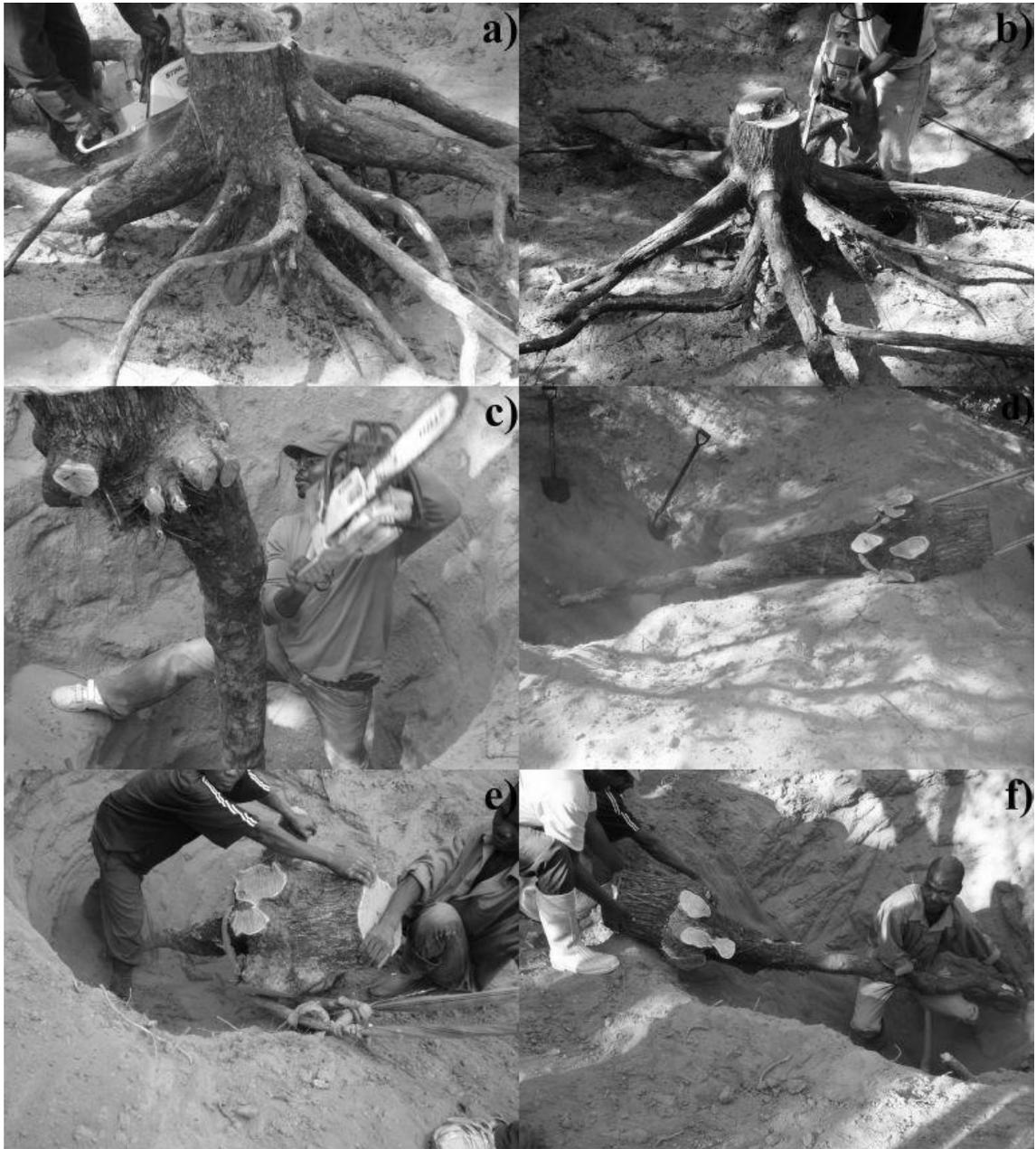
Figure 3. Separation of lateral roots from the root collar/taproot **(a, b, c)**, and removal of the taproot including the root collar and the stump **(d, e, f)**

Fresh weight was obtained for the taproot, each coarse lateral root and for all fine lateral roots. Fresh weight was also obtained for all higher-order lateral roots (mainly secondary roots). A sample was taken from each sub-component, fresh weighed, marked, packed in a bag, and taken to the laboratory for oven drying. For the taproot, the samples were two discs, one taken immediately below the ground level and

another from the middle of the taproot. For the coarse lateral roots, two discs were also taken, one from the insertion point on the taproot and another from the middle of it. For fine roots the sample was 5 to 10% of the fresh weight of all fine lateral roots. Oven drying of all samples was done at 105°C to constant weight, hereafter, referred to as dry weight.

2.2.2 Stem wood and stem bark

Felled trees were scaled up to a 2.5 cm top diameter. The stem was defined as the length of the trunk from the stump to the height that corresponded to 2.5 cm diameter, to standardize with the definitions of fine branches. The remainder (from the height corresponding to 2.5 cm diameter to the tip of the tree) was considered as a fine branch.

First, the stem of each felled tree was divided into 10 segments of equal length, and the diameter of each segment was measured at the midpoint, starting from the bottom of the stem, for volume and form factor determination using Hohenadl formula. The stem was, then, divided into sections, the first with 1.1 m length, the second with 1.7 m, and the remaining with 3 m, except the last, the remainder, which length depended on the length of the stem.

Discs were removed at the bottom and top of the first section, and on the top of the remaining sections; i.e.: discs were removed at heights of 0.2 m (stump height), 1.3 m (breast height), 3 m, and the successive discs were removed at intervals of 3 m to the top of the stem, and their fresh weights measured using a digital scale.

Diameters over and under bark were taken from the discs in the North–south direction (previously marked on the standing tree) with the help of a ruler. The volumes over and under the bark of the stem were obtained by summing up the volumes of each section calculated using Smalian's formula (de Gier 1992; Husch et al. 2003). Bark volume was obtained from the difference between volume over bark and volume under bark.

The discs were dipped in drums filled with water, until constant weight (3 to 4 months), for saturation and subsequent determination of the saturated volume and basic density. The saturated volume of the discs was obtained based on the water displacement method (Brasil et al. 1994) using Archimedes' principle. This procedure was done twice: before and after debarking; hence, saturated volumes under and over the bark were obtained.

Wood discs and barks were oven dried at 105°C to constant weight. Basic density was obtained by dividing the oven dry weight of the discs (with and without bark) by the relevant saturated wood volume (de Gier 1992; Bunster 2006). Therefore, two distinct basic densities were calculated: (1) basic density of the discs with bark and (2) basic density of the discs without bark.

Basic density at point of geometric centroid of each section was estimated using the regression function of density over height (Seifert and Seifert 2014). This density value was taken as representative of each section (Seifert and Seifert 2014).

2.2.3 Crown

The crown was divided into two sub-components: branches and foliage. Primary branches, originating from the stem, were classified in two categories: primary branches with diameters at the insertion point on the stem ≥ 2.5 cm were classified as large branches, and those with diameter < 2.5 cm were classified as fine branches (twigs). Large branches were sampled similarly to coarse roots, and fine branches and foliage were sampled similarly to fine roots. Measurements were also obtained for all higher-order branches.

2.2.4 Tree component dry weights and carbon concentration

Dry weights of the taproot, lateral roots, branches, and foliage were determined by multiplying the ratio of oven-dry- to fresh weight of each sample by the total fresh weight of the relevant component. Dry weights of the root system and crown were obtained by summing up the relevant sub-components' dry weights. Dry weights of each stem section (with and without bark) were obtained by multiplying respective densities by relevant stem section volumes.

Stem (wood + bark) and stem wood dry weights were obtained by summing up each section's dry weight with and without bark, respectively. The dry weight of stem bark was determined from the difference between the dry weights of the stem and stem wood. Dry weights of the major components (root system, shoot system, and crown) and the whole tree were determined by summing the dry weights of their constituent components.

A subsample (n = 17 trees) was randomly selected from the 93 harvested trees (one to two trees per diameter class and location) for carbon analysis. Five samples were randomly selected from each of these 17 trees, from each of the components: roots, leaves, branches, bark, and stem. The samples were pooled and milled together by component to form a composite sample. Carbon concentration in the composite samples was measured using a TruSpec Micro analyser (LECO Corp) at the Central Analytical Facilities, Stellenbosch University (Stellenbosch, South Africa). The average carbon content of the crown was obtained from the average values for branches and foliage. Carbon concentrations for each tree component, with standard deviation (SD) and coefficient of variation (CV, in percentage), are presented in Table 1.

Table 1. Carbon concentration in each tree component (%)

	Roots	Stem wood	Stem bark	Crown
Average	53.14	49.04	45.15	48.67
SD	1.71	1.54	3.93	0.78
CV	3.21	3.15	8.70	1.60

2.3 Data processing and analysis

2.3.1 Biomass modelling and additivity (Article I)

Additivity is a desired trait of biomass models. It means that all model estimates for biomass components (leaves, roots, bark, etc.) if summed up will be equal to the estimation of the total biomass. Different methods to achieve additivity were compared in this thesis.

20

First, several linear and nonlinear regression model forms were tested for each tree component and for the total tree using weighted least squares (WLS). The weight functions were obtained by iteratively finding the optimal weight that homogenises the residuals, and improves other fit statistics. Independent tree component models were fitted with the statistical software package R (R Core Team, 2013) and the functions lm and nls for linear models and nonlinear models (the latter of which using the Gauss-Newton algorithm). The best linear and nonlinear biomass equations selected are given in Eqs.1 and 2, respectively. Among the tested weight functions (1/D, $1/D^2$, 1/DH, 1/DLCL, $1/D^2H$, $1/D^2LCL$), the best weight function was found to be $1/D^2H$, for all tree component equations (linear or nonlinear). Although, the selected weight function might not be the best one among all possible weights, it is the best approximation found.

$$\hat{Y}_{Roots} = b_0 + b_1 D^2 H$$
$$\hat{Y}_{Stem-wood} = b_0 + b_1 D^2 H$$
$$\hat{Y}_{Stem-bark} = b_0 + b_1 D^2 H \quad \text{[Kg]} \tag{1}$$
$$\hat{Y}_{Crown} = b_0 + b_1 D^2 LCL^{0.25}$$
$$\hat{Y}_{Total-tree} = b_0 + b_1 D^2 H$$

$$\hat{Y}_{Roots} = b_0 (D^2 H)^{b_2}$$
$$\hat{Y}_{Stem-wood} = b_0 D^{b_1} H^{b_2}$$
$$\hat{Y}_{Stem-bark} = b_0 D^{b_1} H^{b_2} \quad \text{[Kg]} \tag{2}$$
$$\hat{Y}_{Crown} = b_0 D^{b_1} LCL^{b_2}$$
$$\hat{Y}_{Total-tree} = b_0 (D^2 H)^{b_2}$$

Three methods of enforcing the property of additivity were then tested: (1) the conventional (CON) method, (2) seemingly unrelated regression (SUR) with parameter restriction, and (3) nonlinear seemingly unrelated regression (NSUR) with parameter restriction.

The CON method consists of using the same independent variables and the same weight functions for all tree component models and the total tree model (Parresol 1999), achieving additivity automatically (Goicoa et al. 2011). For this method, the most frequent best linear model form in Eq.1 among tree components was used for all other components and for total tree biomass. The most frequent model form in Eq.1 is $Y = b_0 + b_1 D^2 H + \varepsilon$; where ε is a random deviation possible from the expected relation. Therefore, the structural system of equations for the CON method is given in Eq.3.

$$\hat{Y}_{Roots} = b_{10} + b_{11} D^2 H$$
$$\hat{Y}_{Stem-wood} = b_{20} + b_{21} D^2 H$$
$$\hat{Y}_{Stem-bark} = b_{30} + b_{31} D^2 H$$
$$\hat{Y}_{Crown} = b_{40} + b_{41} D^2 H \quad \text{[Kg]} \tag{3}$$
$$\hat{Y}_{Total-tree} = \hat{Y}_{Roots} + \hat{Y}_{Stem-wood} + \hat{Y}_{Stem-bark} + \hat{Y}_{Crown}$$
$$= (b_{10} + b_{20} + b_{30} + b_{40}) + (b_{11} + b_{21} + b_{31} + b_{41}) D^2 H$$
$$= b_{50} + b_{51} D^2 H$$

21

The SUR (seemingly unrelated regression) method works slightly different and is a multivariate approach, which estimates the different components simultaneously. It is based first on fitting and selecting the best linear models for each tree component. The total tree model was a function (sum) of the independent variables used in each tree component model. Then, all models, including the total, were fitted again simultaneously using joint-generalized least squares (also known as SUR) under the restriction of the coefficients of regression, which ensured additivity.

The best linear model forms were found to be $Y = b_0 + b_1 D^2 H + \mathcal{E}$ for belowground, stem wood, and stem bark biomasses and $Y = b_0 + b_1 D^2 LCL^{0.25} + \mathcal{E}$ for the crown biomass. Summing up the best model forms from each tree component, the model form obtained for the total tree biomass was $Y = b_0 + b_1 D^2 H + b_2 D^2 LCL^{0.25} + \mathcal{E}$.

However, the system of equations obtained by combining the best linear model forms per component under parameter restriction will not yield effective and precise estimates because, according to SAS Institute Inc. (1999), for SUR to be effective, the models must use different regressors. This requirement is not verified, as three of the four components have identical regressors. Indeed, according to Srivastava and Giles (1987) applying SUR to system of the best equations given above is of no benefit when the component equations have identical explanatory variables. Moreover, as stated by Greene (1989) and Bhattacharya (2004), a system of linear SUR equations with identical regressors yields ineffective estimates of coefficient vectors when compared to equation-by-equation ordinary least squares (OLS).

To eliminate the ineffectiveness caused by identical regressors, SUR was applied using second best regression equations for belowground and stem wood biomasses such that the different tree component equations could have different regressors. The resulting system of equations of biomass additivity is given in Eq.4. However, the results of SUR using the best independent model forms are given in Appendices 1 and 2, for demonstration proposes of the ineffectiveness caused by identical regressors.

$$
\begin{aligned}
\hat{Y}_{Roots} &= b_{10} + b_{11}D^2 + b_{12}H \\
\hat{Y}_{Stem-wood} &= b_{20} + b_{21}D^2 \\
\hat{Y}_{Stem-bark} &= b_{30} + b_{31}D^2 H \\
\hat{Y}_{Crown} &= b_{40} + b_{41}D^2 LCL^{0.25} \\
\hat{Y}_{Total} &= (b_{10} + b_{20} + b_{30} + b_{40}) + (b_{11} + b_{21})D^2 + b_{31}D^2 H + b_{41}D^2 LCL^{0.25} + b_{12}H \\
&= b_{50} + b_{51}D^2 + b_{52}D^2 H + b_{53}D^2 LCL^{0.25} + b_{54}H
\end{aligned}
\qquad [Kg] \qquad (4)
$$

Note from the equations shown in Eq.4 that the intercepts of all tree component biomass models are forced (constrained, restricted) to sum up to the intercept of the total tree biomass model, the coefficients of regression for the regressor D^2 in the root system and stem wood biomass models are constrained to sum to the coefficient of regression for D^2 in the total tree biomass model, and the coefficients for the regressors H, $D^2 H$, and $D^2 LCL^{0.25}$ in the root system, stem bark, and crown biomass models, respectively, are constrained to be equal to the coefficients of the same regressors in the total tree biomass model, thereby achieving additivity.

22

The nonlinear seemingly unrelated regression (NSUR) extends the SUR to nonlinear models. NSUR method had the same characteristics and was performed using the same procedures as the SUR method except that the system of equations was composed of nonlinear models. For reference, please see Brandeis et al. (2006), Parresol (2001), Carvalho and Parresol (2003), and Carvalho (2003). The system of equations (including the total tree biomass) obtained by combining the best nonlinear model forms per component under parameter restriction is given in Eq.5.

$$\hat{Y}_{Roots} = b_{10}\left(D^2 H\right)^{b_{11}}$$
$$\hat{Y}_{Stem-wood} = b_{20} D^{b_{21}} H^{b_{22}}$$
$$\hat{Y}_{Stem-bark} = b_{30} D^{b_{31}} H^{b_{32}} \qquad [Kg] \qquad\qquad (5)$$
$$\hat{Y}_{Crown} = b_{41} D^{b_{42}} LCL^{b_{43}}$$
$$\hat{Y}_{Total} = b_{10}\left(D^2 H\right)^{b_{11}} + b_{20} D^{b_{21}} H^{b_{22}} + b_{30} D^{b_{31}} H^{b_{32}} + b_{41} D^{b_{42}} LCL^{b_{43}}$$

Note that the coefficients of regression of each regressor in each tree component model are forced (constrained, restricted) to be equal to coefficients of the equivalent regressor in total tree model, allowing additivity.

The systems of equations in Eqs.4 and 5 were fitted using PROC SYSLIN and PROC MODEL in SAS software (SAS Institute Inc. 1999), respectively, using the ITSUR option. Restrictions (constraints) were imposed on the regression coefficients by using SRESTRICT and RESTRICT statements in PROC SYSLIN and PROC MODEL procedures, respectively. The start values of the parameters in PROC MODEL were obtained by fitting the logarithmized models of each component in Microsoft Excel.

The best tree component and total tree biomass equation were selected by running various possible regressions on combinations of the independent variables (DBH, H, and LCL) and evaluating them using the following goodness of fit statistics: adjusted coefficient of determination (Adj.R^2), standard deviation of the residuals ($S_{y.x}$) and CV of the residuals, mean relative standard error (MRSE), mean residual (MR), and graphical analysis of the residuals. The computation and interpretation of these fit statistics were previously described by Goicoa et al. (2011), Gadow and Hui (1999), Mayer (1941), Magalhães (2008), and Ruiz-Peinado et al. (2011). The best models are those with highest Adj.R^2, smallest $S_{y.x}$, and CV of the residuals, MRSE, and MR; and with the residual plots showing no heteroscedasticity, no dependencies or systematic discrepancies.

In addition to the goodness of fit statistics described above, the methods of enforcing additivity were compared using percent standard error of the expected value and percent standard error of the predicted value, as computed in Table 2. The smaller the percent standard error of the expected and percent standard error of the predicted values is, the better the model in predicting the biomass.

Table 2. Standard error of the expected and predicted values for different methods

Statistic	Absolute form	Relative form
Standard error of the expected value for CON	$S(E(y_0)) = s_{y.x}\sqrt{\dfrac{1}{n} + \dfrac{(x_0 - \bar{x})^2}{SS_x}}$	$S(E(y_0))\% = \dfrac{S(E(y_0))}{\hat{y}_i} \times 100$
Standard error of the predicted value for CON	$S(y_{0i} - \hat{y}) = s_{y.x}\sqrt{1 + \dfrac{1}{n} + \dfrac{(x_0 - \bar{x})^2}{SS_x}}$	$S(y_{0i} - \hat{y})\% = \dfrac{S(y_{0i} - \hat{y})}{\hat{y}_i} \times 100$
Standard error of the expected value for SUR	$S(E(y_0)) = \sqrt{S_{\hat{y}_i}^2} = \sqrt{f_i(b)'\hat{\Sigma}_b f_i(b)}$	$S(E(y_0))\% = \dfrac{S(E(y_0))}{\hat{y}_i} \times 100$
Standard error of the predicted value for SUR	$S(y_{0i} - \hat{y}) = \sqrt{S_{\hat{y}_i}^2 + \hat{\sigma}_{SUR}^2 \hat{\sigma}_{ii}\psi_i(\theta_i)}$	$S(y_{0i} - \hat{y})\% = \dfrac{S(y_{0i} - \hat{y})}{\hat{y}_i} \times 100$
Standard error of the expected value for NSUR	$S(E(y_0)) = \sqrt{S_{\hat{y}_i}^2} = \sqrt{f_i(b)'\hat{\Sigma}_b f_i(b)}$	$S(E(y_0))\% = \dfrac{S(E(y_0))}{\hat{y}_i} \times 100$
Standard error of the predicted value for NSUR	$S(y_{0i} - \hat{y}) = \sqrt{S_{\hat{y}_i}^2 + \hat{\sigma}_{NSUR}^2 \hat{\sigma}_{ii}\psi_i(\theta_i)}$	$S(y_{0i} - \hat{y})\% = \dfrac{S(y_{0i} - \hat{y})}{\hat{y}_i} \times 100$

Sources: Parresol (2001), Lambert et al. (2005), Parresol and Thomas (1991), Snedecor and Cochran (1989), and Yanai et al. (2010).

Where SS_x = sum of squares of the independent variable; $S_{y.x}$ = standard deviation of the residuals; x_0 = particular value of x for which the expected value y is estimated, $E(y_0)$; $S_{\hat{y}_i}^2$ = estimated variance for the *ith* system equation on the observation $\hat{y}_i$; $f_i(b)'$ = a row vector for the *ith* equation from the partial derivates matrix *F(b)*, it is $f_i(b)$ transposed; $\hat{\Sigma}_b$ = estimated covariance matrix of the parameter estimates; $f_i(b)$ = a column vector for the *ith* equation from the partial derivates matrix *F(b)*; $\hat{\sigma}_{SUR}^2$ = SUR system variance; $\hat{\sigma}_{NSUR}^2$ = NSUR system variance; $\hat{\sigma}_{ii}$ = the (i, i) element of the covariance matrix of the residuals $\hat{\Sigma}$ (error covariance matrix), it is the covariance error of the *ith* system equation; and $\psi_i(\theta_i)$ = estimated weight.

SUR and NSUR methods were used instead of, for example, simply summing the best component biomass models (i.e. Harmonization procedure (Návar-Cháidez et al. 2004)), because in the latter case the total biomass is not modelled and therefore its fit statistics are unknown, and because the sum of tree component models with the best fits does not guarantee good fit and unbiased estimates in the total model (Repola 2013). And, further, because SUR and NSUR, unlike the CON method, take into account the contemporaneous correlation among residuals of the component equations (Parresol 1999; Parresol 2001; Carvalho and Parresol 2003; Parresol and Thomas 1991).

Nevertheless, the standard deviation and CV of the residuals for the harmonization approach (HAR) were compared with those obtained for SUR and NSUR approaches. Since, in HAR procedure, the total tree

biomass is obtained simply by summing the best component models, the standard deviation of the residuals can be computed using the variance of a sum (Eq.6) (Parresol 1999; Parresol 2001).

$$S_{y.x(Total)} = \sqrt{\sum_{i=1}^{c} S_{y.x(i)}^2 + 2\sum\sum S_{ij}} \quad [\text{Kg}] \tag{6}$$

where $S_{y.x(Total)}$ and $S_{y.x(i)}$ are the standard deviation of the residuals of the total tree biomass model and of the ith tree component biomass model, respectively, and S_{ij} is the covariance of ith and j^{th} tree component biomass models.

The CV of the residuals is, therefore, computed as

$$CV_{(Total)} = \frac{S_{y.x(Total)}}{\bar{Y}_{total}} \times 100 \ [\%] \tag{7}$$

where $\bar{Y}_{total}$ is the average total tree biomass (per tree).

2.3.2 Estimation of biomass, carbon stocks and error propagation (Article II)

Biomass and carbon stocks and the errors were estimated using the conventional method (Eq. 3). Linear models were preferred over nonlinear models because the conventional method of enforcing additivity is only applicable for linear models (Parresol 1999; Goicoa et al. 2011) and because the procedure of combining the error of the first and second sampling phases (Cunia 1986a) is limited to biomass regressions estimated by linear weighted least squares (Cunia 1986a).

2.3.2.1 Estimation of biomass and carbon stocks

The model form for component and total tree biomass was as follows:

$$Y = b_0 + b_1 D^2 H + \varepsilon \ [\text{Kg}] \tag{8}$$

where D and H represent DBH and total tree-height, respectively, and ε is a random deviation possible from the expected relation. Therefore, the estimated biomass of the kth tree (or tree component) in the hth plot ($\hat{Y}_{hk}$) given by Eq. 8 is determined by Eq. 9:

$$\hat{Y}_{hk} = b_0 + b_1 D_{hk}^2 H_{hk} \ [\text{Kg}] \tag{9}$$

The biomass of plot h ($\hat{Y}_h$) is estimated by summing the individual biomass values ($\hat{Y}_{hk}$) of the n_h trees in plot h as follows:

$$\hat{Y}_h = \sum_{k=1}^{nh} \hat{Y}_{hk} = b_0 n_h + b_1 \sum_{k=1}^{nh} D_{hk}^2 H_{hk} \ [\text{Kg}] \tag{10}$$

where $k = 1, 2, \ldots, n_h$, and $h = 1, 2, \ldots, n_p$, n_p = number of plots in the sample, and n_h = number of trees in the hth plot. Then, dividing Eq.10 by plot size a gives biomass $\hat{Y}$ on an area basis:

$$\hat{Y} = \frac{\hat{Y}_h}{a} = \frac{b_0 n_h}{a} + \frac{b_1 \sum_{k=1}^{nh} D_{hk}^2 H_{hk}}{a} \ [\text{Mg ha}^{-1}] \tag{11}$$

25

Denoting $S_{h0} = \dfrac{n_h}{a}$ and $S_{h1} = \dfrac{\sum\limits_{k=1}^{nh} D_{hk}^2 H_{nh}}{a}$, Eq. 11 can be rewritten as:

$$\hat{Y} = b_0 S_{h0} + b_1 S_{h1} \; [\text{Mg ha}^{-1}] \tag{12}$$

The biomass stock $\bar{Y}$ (average biomass per hectare) is estimated by summing the biomass $\hat{Y}$ of each plot (area basis) and dividing it by the number of plots n_p:

$$\bar{Y} = \dfrac{\sum\limits_{h=1}^{np} \hat{Y}}{n_p} = \dfrac{b_0 \sum\limits_{h=1}^{np} S_{h0}}{n_p} + \dfrac{b_1 \sum\limits_{h=1}^{np} S_{h1}}{n_p} \; [\text{Mg ha}^{-1}] \tag{13}$$

Now, denoting $Z_0 = \dfrac{\sum\limits_{h=1}^{np} S_{h0}}{n_p}$ and $Z_1 = \dfrac{\sum\limits_{h=1}^{np} S_{h1}}{n_p}$, Eq. 13 can be rewritten as follows:

$$\bar{Y} = b_0 Z_0 + b_1 Z_1 = [b]'[Z] \; [\text{Mg ha}^{-1}] \tag{14}$$

where $[b]' = [b_0 \quad b_1]$ is the row vector of the regression coefficient of Eq. 9 (also referred to as the row vector of the estimates from the second sampling phase), and $[Z] = \begin{bmatrix} Z_0 \\ Z_1 \end{bmatrix}$ is the column vector of the estimates from the first phase. As seen in Eq. 14, biomass stock is obtained by combining the estimates from the first and second phases.

Equations 9–14 were applied to estimate biomass stock of each tree component, whole tree, and diameter class. The carbon stock of each tree component was estimated by multiplying the relevant carbon concentration by biomass stock.

2.3.2.2 Error propagation

Biomass stock (Eq. 14) was estimated by combining the estimates of the first and second phases ($[Z]$ and $[b]'$, respectively). Two main sources of error must be accounted for in this calculation. This is, the error resulting from plot-level variability (first sampling phase) and the error from the biomass regression equations (second phase).

Cunia (1965, 1986a, 1986b, 1990) demonstrated that the total variance of the estimated $\bar{Y}$ (mean biomass per hectare) is given by Eq. 15:

$$VAR_t = VAR_1 + VAR_2 = [b]'[S_{zz}][b] + [Z]'[S_{bb}][Z] \; [\text{Mg}^2 \text{ ha}^{-2}] \tag{15}$$

where VAR_1 and VAR_2 are variance components from the first and second sampling phases, respectively; $[b]'$ and $[b]$ are row and column vectors, respectively, of the regression coefficients; $[Z]'$ and $[Z]$ are row

26

and column vectors, respectively, of the estimates from the first phase; $[S_{zz}]$ represents the variance–covariance matrix of vector $[Z]$; and $[S_{bb}]$ represents the variance–covariance matrix of vector $[b]'$ or of the regression coefficients. In this specific case, $[S_{bb}]$ and $[S_{zz}]$ are calculated from Eqs. 16 and 17:

$$[S_{bb}] = \begin{bmatrix} S_{b_0 b_0} & S_{b_0 b_1} \\ S_{b_0 b_1} & S_{b_1 b_1} \end{bmatrix} \tag{16}$$

$$[S_{zz}] = \begin{bmatrix} S_{z_0 z_0} & S_{z_0 z_1} \\ S_{z_0 z_1} & S_{z_1 z_1} \end{bmatrix} \tag{17}$$

where $S_{b_i b_j}$ = covariance of b_i and b_j,

and

$$S_{z_i z_j} = \frac{\sum_{h=1}^{n_p} \left(S_{hi} - \bar{S}_i \right) \left(S_{hj} - \bar{S}_j \right)}{(n_p - 1) n_p} \tag{18}$$

The square root of Eq. 15 is the total standard error (SE) of $\bar{Y}$; the square root of the first component of Eq. 15 $\sqrt{\left[[b]' [S_{zz}] [b] \right]}$ is the standard error of the first phase; and the square root of the second component $\sqrt{\left[[Z]' [S_{bb}] [Z] \right]}$ is the standard error of the second phase.

In this study, the error of $\bar{Y}$ is expressed as the percent SE of the first sampling phase (Eq. 19), the second sampling phase (Eq. 20), and both phases combined (Eq. 21):

$$SE_1(\%) = \frac{\sqrt{\left[[b]' [S_{zz}] [b] \right]}}{\bar{Y}} \times 100 \ [\%] \tag{19}$$

$$SE_2(\%) = \frac{\sqrt{\left[[Z]' [S_{bb}] [Z] \right]}}{\bar{Y}} \times 100 \ [\%] \tag{20}$$

$$SE_t(\%) = \frac{\sqrt{\left[[b]' [S_{zz}] [b] + [Z]' [S_{bb}] [Z] \right]}}{\bar{Y}} \times 100 \ [\%] \tag{21}$$

However, in some cases, the error is expressed as the variance of $\bar{Y}$, especially where the proportional influence of a particular source of error needs to be known, because, unlike the SEs, the variances of the first and second phases are additive, sum to total variance (Cunia 1990).

27

Because carbon stocks are determined by multiplying the carbon concentration by biomass stock, variance of the estimated carbon stock is determined by multiplying the variance of biomass stock by the square of the carbon concentration.

The Monte Carlo error propagation approach was applied to estimate the percent contribution of each variable measurement error to the error of each sampling phase.

In the first sampling phase, the contribution of DBH measurement error, height measurement error, and plot variability were determined. Plot variability was defined as error resulting from variation in the number of trees per hectare (S_{h0}). There were numerous sources of error from the second sampling phase; these sources are described below.

Belowground dry weight was determined by summing the dry weights of lateral roots (coarse and fine) and the taproot (Eq. 22). The sources of error in this calculation are the fresh-weight (FW) and moisture content (MC) determinations:

$$LRFW - LRFW \times LRMC + TRFW - TRFW \times TRMC \ \text{[Kg]} \tag{22}$$

where LR = lateral roots; TR = taproot; $LRFW \times LRMC$ = water weight of lateral roots; and $TRFW \times TRMC$ = water weight of the taproot. Note that MC is a ratio and varies from 0 to 1.

Eq. 22 can be rearranged as:

$$LRFW(1 - LRMC) + TRFW(1 - TRMC) \ \text{[Kg]} \tag{23}$$

Dry weight of stem wood was determined by multiplying the estimated mean stem wood basic density (ρ_{sw}) by its estimated volume (Eq.24):

$$\frac{\Pi}{4} DBH^2 \times H \times ff \times \rho_{sw} \ \text{[Kg]} \tag{24}$$

Because the form factor ff and the value $\frac{\Pi}{4}$ are constants, they do not contribute to error and can be removed to form Eq. 25:

$$DBH^2 \times H \times \rho_{sw} \ \text{[Kg]} \tag{25}$$

Thus, the sources of error in the calculation of stem-wood dry weight are the DBH and height measurements and estimated mean density.

The stem volume obtained by summing the volumes of the constituent stem sections was assumed equal as the volume obtained using form factor; in fact, the mean difference between those two estimates was only 2.3%.

Dry weight of stem bark was calculated as the difference between total stem dry weight (including bark) and dry weight of stem wood (Eq.26), where ρ_s is stem basic density (specific gravity):

$$DBH^2 \times H \times \rho_s - DBH^2 \times H \times \rho_{sw} \ \text{[Kg]} \tag{26}$$

28

The sources of errors in Eq.26 include the DBH and height measurements and the estimated mean stem and stem wood basic densities.

Crown dry weight was determined by summing the dry weights of branches and foliage (Eq.27), with error due to FW and MC determination:

$$BFW - BFW \times BMC + LFW - LFW \times LMC \;\; [Kg] \tag{27}$$

where B = branches; L = leaves; $BFW \times BMC$ = water weight of the branches; and $LFW \times LMC$ = water weight of the foliage.

Eq. 27 can be rearranged as:

$$BFW(1 - BMC) + LFW(1 - LMC) \;\; [Kg] \tag{28}$$

Whole tree dry weight and total error were calculated from the sum of Eqs. 23, 25, 26, and 28.

The contribution of each phase-1 variable measurement error (DBH, total height, and plot variability) to total phase-1 error was determined using Eq. 14 and the phase-1 data; the contribution of error from the second phase was determined from Eqs.23, 25, 26, and 28. These calculations were performed using the 'propagate' package (Spiess 2003) in R (R Core Team 2013). All statistical analyses were performed at the 95% probability level.

The sources of error accounted for in this study are DBH measurement, total tree height estimation and plot variability for phase-1; and DBH and total tree height measurements, stem and stem wood basic density estimation, determination of moisture content (of foliage, branches, and roots), and measurement of fresh weights (of foliage, branches, and roots) for phase-2. Further research is needed to account for other sources of errors not included here, such as the slop of the terrain, distance between the tree and the hypsometer position, diameters at successive heights on the stem, etc.

2.3.3 Biomass expansion factors and root-to-shoot-ratio: measurement uncertainties (Article III)

Biomass expansion factors are another frequently applied method for upscaling biomass and root-to-shoot ratios are often applied to estimate belowground biomass as discussed before.

To apply these methods stem volume was computed using Hohenadl's method (Eq. 29) (Machado and Figueiredo Filho 2005).

$$v_{k2} = \frac{\Pi L}{40}\left(d_{.05}^2 + d_{.15}^2 + d_{.25}^2 + d_{.35}^2 + d_{.45}^2 + d_{.55}^2 + d_{.65}^2 + d_{.75}^2 + d_{.85}^2 + d_{.95}^2\right) \;\; [\text{m}^3] \tag{29}$$

where v_{k2} is the stem volume of the kth tree from the second sampling phase, L is the stem length (in meters), and $d_{.k}$ is the diameter (in meters) measured at the proportional distance along the stem of the kth tree.

The individual stem volume of the kth tree of the hth plot from the first sampling phase (v_{hk1}) was calculated using Eq. 30 as follows:

$$v_{hk1} = \frac{\Pi}{4} DBH^2 \times L \times f_h \;\; [\text{m}^3] \tag{30}$$

29

where f_h is the Hohenadl form factor of the trees from the second sampling phase, obtained using Eq. 31 as:

$$f_h = 0.1\left(1 + \frac{d_{.15}^2}{d_{.05}^2} + \frac{d_{.25}^2}{d_{.05}^2} + \frac{d_{.35}^2}{d_{.05}^2} + \frac{d_{.45}^2}{d_{.05}^2} + \frac{d_{.55}^2}{d_{.05}^2} + \frac{d_{.65}^2}{d_{.05}^2} + \frac{d_{.75}^2}{d_{.05}^2} + \frac{d_{.85}^2}{d_{.05}^2} + \frac{d_{.95}^2}{d_{.05}^2}\right) \text{ [dimensionless]} \quad (31)$$

The main auxiliary variable (the first-phase variable) is the stand-level stem volume (m³ ha⁻¹), estimated from Eq.32 as follows:

$$V_1 = \frac{\sum_{h=1}^{n_p}\sum_{k=1}^{n_h} v_{hk1}}{n_p \times a} = \bar{v}_1 \times N_1 \text{ [m}^3\text{ ha}^{-1}] \quad (32)$$

where n_h is the number of trees in the hth plot, n_p is the number of plots in the sample, a is the plot area (ha), $\bar{v}_1$ is the average stem volume of the trees of the first phase (m³), and N_1 is the average number of trees per hectare estimated from the first sampling phase. Stem height of trees from the first phase was obtained by subtracting predefined stump height from the whole-tree height (H) to standardize the definitions of stem height and stem length (for phase-1 trees).

The BEF of the cth component of the kth tree (BEF_{kc}) of the second sampling phase were calculated as the ratio of tree component biomass y_{kc2} to stem volume v_{k2} (Lehtonen et al. 2004; Cháidez 2009; Dutca et al. 2010; Lehtonen et al. 2007; Marková and Pokorný 2011) (Eq.33) and the average (BEF_c) was taken as the component BEF (Eq. 34) of the woodland. This process enabled to convert stem volume to biomass. The root-to-shoot ratio (R/S) was determined as the ratio of BGB to AGB (IPCC 2006; Mokany et al. 2006; Ryan et al. 2011) for each tree (Eq.35); the average value was taken as the overall vegetation R/S (Eq.36).

$$BEF_{kc} = \frac{y_{kc2}}{v_{k2}} \text{ [Mg m}^{-3}] \quad (33)$$

$$BEF_c = \frac{\sum_{k=1}^{m_2} BEF_{kc}}{m_2} \text{ [Mg m}^{-3}] \quad (34)$$

$$(R/S)_k = \frac{y_{Root_{k2}}}{y_{Shoot_{k2}}} \text{ [dimensionless]} \quad (35)$$

$$R/S = \frac{\sum_{k=1}^{m_2} (R/S)_k}{m_2} \text{ [dimensionless]} \quad (36)$$

where R/S_k is the root-to-shoot ratio of the kth tree of the second sampling phase; $y_{Root_{k2}}$ and $y_{Shoot_{k2}}$ represent BGB and AGB, respectively, of the kth tree of the second phase; and m_2 is the total number of trees in the second sampling phase.

The average tree component biomass stock $\hat{Y}_c$ (Mg ha⁻¹) was estimated as the product of the respective component BEF_c values and V_1 (Eq. 37):

$$\hat{Y}_c = BEF_c \times V_1 = \hat{Y}_{kc} \times N_1 \text{ [Mg ha}^{-1}] \quad (37)$$

30

where

$$\hat{Y}_{kc} = BEF_c \times \bar{v}_1 \ [\text{Mg}] \tag{38}$$

is the estimated average component biomass per tree, which yields $\hat{Y}_c$ when multiplied by the number of trees per hectare.

BEF_{kc} (Eq.33) is the ratio of biomass of a tree component to stem volume; therefore, BEF_c (Eq.34) is a mean ratio (not a ratio of means). These variables represent double sampling with mean-of-ratios estimators and dependent phases, and the uncertainty (variance and standard error) of the estimated BEF_c and $\hat{Y}_c$ must be computed accordingly (as for R/S).

The variance of the estimated $\hat{Y}_{kc}$ (Eq. 38) was calculated according to Freese (1962, 1984):

$$VAR_{\hat{Y}_{KC}} = \bar{v}_1^2 \left(\frac{S^2_{BEF_C}}{m_2} \right)\left(1 - \frac{m_2}{m_1} \right) + \frac{S^2_{y_{C2}}}{m_1}\left(1 - \frac{m_1}{M} \right) \ \ [\text{Mg}^2] \tag{39}$$

Rearranging Eq.38 as $BEF_c = \dfrac{\hat{Y}_{kc}}{\bar{v}_1}$, the variance of the estimated BEF_c becomes (de Vries 1986):

$$VAR_{BEF_C} = \frac{VAR_{\hat{Y}_{KC}}}{\bar{v}_1^2} = \left(\frac{S^2_{BEF_C}}{m_2} \right)\left(1 - \frac{m_2}{m_1} \right) + \left(\frac{1}{\bar{v}_1^2} \right)\left(\frac{S^2_{y_{C2}}}{m_1} \right)\left(1 - \frac{m_1}{M} \right) \ \ [\text{Mg}^2\,\text{m}^{-6}] \tag{40}$$

Similarly, the variance of the estimated $\hat{Y}_c$ is (de Vries 1986):

$$VAR_{\hat{Y}_C} = N_1^2 \times \left[\bar{v}_1^2 \left(\frac{S^2_{BEF_C}}{m_2} \right)\left(1 - \frac{m_2}{m_1} \right) + \frac{S^2_{y_{C2}}}{m_1}\left(1 - \frac{m_1}{M} \right) \right] \ \ [\text{Mg}^2\,\text{ha}^{-2}] \tag{41}$$

and the variance of the estimated R/S is

$$VAR_{R/S} = \left(\frac{S^2_{R/S}}{m_2} \right)\left(1 - \frac{m_2}{m_1} \right) + \left(\frac{1}{\bar{y}^2_{Shoot}} \right)\left(\frac{S^2_{y_{Root2}}}{m_1} \right)\left(1 - \frac{m_1}{M} \right) \ \text{[dimensionless]} \tag{42}$$

where

$$S^2_{BEF_C} = \frac{\sum BEF_{kc}^2 - \dfrac{\left(\sum BEF_{kc} \right)^2}{m_2}}{m_2 - 1} \ [\text{Mg}^2\,\text{m}^{-6}] \tag{43}$$

is the variance of BEF_c for the second phase;

$$S^2_{y_{C2}} = \frac{\sum y_{kc2}^2 - \dfrac{\left(\sum y_{kc2} \right)^2}{m_2}}{m_2 - 1} \ [\text{Mg}^2] \tag{44}$$

is the variance of y_{c2}; y_{c2} is the component biomass for the second phase;

$$S^2_R = \frac{\sum \left(R/S \right)_k^2 - \dfrac{\left(\sum \left(R/S \right)_k \right)^2}{m_2}}{m_2 - 1} \ \text{[dimensionless]} \tag{45}$$

31

is the variance of R/S for the second phase;

$$S^2_{y_{Root2}} = \frac{\sum y^2_{Root_{i_2}} - \frac{\left(\sum y_{Root_{i_2}}\right)^2}{m_2}}{m_2 - 1} \ [Mg^2] \tag{46}$$

is the variance of $y_{Root_{i_2}}$; $y_{Root_{i_2}}$ is the BGB of trees of the second phase; $\bar{y}_{Shoot_1}$ is the average AGB per tree for the first sampling phase; and m_1, m_2, and M are the number of trees in the first sampling phase, the second sampling phase, and the entire population, respectively. The finite population correction factor $\left(1 - \frac{m_1}{M}\right)$ was eliminated because m_1 was very small relative to M, which was unknown.

The square root of Eqs.40 and 41 is the absolute standard error of the estimated BEF_c and $\hat{Y}_c$, respectively; dividing these values by BEF_c and $\hat{Y}_c$ and then multiplying them by 100 provides the respective percent standard error. The absolute and percent 95% confidence limits (CI) are computed by multiplying the absolute and percent standard error by the Student's t-value (t). The absolute and percent standard errors of R/S are computed analogously.

The percent 95% confidence limit (Eq.47) is also referred as percent sampling error (Sanquetta et al. 2006).

$$95\% CI_{\%} = E_{\%} = \pm \frac{t \times SE}{\bar{X}} \times 100 \ [\%] \tag{47}$$

where SE is the standard error and $\bar{X}$ is the average BEF_c, $\hat{Y}_c$ or R/S.

In this study, uncertainty is expressed as the percent SE and as the 95% confidence interval (CI) to facilitate comparison with existing studies as, for the knowledge of the author, the existing studies reporting BEFs and R/S with known uncertainty use either percent SE (Lehtonen et al. 2004; Lehtonen et al. 2007; Jalkanen et al. 2005) or percent 95% CI (IPCC 2003; Tobin and Nieuwenhuis 2007; Green et al. 2007) to express the uncertainty.

Because, in many studies, BEF is found to vary with tree size (Brown et al. 1989; Lehtonen et al. 2004; Cháidez 2009; Dutca et al. 2010; Sanquetta et al. 2011), the dependence of the component BEF values on DBH and tree-height was analysed by linear regression of BEF_c against DBH and tree-height and testing the significance of the regression against the null hypothesis of slope = 0 using Student's t-tests; and by testing the significance of the Pearson´s correlation coefficient. However, the linear regression and the Pearson´s correlation coefficient detect only linear dependence; do not detect nonlinear or nonmonotone dependencies (Székelly and Rizzo 2009). Therefore, distance correlation, distance covariance, and distance covariance test of independence (Székelly et al. 2007; Székelly and Rizzo 2009) were used to address possible nonlinear dependencies between the variables under study. Distance correlation is a new dependence coefficient that measures all types of dependencies between random vectors X and Y in arbitrary dimension (Székelly and Rizzo 2009). Therefore, the distance covariance test of independence detects any nonlinear and

32

nonmonotone dependence between two random variables (Székelly and Rizzo 2009). The relationship of R/S to DBH, total tree-height, AGB, BGB, and total biomass was examined by the same procedures. All analyses were performed at the 5% significance level using Microsoft Excel Data Analysis Tools and using the "Energy" package (Rizzo and Székelly 2015) in R (R Core Team 2015).

Further, the default IPCC aboveground BEF ($BEF_{c(IPCC)}$) for tropical broadleaf species and the respective BEF-based biomass density ($\hat{Y}_{c(IPCC)}$), computed using the default BEF and the volume estimated in this study, were compared with the aboveground BEF from this study and the respective BEF-based biomass density.

The default BEF-based biomass density was computed as follows (Eq. 48):

$$\hat{Y}_{c(IPCC)} = BEF_{c(IPCC)} \times V_1 \quad [\text{Mg ha}^{-1}] \tag{48}$$

The $BEF_{c(IPCC)}$ and V_1 are obtained from independent samples (separate surveys), therefore, the uncertainty (percent SE) of $\hat{Y}_{c(IPCC)}$ can be computed as in Eq. 49 (Freese 1962; Freese 1984; IPCC 2003; Chave et al. 2004; Jalkanen et al. 2005; Green et al. 2007; Tobin and Nieuwenhuis 2007):

$$SE\% = \sqrt{SE\%^2_{BEF_{C(IPCC)}} + SE\%^2_{V_1}} \quad [\%] \tag{49}$$

where $SE^2_{BEF_{C(IPCC)}}$ $SE^2_{V_1}$ are percent standard errors associated with $BEF_{c(IPCC)}$ and V_1, respectively.

2.3.4 Below- and aboveground architecture: topological analysis of the root and shoot systems (Article IV)

The altitude (a) and magnitude (μ) of topological parameters were determined for each root and shoot system. Altitude refers to the number of links in the longest individual path in the system (Fitter 1987; Fitter and Stickland 1991; Echeverria 2008), from the root or shoot base to an external link (Coll et al. 2008; Echeverria 2008), and magnitude refers to the total number of external links (those ending with a meristem; Fitter et al. 1991; Fitter and Stickland 1991; Riccardo 2007; Coll et al. 2008) (Figure 4).
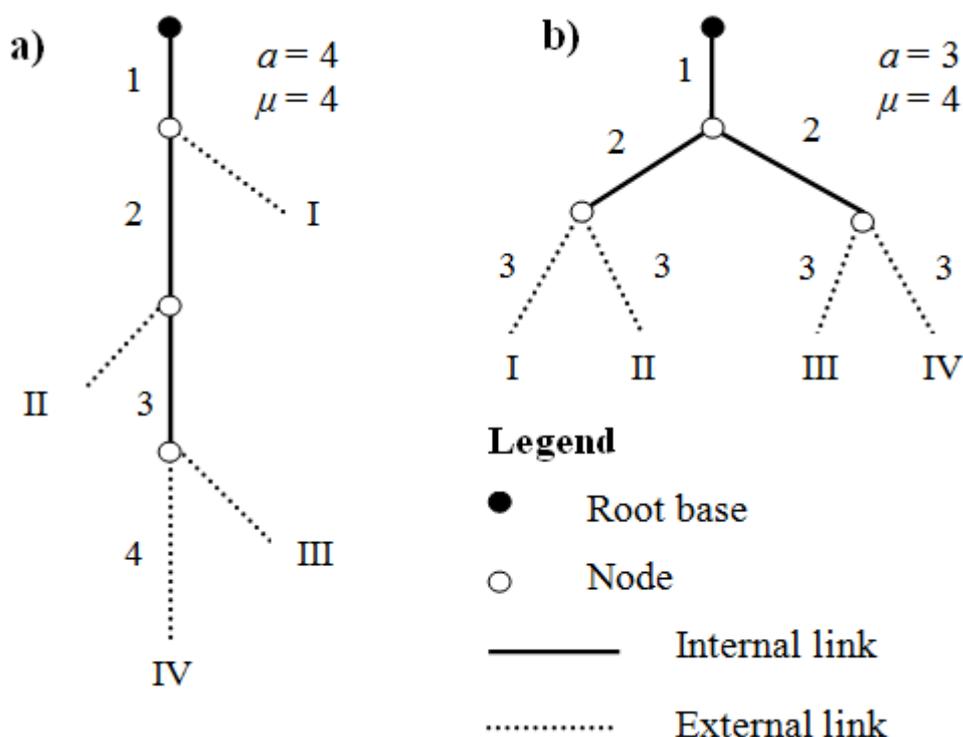
Figure 4. Altitude and magnitude for (**a**) herringbone and (**b**) dichotomous root systems. The altitude is numbered in Arabic numerals and the magnitude is numbered in Roman numerals

The branching tendency of the root and shoot systems to one of the two extremes of branching patterns, herringbone and dichotomous, was estimated by calculating two distinct indexes, the topological index (TI) and the topological trend (TT). TI was computed as the slope of the linear regression between $\log_{10}(a)$ and $\log_{10}(\mu)$ as proposed by Fitter et al. (1991); it can also be computed as follows: $\log_{10}(a)$: $\log_{10}(\mu)$ ratio (Riccardo 2007; Glimskar 2000), in the cases of single root or shoot systems. TI values close to 1 are associated with herringbone branching pattern and those close to 0.53 are associated with random growth of the roots or branches (Fitter et al. 1991). TT was computed using Eq. 50 (Trencia 1995). TT values close to 1 are associated with herringbone branching pattern, and those close to 0 are associated with dichotomous branching pattern (Trencia 1995). Therefore, TI values were tested under the null hypothesis of being equal to 1 and 0.53, and average TT values were tested under the null hypothesis of being equal to 1 and 0 by using Student's t-test.

$$TT = [Pe0 - Pe_{(min)}]/[Pe_{(max)} - Pe_{(min)}] \text{ [dimensionless]} \tag{50}$$

where Pe0 is the number of observed Pe, and Pe (external path length) is the sum of the number of links in all paths from all external links to the base link (Fitter 1987). $Pe_{(max)}$ and $Pe_{(min)}$ are the possible maximum and minimum Pe values, respectively, and are computed as $Pe_{(max)} = 1/2 (\mu^2 + 3\mu - 2)$ and $Pe_{(min)} = \mu(a_{min} + 1) - 2a_{min} - 1$, where $a_{min} = \log_2(\mu - 1) + 2$.

The proportionality factor (p), a parameter that describes the changes in cross-sectional area (CSA) from parent root or branch to the total daughter roots or branches (van Noordwijk and Mulia 2002), i.e. the

34

changes of CSA during branching (Soethe et al. 2007) was computed using Eq. 51. The allocation factor (q), a parameter that describes the equity in CSA among daughter roots or branches (van Noordwijk and Mulia 2002) was computed using Eq. 52. Since only the primary roots or branches were considered, the parent root or branch was always the taproot or stem and the daughter roots or branches included the taproot or the stem after branching and the daughter roots or branches after branching.

$$p = \frac{D^2 before\ branching}{\sum D^2 after\ branching} \quad \text{[dimensionless]} \tag{51}$$

$$q = \frac{\max D^2 after\ branching}{\sum D^2 after\ branching} \quad \text{[dimensionless]} \tag{52}$$

where D is the root or branch diameter.

The Leonardo da Vinci rule or the area-preserving branching further substantiated by eco-physiological principles by Shinozaki et al. (1964) with their pipe model theory was tested for the root and shoot systems by using four different methods. First, the average parameters p and q calculated for each *ith* node of the 93 trees and for the entire population of nodes were tested under the null hypothesis of being equal to 1 and 0.5, respectively, by using Student's *t*-test. Second, these parameters (p and q) were tested for independence to the link diameter by running a linear regression of p and q against the link diameter and testing the significance of the regression slope. Third, the diameter exponent Δ from Eq. 53 of each stem or taproot node in each tree was estimated separately by nonlinear optimisation using Newton coordinate search, and the average was obtained per *ith* node and per total number of nodes. The diameter exponent is the value of exponent Δ that is used to solve Eq. 53.

$$d_b^\Delta = \sum_{a=1}^{n} d_a^\Delta \quad \text{[cm}^\Delta\text{]} \tag{53}$$

where d_b is the distal diameter before branching, and d_a is the proximal diameter after branching. Finally, assuming $\Delta = 2$, the regression through the origin (RTO) of the CSA before branching against total CSA after branching was run by using Eq.54 reported by Spek and van Noordwijk (1994).

$$d_b^2 = \alpha \sum_{a=1}^{n} d_a^2 \quad \text{[cm}^2\text{]} \tag{54}$$

The average parameter Δ and the regression slope α were tested under the null hypothesis of being equal to 2 and 1, respectively, by using Student's *t*-test. The regression slope α is also referred to as the proportionality factor (p) by some authors such as Oppelt et al. (2001), although their values estimated from Eqs.51 and 54 are distinct. In this study, these parameters were treated distinctly.

In the cases where the average parameter p and slope α were not statistically different from 1 and the average parameter Δ was not statistically different from 2, the area-preserving branching was confirmed. This was because if $p = 1$ (i.e. $\Delta = 2$ or $\alpha = 1$), the CSA does not change across a branching point (node), whereas if $p > 1$ (i.e. $\Delta > 2$ or $\alpha > 1$), the CSA decreases from the parent to daughter and, if $p < 1$ (i.e. $\Delta < 2$

35

or $\alpha < 1$), it increases (Kalliokoski 2011; Oppelt et al. 2001; Richardson and zu Dohna 2003). Further, in the cases where the average parameter q was not found to be statistically different from 0.5, equity in CSA was implied among daughter roots or branches.

Furthermore, in the cases in which the area-preserving branching was observed for all nodes across the stem or taproot, the self-similar branching pattern was confirmed (van Noordwijk and Mulia 2002; Soethe et al. 2007 and Richardson and zu Dohna 2003). In other words, if the branching parameters (p and q) for all nodes across the stem or taproot were not found to be dependent on the link diameter, the self-similar branching pattern was confirmed (Salas et al. 2004; van Noordwijk and Purnomosidhi 1995). All the statistical analyses were performed at the 5% significance level using Microsoft Excel Data Analysis Tools.

3. RESULTS

3.1 Descriptive statistics of the collected data

The number of trees recorded during the first sampling phase ranged from approximately 500 to >1000 ha^{-1} with an average of 1236 ha^{-1}, distributed in each diameter class as shown in the Figure 5 – diameter distribution histogram – which follows a pattern of an inverse J-shaped curve, typical of an uneven-aged forest. The size and volume of the trees varied substantially (Table 3). The average AGB per tree $\left(\bar{y}_{Shoot}\right)$ was 97.95 kg. The dry weight of the components measured destructively during the second sampling phase, as well as Hohenadl form factor and stem volume, also varied considerably (Table 4).
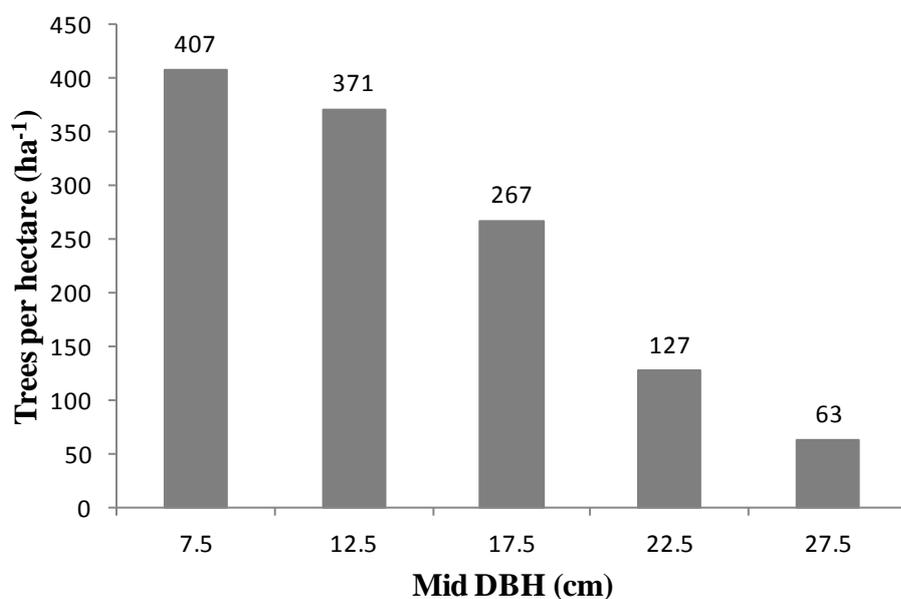
Figure 5. Diameter distribution histogram of phase-1 sampled *A. johnsonii* trees

Table 3. Values of variables estimated for 3574 *A. johnsonii* trees in 23 plots during the first sampling phase

Statistic	Tree-density (trees.ha^{-1})	Basal area (m^2/ha)	Stem volume (m^3/ha)	DBH (cm)	H (m)	L (m)
Average	1236.2187	21.2856	115.3149	13.4112	10.5616	10.4272
Minimum	541.1268	15.2386	66.8999	5.0000	1.8000	1.6000
Maximum	2220.2115	30.0053	170.4468	50.0000	22.5000	22.3000
SD	476.7204	4.1198	25.4407	6.2879	2.7637	2.7901
CV (%)	38.5628	19.3549	22.0900	46.8856	26.1678	26.7583
SE	99.4031	0.8590	5.3048	0.1052	0.0462	0.0467
SE (%)	8.0409	4.0358	4.6061	0.7843	0.4377	0.4476

DBH = diameter at breast height; H = total tree height; L = stem height; SD = standard deviation; CV = coefficient of variation; SE = standard error.

Table 4. Values of variables for 93 *Androstachys johnsonii* trees (a subset of the trees from phase-1) obtained during the second phase using destructive sampling

	Second phase variables	Average	Minimum	Maximum	SD	CV (%)
	Taproot + stump	23.651	1.474	71.926	18.926	80.019
	Lateral roots	24.083	0.746	100.815	23.945	99.428
	Root system	**47.735**	**2.545**	**162.105**	**41.210**	**86.331**
	Stem wood	124.068	4.947	357.348	99.497	80.196
	Stem bark	14.198	0.677	55.805	12.372	87.138
Component dry weight (kg)	**Stem**	**138.267**	**5.636**	**413.153**	**110.577**	**79.974**
	Branches	55.586	2.583	211.320	57.355	103.183
	Foliage	2.807	0.333	15.100	2.493	88.818
	Crown	**58.393**	**3.038**	**216.695**	**59.077**	**101.172**
	Shoot system	**196.659**	**9.823**	**590.863**	**163.713**	**83.247**
	Total tree	**244.394**	**12.484**	**752.571**	**204.330**	**83.607**
	Diameter at breast height (DBH) (cm)	17.5860	5.0000	32.0000	7.5122	42.7167
	Total height (TH) (m)	12.3230	5.6900	16.0000	2.1381	17.3508
Dendrometric variables	Stem length (H) (m)	10.7470	4.2500	14.8400	2.4456	22.7562
	Stem volume (v_2) (m^3)	0.1890	0.0083	0.5806	0.1512	79.9826
	Hohenadal form factor (f_h)	0.4460	0.3002	0.6128	0.0592	13.2716

The major components and their values are indicated in bold font. SD = standard deviation; CV = coefficient of variation

3.2 Biomass modelling and additivity (Article I)

3.2.1 Independent tree component and total tree models

The fit statistics and the coefficient of regression for the best tree component and total tree models are given in Table 5 for linear and nonlinear models.

Table 5. Regression coefficients and goodness of fit statistics for the best linear and nonlinear models in Eqs.3 and 4, respectively

Tree component	Weight function	b_0 (± SE)	b_1 (± SE)	b_2 (± SE)	Adj.R^2(%)	$S_{y.x}$(kg)	CV(%)	MRSE (kg)	MR (kg)
				Linear models					
Roots	1/D^{2}H	0.2522 (± 0.6334)	0.0097 (± 0.0002)*		94.94	9.59	20.10	0.1520	-2.05E-14
Stem wood	1/D^{2}H	0.6616 (± 1.1451)	0.0251 (± 0.0004)*		97.49	19.66	15.84	0.0255	-7.96E-16
Stem bark	1/D^{2}H	0.1895 (± 0.3503)	0.0028 (± 0.0001)*		84.24	4.97	34.97	0.3397	-1.96E-16
Crown	1/D^{2}H	− 1.9106 (± 1.5216)	0.0984 (± 0.0044)*		84.24	27.06	46.34	1.0292	-2.43E-01
Total tree	1/D^{2}H	1.4066 (± 2.1984)	0.0494 (± 0.0008)*		97.61	34.92	14.29	0.0247	-1.24E-15
				Nonlinear models					
Roots	1/D^{2}H	0.0091 (± 0.0024)*	1.0074 (± 0.0841)*		94.94	10.40	21.79	0.1480	1.90E-05
Stem wood	1/D^{2}H	0.0197 (± 0.0063)*	1.8210 (± 0.0567)*	1.3081 (± 0.1559)*	97.71	18.83	15.18	0.0272	-3.40E-04
Stem bark	1/D^{2}H	0.0022 (± 0.0019)	1.7451 (± 0.1564)*	1.4084 (± 0.4355)	84.84	5.70	40.11	0.3770	-2.04E-03
Crown	1/D^{2}H	0.0350 (± 0.0137)*	2.1318 (± 0.1385)*	0.5290 (± 0.1482)*	84.42	26.89	46.05	0.5396	-2.59E-01
Total tree	1/D^{2}H	0.0533 (± 0.0093)*	0.9920 (± 0.0196)*		97.60	38.68	15.83	0.1192	1.10E-05

SE = standard error; "*" = significant at α ≥ 5%; " " = not significant at any probability level

All linear and nonlinear regression equations yielded satisfactory fit statistics. The linear models presented an adjusted R^2 varying from 84.24% for stem bark and crown biomass regressions to 97.61% for total tree biomass regression; the precision, as measured by the coefficient of variation (CV) of the residuals, varied from 14.29% for total tree biomass regression to 46.34% for crown biomass regression. The adjusted R^2 for nonlinear models varied in a comparable range from 84.42% for crown biomass regression to 97.60% for total tree biomass regression, and the CV of the residuals varied from 15.18% to 46.05%. For both, linear or nonlinear models, the bias, as measured by the mean residual (MR), were found to be statistically not significant using Student's t-test, and comparatively poorer fit statistics were obtained for stem bark and crown biomass regressions.

3.3.2 Forcing additivity

In the models in Eq.1, the most frequent best linear model form was $Y = b_0 + b_1 D^2 H + \varepsilon$, which was found to be the best for the root system, stem wood, stem bark, and total tree biomasses. This model form was also ranked as the second model form for crown biomass. Therefore, to enforce additivity using the CON approach, this model form was generalized for all tree components and for total tree biomasses, as can be seen from Eq.3. Tables 6 and 7 illustrate the regression coefficients, and the goodness of fit statistics, respectively, for the CON method presented in Eq.3, the SUR method in Eq.4 and the NSUR method in Eq.5.

Table 6. Coefficients of regression for CON, SUR and NSUR methods

Tree component	Weight function	b_0 (± SE)	b_1 (± SE)	b_2 (± SE)	b_3 (± SE)	b_4 (± SE)
			CON method			
Roots	$1/D^2H$	0.2522 (± 0.6334)	0.0097 (± 0.0002)*			
Stem wood	$1/D^2H$	0.6616 (± 1.1451)	0.0251 (± 0.0004)*			
Stem bark	$1/D^2H$	0.1895 (± 0.3503)	0.0028 (± 0.0001)*			
Crown	$1/D^2H$	0.3033 (± 1.5640)	0.0118 (± 0.0006)*			
Total tree	$1/D^2H$	1.4066 (± 2.1984)	0.0494 (± 0.0008)*			
			SUR method			
Roots	$1/D^2H$	1.6513 (± 2.3498)	0.1016 (± 0.0040)*	− 0.4056 (± 0.2584)		
Stem wood	$1/D^2H$	− 3.8911 (± 0.9553)*	0.2106 (± 0.0047)*			
Stem bark	$1/D^2H$	0.1285 (± 0.3260)	0.0014 (± 0.0001)*			
Crown	$1/D^2H$	− 1.9730 (± 1.5045)	0.1114 (± 0.0044)*			
Total tree	$1/D^2H$	− 4.0843 (± 3.1723)	0.3122 (± 0.0068)*	0.0014 (± 0.0001)*	0.1114 (± 0.0044)*	− 0.4056 (± 0.2584)
			NSUR method			
Roots	$1/D^2H$	0.0075 (± 0.0022)*	1.0137 (± 0.0326)*			
Stem wood	$1/D^2H$	0.0131 (± 0.0040)*	1.7962 (± 0.0549)*	1.4113 (± 0.1470)*		
Stem bark	$1/D^2H$	0.0001 (± 0.0011)	1.6545 (± 0.1942)*	1.7332 (± 0.5460)*		
Crown	$1/D^2H$	0.0407 (± 0.0159)*	2.2302 (± 0.1343)*	0.3146 (± 0.1214)*		
Total tree	$1/D^2H$					

SE = standard error; "*" = significant at $\alpha \geq 5\%$; " " = not significant at any probability level

Table 7. Fit statistics for CON, SUR and NSUR methods

Tree component	Weight function	Adj.R^2(%)	S$_{y.x}$ (kg)	CV(%)	MRSE (kg)	MR (kg)	$\hat{\sigma}_{ii}$	$\hat{\sigma}^2_{SUR}$	$\hat{\sigma}^2_{NSUR}$
				CON method					
Roots	1/D^{2}H	94.94	9.59	20.10	0.1520	-2.05E-14	–		
Stem wood	1/D^{2}H	97.49	19.66	15.84	0.0255	-7.96E-16	–		
Stem bark	1/D^{2}H	84.24	4.97	34.97	0.3397	-1.96E-16	–	–	–
Crown	1/D^{2}H	82.16	25.11	43.01	1.5596	1.71E-15	–		
Total tree	1/D^{2}H	97.61	34.92	14.29	0.0247	-1.24E-15	–		
				SUR method					
Roots	1/D^{2}H	82.44	22.06	46.24	0.1378	0.1769*	0.0581		
Stem wood	1/D^{2}H	72.47	60.59	48.83	0.1732	0.6599*	0.5943		
Stem bark	1/D^{2}H	52.84	10.56	74.38	0.2403	0.0930*	0.0157	0.9906	–
Crown	1/D^{2}H	81.96	27.22	46.62	1.4330	– 0.1188*	0.1053		
Total tree	1/D^{2}H	86.88	96.67	39.56	0.0791	0.8109*	9.1562		
				NSUR method					
Roots	1/D^{2}H	92.76	12.84	26.92	0.1168	0.0805*	0.0244		
Stem wood	1/D^{2}H	92.27	35.66	28.74	0.0440	0.3116*	0.1718		
Stem bark	1/D^{2}H	78.12	6.85	48.25	0.2084	0.0423*	0.0072	–	4.7801
Crown	1/D^{2}H	85.27	26.41	45.23	0.8348	– 0.0049	0.0859		
Total tree	1/D^{2}H	67.76	53.32	21.82	0.0321	0.4296*	6.7590		

"*" = significant at α ≥ 5%; " " = not significant at any probability level

Tables 8 and 9 show the tests of significance of the restrictions imposed for weighted SUR and weighted NSUR, respectively. All the tests were found to be highly significant.

Table 8. *t*-test for the restriction imposed for weighted SUR.

Restriction	DF	Parameter estimate	Standard error	t value	Pr > |t|
b$_{50}$ = b$_{10}$ + b$_{20}$ + b$_{30}$ + b$_{40}$	– 1	0.6255	0.1204	5.2	<.0001
b$_{51}$ = b$_{11}$ + b$_{21}$	– 1	2230.6100	355.5158	6.27	<.0001
b$_{52}$ = b$_{31}$	– 1	390.4832	43.5058	8.98	<.0001
b$_{53}$ = b$_{42}$	– 1	227.0888	24.8863	9.13	<.0001
b$_{54}$ = b$_{12}$	– 1	4.7892	1.4875	3.22	0.0010

Note: The restrictions are as stated in the Eq. (4).

**Table 9.** *t*-test for the restriction imposed for weighted NSUR.

Restriction	Parameter estimate	Standard error	t value	Pr > |t|
Res1	− 3162.70	356.20	− 8.88	<.0001
Res2	− 210.46	23.76	− 8.86	<.0001
Res3	− 4392.79	489.80	− 8.97	<.0001
Res4	− 178.30	19.99	− 8.92	<.0001
Res5	− 150.95	16.78	− 9.00	<.0001
Res6	− 6811.46	732.60	− 9.30	<.0001
Res7	− 20.27	2.19	− 9.25	<.0001
Res8	− 17.20	1.85	− 9.31	<.0001
Res9	− 877.64	94.86	− 9.25	<.0001
Res10	− 111.99	12.20	− 9.18	<.0001
Res11	− 84.74	8.80	− 9.63	<.0001

Note: Res1 to res11 are the restrictions imposed to each of the 11 regression coefficients in the total tree model, as stated in Eq. (5).

3.3.2.1 The CON method

The results of the CON method were the same as for equation-by-equation WLS in Table 5, except that the model for crown biomass was replaced in order to use the same regressors as the remaining tree components. Better performances were found for total tree, belowground, and stem wood biomass regressions.

The graphs of the residuals against predicted values for the CON method are presented in Figure 6 and did not show a significant heteroscedasticity to impact the adjustement. The cluster of points was contained in a horizontal band, showing no particular trend, with the residuals almost evenly distributed under and over the axis of abscissas, meaning that there were not obvious model defects.


(a)

(b)
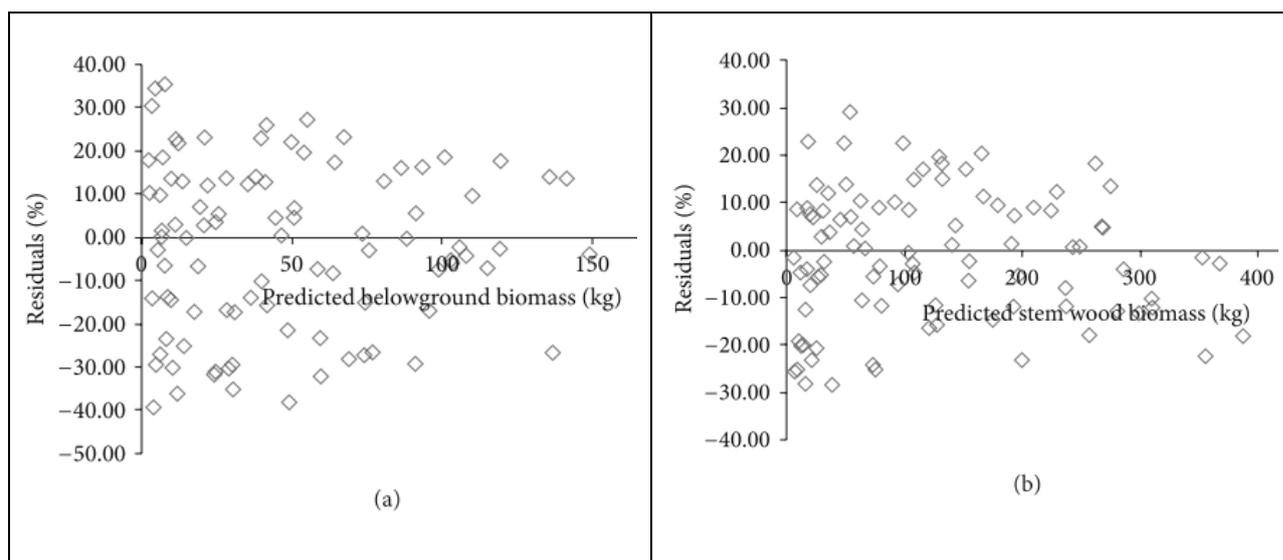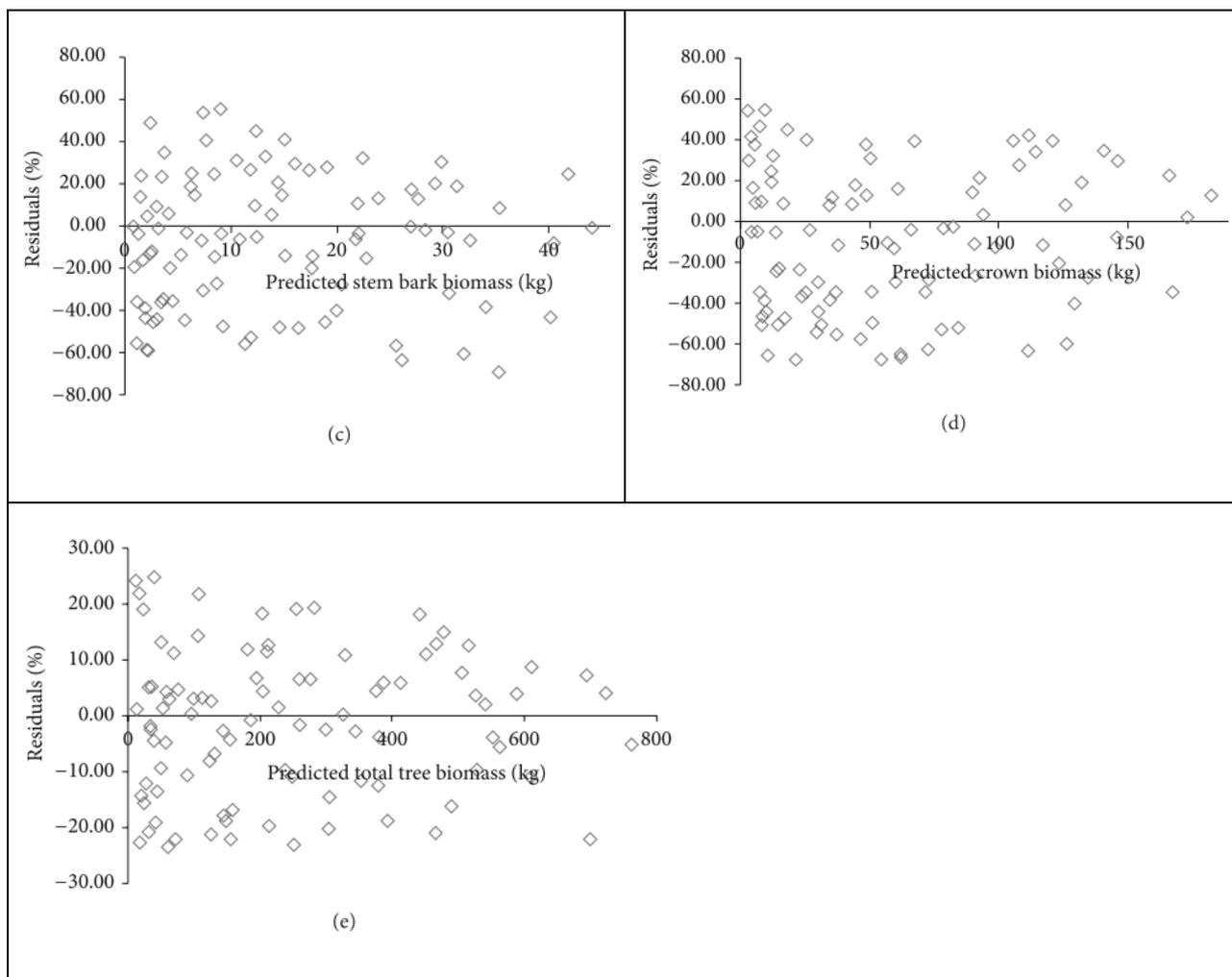
Figure 6. Residuals against predicted biomass for the CON method: **a)** belowground, **b)** stem wood, **c)** stem bark, **d)** crown, and **e)** total tree biomass

3.3.2.2 SUR method

As can be seen in Tables 6 and 7, the adjusted R^2 varied from 52.84% for stem bark to 86.88% for total tree biomass regression, and the CVs of the residuals varied from 39.56% for total tree biomass regression to 74.38% for stem bark. All tree components and total tree models were found to be biased, and all of these models underestimated the biomass, except for the crown biomass, which was overestimated, as was observed from the mean residual (MR). Using Student's *t*-test, these biases (MRs) were found to be statistically significant (statistically different from zero).

The biases, model defects (under and/or overestimation, heteroscedasticity), and patterns that indicated systematic discrepancies are illustrated by the graph of the residuals in Figure 7. Analyses of the residuals for SUR did not reveal heteroscedasticity but showed that symmetry of the residuals was only verified for BGB model (Figure 7a). The residuals for stem wood, stem bark and total tree biomass were mostly agglomerated above the axis of abscissas, meaning that the designed models predicted biomass values smaller than the observed ones, underestimating the biomass (producing positive residuals). Overestimation was observed for the model of crown biomass.

42
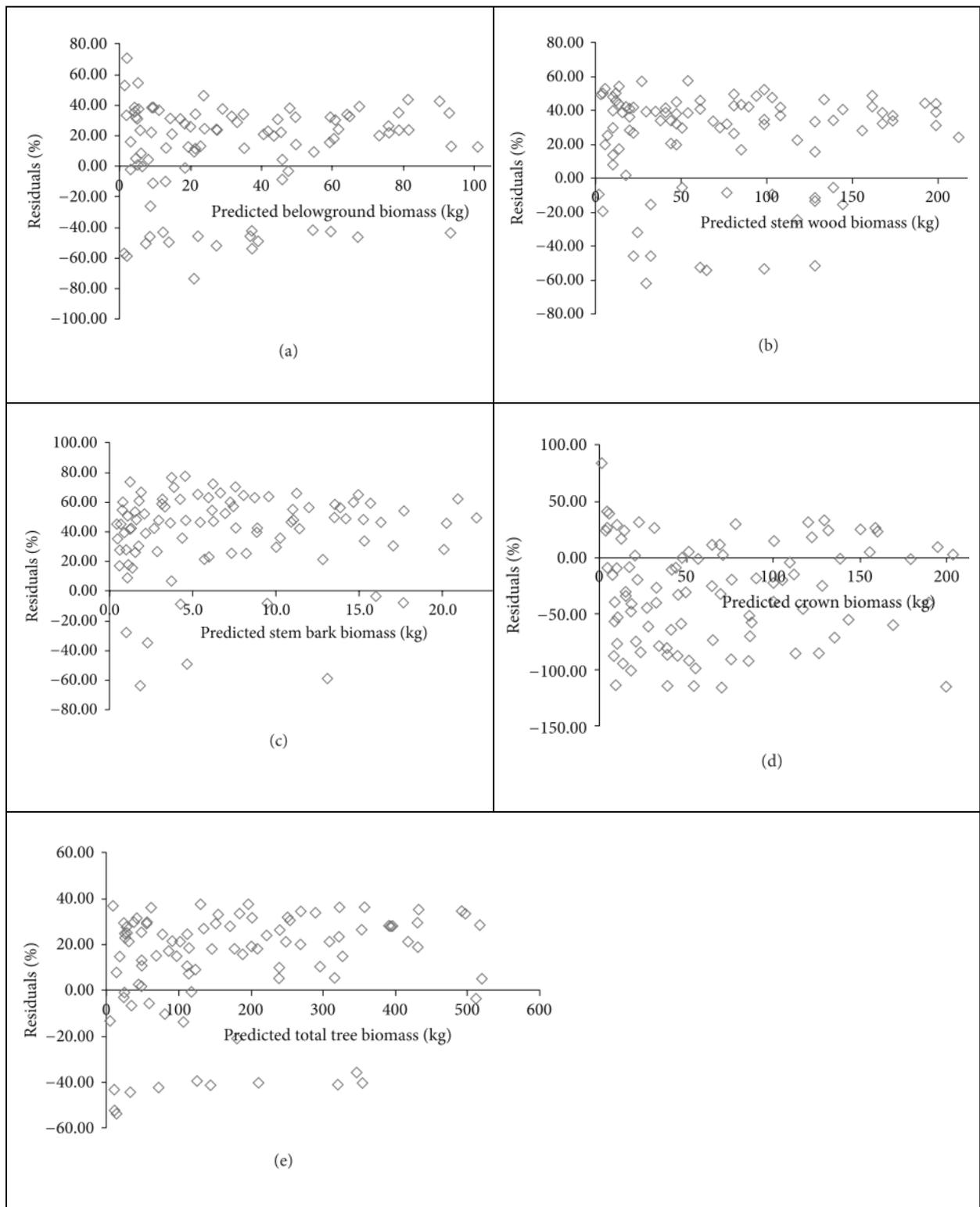
Figure 7. Residuals against the predicted biomass for the SUR method: **a)** belowground, **b)** stem wood, **c)** stem bark, **d)** crown, and **e)** total tree biomass.

3.3.2.3 NSUR method

Component models (Tables 6 and 7) showed an adjusted R^2 varying from 78.12% for stem bark to 92.76% for roots. The lowest adjusted R^2 was found for the total tree model (67.76%). The CVs of the residuals varied from 21.82% for total tree to 48.25% for the stem bark model. All tree components (except the crown)

43

and the total tree models were biased, underestimating the biomass significantly, as shown by the observation that the MRs were significantly different from zero.

Overall, the distribution of the residuals (Figure 8) was satisfactory. Minor defects were found for crown and total tree models.
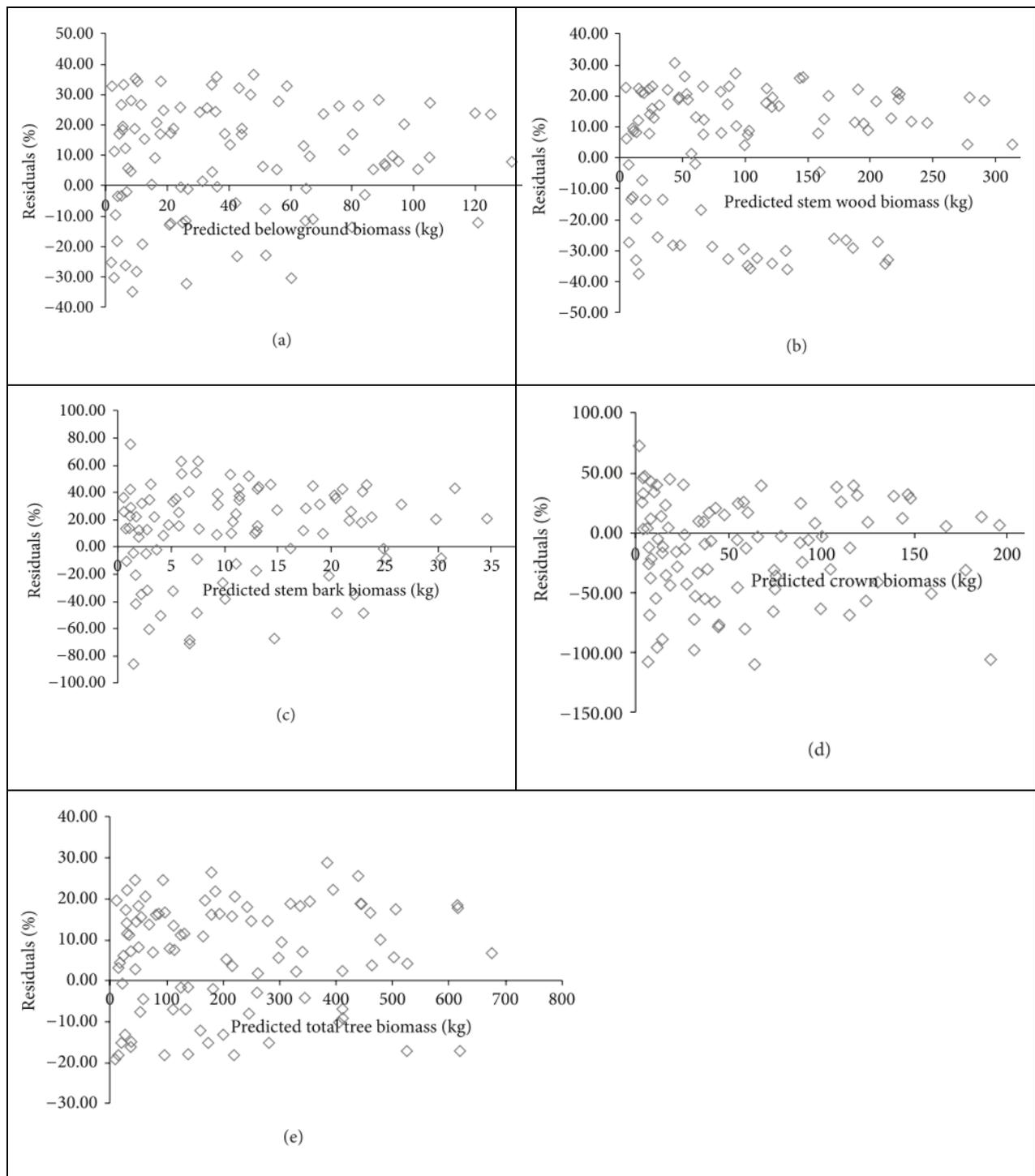
Figure 8. Residuals against predicted biomass for the NSUR method: **a)** belowground, **b)** stem wood, **c)** stem bark, **d)** crown, and **e)** total tree biomass.

44

Comparing the different methods based on the relative standard errors of the expected and predicted values for total tree biomass, computed from 11 randomly selected trees from different diameter classes (Table 10), it was found that the conventional method had the smallest average standard errors of the expected and predicted total tree biomass values (2.02% and 2.20%, respectively), followed by the NSUR method (3.52% and 3.68%, respectively), and lastly the SUR method (7.72% and 7.75%, respectively). These data indicated that the CON method yielded narrower confidence and prediction intervals than the NSUR and SUR methods.

Table 10. Relative standard errors (%) of the expected and predicted total tree biomass values for 11 randomly selected trees

D (cm)	H (m)	CH (m)	LCL (m)	CON $S(E(y_0))\%$	CON $S(y_{0i} - \hat{y})\%$	SUR $S(E(y_0))\%$	SUR $S(y_{0i} - \hat{y})\%$	NSUR $S(E(y_0))\%$	NSUR $S(y_{0i} - \hat{y})\%$
5.00	7.60	6.50	1.10	9.8935	10.7478	57.0913	57.3862	7.7570	9.4475
8.00	9.16	2.12	7.04	2.4664	2.8828	7.7433	7.7598	5.7686	5.8364
10.00	9.59	1.55	8.04	0.9218	1.3087	4.1622	4.1682	4.9674	4.9854
12.50	13.40	5.80	7.60	0.4477	0.6223	2.8034	2.8049	3.3916	3.3943
15.00	13.12	2.23	10.89	0.7874	0.8454	2.0203	2.0209	3.1360	3.1370
17.50	13.95	8.07	5.88	1.0461	1.0676	1.8206	1.8209	2.4721	2.4726
20.00	13.85	4.60	9.25	1.1791	1.1906	1.7894	1.7895	2.1321	2.1324
22.50	13.04	6.00	7.04	1.2514	1.2590	1.7775	1.7775	2.0573	2.0575
25.00	14.53	4.50	10.03	1.3547	1.3584	1.8523	1.8523	2.0828	2.0828
27.50	13.46	2.89	10.57	1.3843	1.3873	1.9000	1.9000	2.2690	2.2690
30.50	15.05	2.16	12.89	1.4515	1.4529	1.9571	1.9571	2.6660	2.6660
Average				2.0167	2.1930	7.7198	7.7489	3.5182	3.6801

D = DBH; H = tree height; CH = crown height; LCL = live crown length; $S(E(y_0))\%$ = relative standard error of the expected value; $S(y_{0i} - \hat{y})\%$ = relative standard error of the predicted value.

Figure 9 shows that the SUR method described the data quite poorly, whereas the CON and NSUR methods described the data satisfactorily, even for the total tree model, for which the SUR method had the higher adjusted R^2 value than the NSUR method. The predicted regression lines in the Figure 9 were obtained from 11 randomly selected trees from different diameter classes (2 trees per diameter class, except the last where only 1 tree was selected due to fewer representative trees); therefore the lines are function of changing all variables (refer to Table 10), hence exhibiting waves, since other variables (H, CH, LCL) did not necessarily increase as DBH increased.
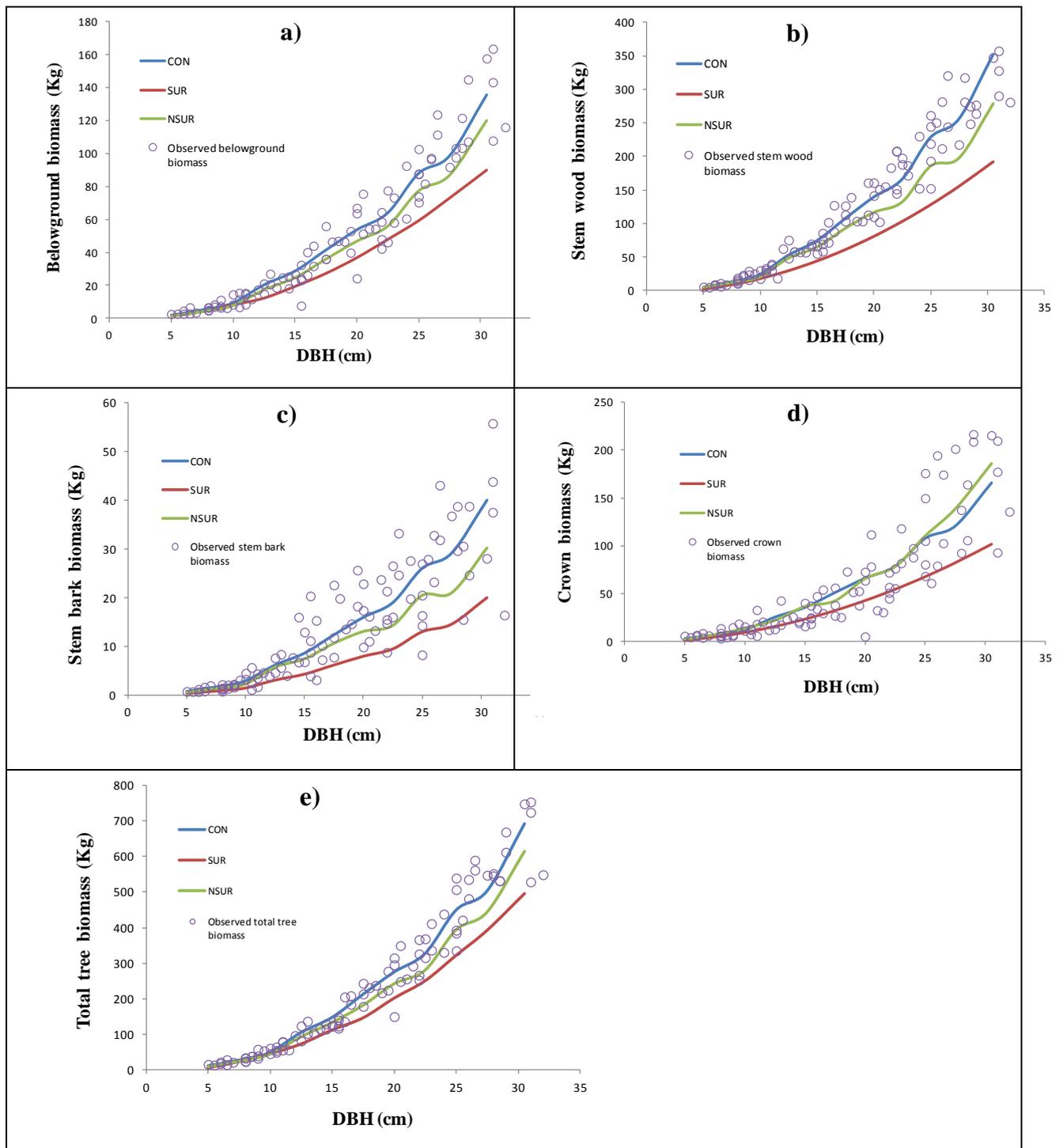
Figure 9. Observed biomass vs. DBH values and regression lines obtained from the different methods of achieving additivity for **a)** belowground, **b)** stem wood, **c)** stem bark, **d)** crown, and **e)** total tree biomass.

3.3 Estimation of biomass, carbon stocks and error propagation (Article II)

3.3.1 Biomass and carbon stocks

Biomass stock (from Eq.14) and the corresponding carbon stock (Mg ha^{-1}), are presented in Tables 11 and 12, respectively. The whole tree and aboveground biomass stocks were 167 and 134 Mg ha^{-1}, respectively.

46

Stem wood formed the largest share of biomass for all diameter classes, followed by the crown. The proportional distribution of biomass at the forest scale was as follows: stem wood, 51%; crown, 24%; belowground biomass, 19%; and stem bark, 6%.

Table 11. Biomass stock (Mg ha^{-1}) for each tree component and diameter class

Tree component	Diameter class (cm)					
	[5–10[	[10–15[	[15–20[	[20–25[	[25–30+]	Total
Belowground	1.88	5.85	9.27	7.93	4.20	32.60
Stem wood	4.89	15.22	24.12	20.64	10.93	84.79
Stem bark	0.60	1.77	2.77	2.36	1.25	9.77
Crown	2.30	7.16	11.35	9.71	5.14	39.90
Whole tree	9.67	29.99	47.51	40.64	21.52	167.05
Harvested trees	18.00	18.00	18.00	17.00	22.00	93.00

Table 12. Carbon stock (Mg ha^{-1}) for each tree component and diameter class

| Tree component	Diameter class (cm)					
	[5–10[	[10–15[	[15–20[	[20–25[	[25–30+]	Total
Belowground	1.00	3.11	4.93	4.22	2.23	17.32
Stem wood	2.40	7.46	11.83	10.12	5.36	41.58
Stem bark	0.27	0.80	1.25	1.06	0.56	4.41
Crown	1.12	3.48	5.52	4.73	2.50	19.42
Whole tree	4.79	14.85	23.53	20.13	10.66	82.73
Harvested trees	18.00	18.00	18.00	17.00	22.00	93.00

The 15–20 and 20–25 cm diameter classes represented >50% of the total forest biomass stock (Figure 10) and of the total basal area (Figure 11); however, only ~30% of all trees were in these size classes (Figure 5).
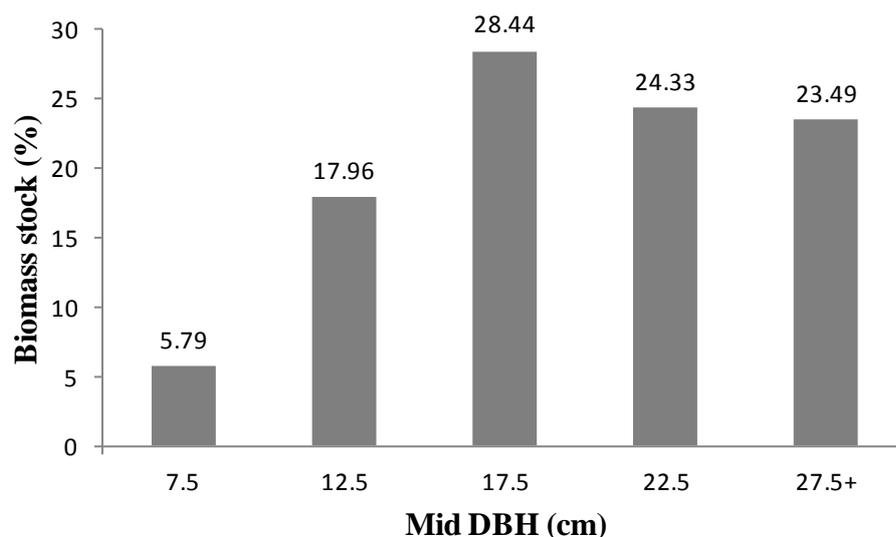
Figure 10. Proportion of total biomass stock (obtained using phase-1 data) for each diameter class in Mecrusse woodlands of the study area

47
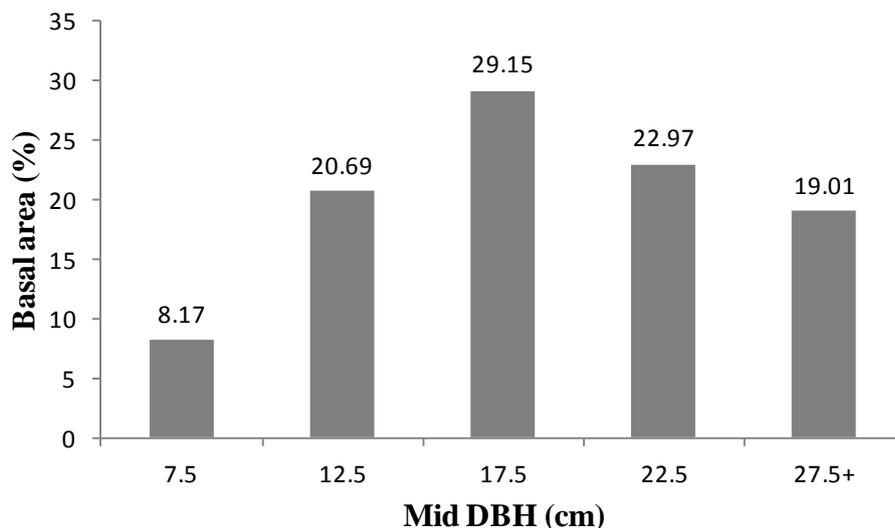
Figure 11. Percent basal area distribution for each diameter class in Mecrusse woodlands in the study area

Note that the DBH of *A. johnsonii* rarely exceeds 35 cm (here, <1% of trees during the first sampling phase); therefore, trees encountered in diameter classes larger than the highest class in Figure 5 ($25 \leq DBH < 30$) were considered as belonging to this diameter class.

3.3.2 Error Propagation

Low variance in the estimates of biomass stock indicated that there was a high level of precision in the estimates (Table 13). The largest error was observed for stem bark and crown; the goodness of fit for these components was poorer in the models (smaller R^2 and higher CV of the residuals; Table 7), which explained the higher error. For the crown, the error in the allometric equations (second sampling phase) was equal to the error of plot-level variability (differences in the number of trees per plot in the first sampling phase). In contrast, more of the variance for belowground, stem wood, stem bark, and total biomass was attributable to plot-level variability than to the allometric equations (Table 14).

Table 13. Variance ($Mg^2 \ ha^{-2}$), absolute standard error ($Mg \ ha^{-1}$), and percent standard errors of the estimates of biomass stock for each tree component and sampling phase

Tree component	VAR_1	VAR_2	VAR_t	SE_1	SE_2	SE_t	SE_1 (%)	SE_2 (%)	SE_t (%)
Belowground	2.20	0.54	2.74	1.48	0.74	1.66	4.55	2.26	5.08
Stem wood	14.89	1.77	16.66	3.86	1.33	4.08	4.55	1.57	4.81
Stem bark	0.19	0.17	0.36	0.44	0.41	0.60	4.50	4.17	6.13
Crown	3.30	3.30	6.60	1.82	1.82	2.57	4.55	4.55	6.44
Whole tree	57.74	6.52	64.26	7.60	2.55	8.02	4.55	1.53	4.80

Subscripts 1 and 2 indicate the first and second sampling phases, respectively; subscript t indicates the total variance or standard error for a given component.

48

Table 14. Percentage of total error (as variance) attributed to each sampling phase

Tree component	Percentage of total variance attributed to the first phase	Percentage of total variance attributed to the second phase
Belowground	80	20
Stem wood	89	11
Stem bark	54	46
Crown	50	50
Total tree	90	10

Actual whole tree biomass stock (from 95% CI) was between 151 and 183 Mg ha^{-1} (Table 15). Carbon stock (Mg ha^{-1}) varied from approximately 75–91 Mg ha^{-1} (Table 16). DBH measurement error contributed close to two-thirds of the error from the first sampling phase, while the tree height measurement error contributed more than one third. Plot-level variability contributes negligibly to the uncertainty (Table 17).

Table 15. Biomass stocks and 95% confidence limits

Tree component	Biomass stock (Mg ha^{-1})	95% Confidence limit (Mg ha^{-1})	95% Confidence limit (%)
Belowground	32.60	± 3.31	± 10.16
Stem wood	84.79	± 8.16	± 9.63
Stem bark	9.77	± 1.20	± 12.26
Crown	39.90	± 5.14	± 12.88
Total tree	167.05	± 16.03	± 9.60

Table 16. Carbon stocks and 95% confidence limits

Tree component	Carbon stock (Mg ha^{-1})	95% Confidence limit (Mg ha^{-1})	95% Confidence limit (%)
Belowground	17.32	± 1.76	± 10.16
Stem wood	41.58	± 4.00	± 9.63
Stem bark	4.41	± 0.54	± 12.26
Crown	19.42	± 2.50	± 12.88
Total tree	82.73	± 7.94	± 9.60

Table 17. Percent contribution of the error of each variable to the error of the first sampling phase

Source of error	Percent contribution to the error
DBH measurement	62.1
Total tree height estimation	37.88
Plot variability	0.02

In the second sampling phase (using allometric equations), fresh-weight measurement error accounted for >90% of the total error in biomass calculations. The majority of the error in stem bark and stem wood calculations arose from the errors of basic density estimation and DBH measurements, respectively, while DBH measurement error accounted for most of the error in whole tree biomass calculations (Table 18).

49

Note that the stem wood basic density estimation is not included as a source of error for the whole tree. The whole tree biomass is obtained by summing Eqs.23, 25, 26, and 28; as for the errors. However, by summing Eqs.25 and 26 the result is $DBH^2 \times H \times \rho_s$, which excludes stem wood basic density (ρ_{sw}). In fact, the stem biomass ($DBH^2 \times H \times \rho_s$) includes both stem wood (Eq.25) and stem bark biomass (Eq.26); as for stem density (ρ_s).

Table 18. Percent contribution of the error of each variable to the error of the second sampling phase

Tree component	Source of error	Contribution to the total error (%)
Belowground	Measurement of the fresh weight of the lateral roots	41.40
	Measurement of the fresh weight of the taproot	56.02
	Determination of MC of the lateral roots	0.99
	Determination of MC of the taproot	1.58
Stem wood	DBH measurement	66.27
	Total height measurement	20.04
	Stem wood density estimation	13.70
Stem bark	DBH measurement	12.92
	Total height measurement	3.91
	Stem density estimation	40.58
	Stem wood density estimation	42.59
Crown	Measurement of the fresh weight of the branches	81.87
	Measurement of the fresh weight of the foliage	10.46
	Determination of MC of the branches	5.10
	Determination of MC of the foliage	2.57
Whole tree	Measurement of the fresh weight of the lateral roots	8.3E-04
	Measurement of the fresh weight of the taproot	1.1E-03
	Determination of MC of lateral roots	2.0E-05
	Determination of MC of taproot	3.2E-05
	DBH measurement	66.11
	Total height measurement	19.99
	Stem density estimation	13.89
	Measurement of the fresh weight of the branches	1.8E-03
	Measurement of the fresh weight of the foliage	2.3E-04
	Determination of MC of branches	1.1E-04
	Determination of MC of foliage	5.6E-05

3.4 Biomass expansion factors and root-to-shoot-ratio: measurement uncertainties (Article III)

3.4.1 Biomass expansion factors

The total tree and aboveground BEFs were approximately 131% and 105% of the stem volume, respectively (Table 19). For the major components, the stem had the highest BEF contribution. Its value was more than

two-fold higher than the BEF of crowns and roots. The standard error of all estimates was <11%; stem estimates were the most precise, and foliage estimates had the largest error (Table 19).

Table 19. Component biomass expansion factors (BEF_c), their variances (VAR_{BEF}), standard errors (SE), and 95% confidence intervals (CI) for *Androstachys johnsonii* trees

#	Tree component	BEF_c (Mg m^{-3})	VAR_{BEF} (Mg^2 m^{-6})	SE (Mg m^{-3})	SE (%)	95% CI (Mg m^{-3})	95% CI (%)
1	Taproot + stump	0.1407	3.6E-05	0.0060	4.2382	± 0.0119	± 8.4764
2	Lateral roots	0.1162	4.4E-05	0.0067	5.7232	± 0.0133	± 11.4465
3	**Root system (1 + 2)**	**0.2569**	**1.0E-04**	**0.0100**	**3.8930**	**± 0.0200**	**± 7.7860**
4	Stem wood	0.6569	3.6E-04	0.0191	2.9046	± 0.0382	± 5.8092
5	Stem bark	0.0765	1.3E-05	0.0036	4.7534	± 0.0073	± 9.5068
6	**Stem (4 + 5)**	**0.7334**	**4.4E-04**	**0.0210**	**2.8615**	**± 0.0420**	**± 5.7230**
7	Branches	0.2928	3.1E-04	0.0177	6.0590	± 0.0355	± 12.1180
8	Foliage	0.0242	6.6E-06	0.0026	10.6242	± 0.0051	± 21.2483
9	**Crown (7 + 8)**	**0.3170**	**3.6E-04**	**0.0190**	**5.9973**	**± 0.0380**	**± 11.9946**
10	**Shoot system (6 + 9)**	**1.0504**	**1.2E-03**	**0.0340**	**3.2345**	**± 0.0679**	**± 6.4690**
11	**Total tree (3 + 10)**	**1.3072**	**1.8E-03**	**0.0428**	**3.2736**	**± 0.0856**	**± 6.5472**

The major components and their values are indicated in bold font. SE = standard error; CI = confidence limit.

Using linear regression, Pearson´s correlation coefficient test of significance, and distance covariance (dcov) test of independence, the BEF of taproots, lateral roots, and foliage was found to be DBH-dependent (Tables 20 and 21). They showed a weak but significant dependence. Other seven component BEFs and total tree BEF were not found to have any kind of dependence on DBH (neither linear nor nonlinear). The strongest DBH-dependence was found for foliage BEF (adjusted $R^2 = 0.2900$, r = − 0.5329, dcor = 0.5874). Seven component BEFs were linearly tree height-dependent (Table 22); however, using dcov test of independence, only 5 component BEFs were tree height-dependent; i.e. the linear dependence of crown and shoot system BEFs on tree height was not detected by dcov test of independence (Table 23). The BEF of foliage was the most strongly dependent on both DBH and tree-height. Component BEF values decreased with increasing tree-height and DBH (except for the relationship between lateral roots and DBH).

Table 20. Linear regression test for dependence of biomass expansion factors (BEF) on diameter at breast height (DBH) in *A. johnsonii*

#	Tree component	BEF=b_0+b_1DBH			
		b_0 ($\pm$ SE)	b_1 ($\pm$ SE)	Probability	Adjusted R^2
1	Taproot + stump	0.1890 ($\pm$ 0.0115)	$-$ 0.0027 ($\pm$ 0.0006)	0.0000	0.1768
2	Lateral roots	0.0789 ($\pm$ 0.0125)	0.0021 ($\pm$ 0.0007)	0.0017	0.0933
3	**Root system (1 + 2)**	**0.2679 ($\pm$ 0.0175)**	$-$ **0.0006 ($\pm$ 0.0009)**	**0.4963**	$-$ **0.0058**
4	Stem wood	0.6482 ($\pm$ 0.0176)	0.0005 ($\pm$ 0.0009)	0.5911	$-$ 0.0078
5	Stem bark	0.0798 ($\pm$ 0.0075)	$-$ 0.0002 ($\pm$ 0.0004)	0.6314	$-$ 0.0084
6	**Stem (4 + 5)**	**0.7280 ($\pm$ 0.0179)**	**0.0003 ($\pm$ 0.0009)**	**0.7435**	$-$ **0.0098**
7	Branches	0.2821 ($\pm$ 0.0376)	0.0006 ($\pm$ 0.0020)	0.7583	$-$ 0.0099
8	Foliage	0.0557 ($\pm$ 0.0055)	$-$ 0.0018 ($\pm$ 0.0003)	0.0000	0.2870
9	**Crown (7 + 8)**	**0.3378 ($\pm$ 0.0411)**	$-$ **0.0012 ($\pm$ 0.0021)**	**0.5838**	$-$ **0.0076**
10	**Shoot system (6 + 9)**	**1.0658 ($\pm$ 0.0445)**	$-$ **0.0009 ($\pm$ 0.0023)**	**0.7080**	$-$ **0.0094**
11	**Total tree (3 + 10)**	**1.3336 ($\pm$ 0.0574)**	$-$ **0.0015 ($\pm$ 0.0030)**	**0.6192**	$-$ **0.0082**

The major components and their values are indicated in bold font. b_0 and b_1 are regression parameters; SE = standard error; probability refers to the significance of the regression.

Table 21. Pearson´s correlation coefficient test of significance, and distance covariance test of independence of biomass expansion factors (BEF) on diameter at breast height (DBH) in *A. johnsonii*

#	Tree component	BEF vs. DBH				
		Pearson´s correlation test		Distance covariance test of independence		
		r	Probability	dcov	dcor	Probability
1	Taproot + stump	$-$ 0.4310	1.6E-05	0.1802	0.4668	0.0150
2	Lateral roots	0.3211	0.0017	0.1670	0.4377	0.0150
3	**Root system (1 + 2)**	$-$ **0.0714**	**0.4963**	**0.1154**	**0.2546**	**0.0700**
4	Stem wood	0.0564	0.5911	0.0671	0.1430	0.7650
5	Stem bark	$-$ 0.0504	0.6314	0.0442	0.1468	0.5200
6	**Stem (4 + 5)**	**0.0344**	**0.7435**	**0.0677**	**0.1428**	**0.7450**
7	Branches	0.0323	0.7583	0.1567	0.2190	0.2950
8	Foliage	$-$ 0.5429	1.9E-08	0.1521	0.5874	0.0150
9	**Crown (7 + 8)**	$-$ **0.0575**	**0.5838**	**0.1684**	**0.2274**	**0.2450**
10	**Shoot system (6 + 9)**	$-$ **0.0394**	**0.7080**	**0.1738**	**0.2260**	**0.3300**
11	**Total tree (3 + 10)**	$-$ **0.0522**	**0.6192**	**0.2132**	**0.2432**	**0.2750**

The major components and their values are indicated in bold font. r = Perason´s correlation coefficient; dcov = distance covariance; dcor = distance correlation; probability refers to the significance of the test.

Table 22. Linear regression test for dependence of biomass expansion factors (BEF) on total tree-height (H) in *Androstachys johnsonii*

#	Tree component	b_0 (± SE)	b_1 (± SE)	Probability	Adjusted R^2
			BEF=b_0+b_1H		
1	Taproot + stump	0.2884 (± 0.0248)	− 0.0120 (± 0.0020)	0.0000	0.2787
2	Lateral roots	0.1178 (± 0.0304)	− 0.0001 (± 0.0024)	0.9585	− 0.0110
3	**Root system (1 + 2)**	**0.4061 (± 0.0371)**	**− 0.0121 (± 0.0030)**	**0.0001**	**0.1456**
4	Stem wood	0.6697 (± 0.0404)	− 0.0010 (± 0.0032)	0.7486	− 0.0098
5	Stem bark	0.1018 (± 0.0170)	− 0.0021 (± 0.0014)	0.1345	0.0137
6	**Stem (4 + 5)**	**0.7715 (± 0.0409)**	**− 0.0031 (± 0.0033)**	**0.3461**	**− 0.0011**
7	Branches	0.4745 (± 0.0844)	− 0.0147 (± 0.0068)	0.0314	0.0394
8	Foliage	0.1142 (± 0.0118)	− 0.0073 (± 0.0009)	0.0000	0.3911
9	**Crown (7 + 8)**	**0.5887 (± 0.0900)**	**− 0.0221 (± 0.0072)**	**0.0029**	**0.0835**
10	**Shoot system (6 + 9)**	**1.3603 (± 0.0969)**	**− 0.0251 (± 0.0077)**	**0.0016**	**0.0939**
11	**Total tree (3 + 10)**	**1.7664 (± 0.1230)**	**− 0.0373 (± 0.0098)**	**0.0003**	**0.1267**

The major components and their values are indicated in bold font. b_0 and b_1, regression parameters; SE, standard error; probability refers to the significance of the regression.

Table 23. Pearson´s correlation coefficient test of significance and distance covariance test of independence of biomass expansion factors (BEF) on total tree-height (H) in *A. johnsonii*

#	Tree component	r	Probability	dcov	dcor	Probability
		Pearson´s correlation test		Distance covariance test of independence		
1	Taproot + stump	− 0.5353	3.2E-08	0.1106	0.5672	0.0150
2	Lateral roots	− 0.0055	0.9585	0.0516	0.2679	0.1550
3	**Root system (1 + 2)**	**− 0.3936**	**9.5E-05**	**0.0918**	**0.4009**	**0.0150**
4	Stem wood	− 0.0337	0.7486	0.0370	0.1562	0.6350
5	Stem bark	− 0.1564	0.1345	0.0249	0.1636	0.5250
6	**Stem (4 + 5)**	**− 0.0988**	**0.3461**	**0.0439**	**0.1833**	**0.3750**
7	Branches	− 0.2233	0.0314	0.0844	0.2334	0.2400
8	Foliage	− 0.6306	1.2E-11	0.0835	0.6386	0.0150
9	**Crown (7 + 8)**	**− 0.3057**	**0.0029**	**0.1089**	**0.2910**	**0.0600**
10	**Shoot system (6 + 9)**	**− 0.3220**	**0.0016**	**0.1131**	**0.2911**	**0.1300**
11	**Total tree (3 + 10)**	**− 0.3691**	**0.0003**	**0.1495**	**0.3376**	**0.0400**

The major components and their values are indicated in bold font. r = Pearson´s correlation coefficient; dcov = distance covariance; dcor = distance correlation; probability refers to the significance of the test.

3.4.2 Biomass stock

Total tree biomass was approximately 25% higher than AGB (Table 24). The root system, stem, and crown observed biomass stocks of 29.62, 84.57, and 36.55 Mg ha^{-1}, respectively. Stem biomass stock accounted for approximately 70% of AGB and 56% of the total tree biomass stock. As expected, the estimates of biomass stocks are as precise as the estimates of BEFs.

Table 24. Biomass stock ($\hat{Y}_c$), variance ($VAR_{\hat{Y}_c}$), standard error (SE), and 95% confidence intervals (CI) for each component in *Androstachys johnsonii* trees

#	Tree component	$\hat{Y}_c$ (Mg ha^{-1})	$VAR_{\hat{Y}_c}$ (Mg^2 ha^{-2})	SE (Mg ha^{-1})	SE (%)	95% CI (Mg ha^{-1})	95% CI (%)
1	Taproot + stump	16.2192	0.4725	0.6874	4.2382	± 1.3748	± 8.4764
2	Lateral roots	13.4005	0.5882	0.7669	5.7232	± 1.5339	± 11.4465
3	**Root sytem (1 + 2)**	**29.6197**	**1.3296**	**1.1531**	**3.8930**	**± 2.3062**	**± 7.7860**
4	Stem wood	75.7526	4.8413	2.2003	2.9046	± 4.4006	± 5.8092
5	Stem bark	8.8182	0.1757	0.4192	4.7534	± 0.8383	± 9.5068
6	**Stem (4 + 5)**	**84.5708**	**5.8565**	**2.4200**	**2.8615**	**± 4.8400**	**± 5.7230**
7	Branches	33.7612	4.1845	2.0456	6.0590	± 4.0912	± 12.1180
8	Foliage	2.7923	0.0880	0.2967	10.6242	± 0.5933	± 21.2483
9	**Crown (7 + 8)**	**36.5535**	**4.8058**	**2.1922**	**5.9973**	**± 4.3844**	**± 11.9946**
10	**Shoot system (6 + 9)**	**121.1243**	**15.3491**	**3.9178**	**3.2345**	**± 7.8356**	**± 6.4690**
11	**Total tree (3 + 10)**	**150.7440**	**24.3521**	**4.9348**	**3.2736**	**± 9.8696**	**± 6.5472**

3.4.3 Root-to-shoot ratio

The average root-to-shoot biomass ratio was 0.24 (minimum = 0.07, maximum = 0.35, SD = 0.04, CV = 16.8%). The uncertainty (SE) of the estimated R/S was 3.4% (CI = 6.78%). The root-to-shoot ratio was neither linear nor nonlinearly dependent on any of the four tested variables (DBH, tree height, AGB, and BGB) (Tables 25 and 26). The BGB density calculated based on R/S was 29.26 Mg ha^{-1} (SE = 3.4%), which was 1.20% smaller and 13.73% more precise than the BGB density estimate based on BEF.

Table 25. Linear regression test of dependence of root-to-shoot ratio on diameter at breast height (DBH), total tree-height (H), aboveground biomass (AGB), belowground biomass (BGB), and total biomass (TB) in *Androstachys johnsonii* trees

#	Regression equation	b_0 (± SE)	b_1 (± SE)	Probability	Adjusted R^2
1	R/S = b_0 + b_1DBH	0.24051 (± 0.01080)	0.00006 (± 0.00057)	0.9154	− 0.0109
2	R/S = b_0 + b_1H	0.27807 (± 0.02454)	− 0.00296 (± 0.00196)	0.1347	0.0137
3	R/S = b_0 + b_1AGB	0.27015 (± 0.00662)	0.00001 (± 0.00003)	0.7812	− 0.0101
4	R/S = b_0 + b_1BGB	0.23354 (± 0.00634)	0.00017 (± 0.00010)	0.0997	0.0188
5	R/S = b_0 + b_1TB	0.23876 (± 0.00659)	0.00001 (± 0.00002)	0.5802	− 0.0076

b_0 and b_1 are regression parameters; SE = standard error; probability refers to the significance of the regression.

Table 26. Pearson´s correlation coefficient test of significance and distance covariance test of independence of root-to-shoot ratio on diameter at breast height (DBH), total tree-height (H), aboveground biomass (AGB), belowground biomass (BGB), and total biomass (TB) in *Androstachys johnsonii* trees

# Pair of variables	Pearson´s correlation test		Distance covariance test of independence		
	r	Probability	dcov	dcor	Probability
1 R/S vs. DBH	0.0112	0.9154	0.0554	0.1573	0.8650
2 R/S vs. H	− 0.1563	0.1347	0.0473	0.2662	0.0650
3 R/S vs. AGB	0.0292	0.7812	0.2475	0.1518	0.8200
4 R/S vs. BGB	0.1718	0.0997	0.1575	0.1951	0.2900
5 R/S vs. TB	0.0581	0.5802	0.2763	0.1519	0.8100

r = Perason´s correlation coefficient; dcov = distance covariance; dcor = distance correlation; probability refers to the significance of the test.

3.5 Below- and aboveground architecture: topological analysis of the root / shoot systems (Article IV)

3.5.1 Topology

The branching topology of the root and shoot systems of *A. johnsonii* can be considered as perfectly to nearly herringbone, respectively, i.e. the stem or taproot is the main axis (Kalliokoski 2011) and the longest and thickest branch (Richardson and zu Dohna 2003; Figure 12) as opposed to dichotomous branching topology where the parent branch divides into two daughter branches of the same size (Richardson and zu Dohna 2003), i.e. branching occurs with equal probability on all links (Kalliokoski 2011). However, while the shoot system occasionally violated the definition of herringbone branching by having branching laterals, the root system conformed to the definition by Riccardo (2007) and Kalliokoski (2011) since it mostly had non-branching laterals.
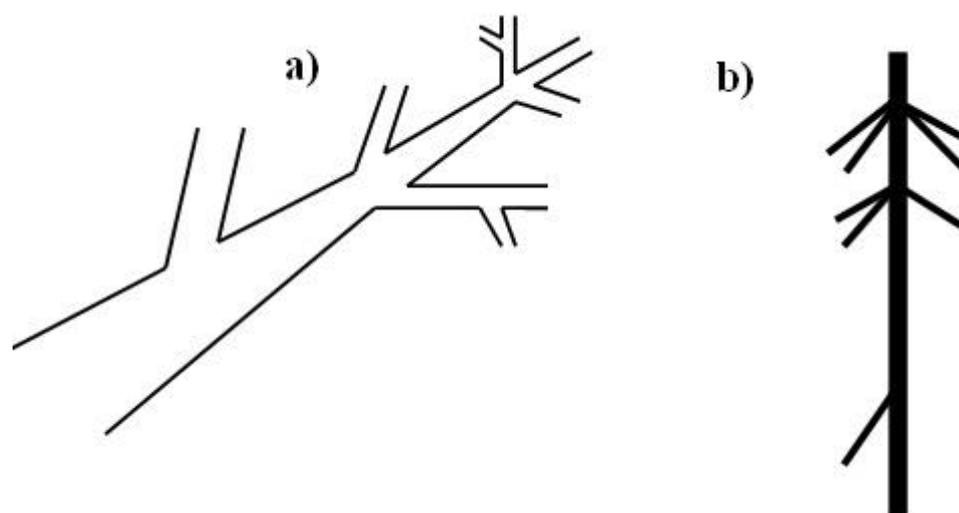
Figure 12. Topological representation of the **(a)** shoot system and **(b)** root system. All the laterals of the root system emerge from the main axis (taproot); however, in the shoot system, branching of some primary laterals is noted

55

The shoot system consisted mostly of 7 nodes with an average of 2 laterals per node, a minimum of 1 and maximum of 4. The root system, on the other hand, consisted mostly of 4 nodes with 75% of the laterals located in the first and second nodes. The average number of laterals per node in the root system was 4 and 3 for the first and second nodes, respectively, and 2 per remaining nodes; the minimum and maximum numbers of laterals per node were 1 and 11, respectively. Table 27 provides details on the number of nodes and laterals per node for the root and shoot systems.

Table 27. Summary description of the number of nodes and laterals in the sampled trees

		First node	Second node	Third node	Fourth node	Fifth node	Sixth node	Seventh node	Total
Shoot system	Number of nodes in the sampled trees	86.00	80.00	69.00	44.00	23.00	6.00	1.00	309.00
	Number of branches after bifurcation	175.00	168.00	158.00	110.00	57.00	20.00	3.00	691.00
	Average number of branches per node per tree	2.03	2.10	2.29	2.50	2.48	3.33	3.00	17.74
	Number of lateral branches after bifurcation (excluding the stem)	172.00	160.00	141.00	93.00	48.00	17.00	2.00	633.00
	Average number of lateral branches per node per tree (excluding the stem)	2.00	2.00	2.04	2.11	2.09	2.83	2.00	15.08
Root system	Number of nodes in the sampled trees	73.00	40.00	19.00	1.00				133.00
	Number of lateral roots after bifurcation	386.00	160.00	43.00	3.00				592.00
	Average number of lateral roots after bifurcation per node per tree	5.29	4.00	2.26	3.00				14.55
	Number of lateral roots after bifurcation (excluding the taproot)	327.00	134.00	39.00	2.00				502.00
	Average number of lateral roots after bifurcation per node per tree (excluding the taproot)	4.48	3.35	2.05	2.00				11.88

In all, 81% of the stem nodes had only 1 lateral; 15%, had 2 and 3; and 1%, had 3 and 4 laterals. Further, 32% of the taproot nodes had only 1 lateral, and 17, 13, and 6% had 2, 3, and 4 laterals, respectively; in 32% of the nodes, the number of laterals varied from 5 to 11. In the shoot system, the laterals per node increased with height; on the other hand, in the root system, the laterals decreased with depth. The diameters of the laterals at the insertion point decreased with height (aboveground) and depth (belowground).

In the shoot system, the average link length per tree varied from 115 to 719 cm, with an overall weighted average of 193 cm; on the other hand, in the root system, it varied from 35 to 235 cm, with an overall weighted average of 90 cm. The average link diameter in the shoot system was 9.73 cm, varying from a minimum of 2.5 to a maximum of 32 cm; in the root system, the average link diameter was 12.59 cm, ranging from 3.5 to 47 cm. The biomass allocated in each tree component is given in the Table 28; where it can be seen that higher-order roots account, on average, with 2.922% (0.704 kg) of the biomass of all lateral roots (24.083 kg); and higher-order branches account with 5.631% (3.130 kg) of the biomass of all branches (55.586 kg).

Table 28. Summary basic statistics of the biomass per tree (kg) allocated in different tree components

#	Tree component	Minimum (kg)	Mean (kg)	Maximum (kg)	SD (kg)	CV (%)
1	Taproot	1.474	23.651	71.926	18.926	80.019
2	Primary lateral roots	0.000	23.379	95.737	22.551	112.085
3	Higher-order lateral roots	0.000	0.704	5.600	2.267	57.200
4	**Lateral roots (2 + 3)**	**0.746**	**24.083**	**100.815**	**23.945**	**99.428**
5	**Root system (1 + 4)**	**2.545**	**47.735**	**162.105**	**41.210**	**86.331**
6	Stem	5.636	138.267	413.153	110.577	79.974
7	Primary branches	2.310	52.456	209.586	57.492	109.600
8	Higher-order branches	0.000	3.130	12.858	1.954	62.437
9	**Branches (7 + 8)**	**2.583**	**55.586**	**211.320**	**57.355**	**103.183**
10	**Shoot system (6 + 9)**	**9.823**	**196.659**	**590.863**	**163.713**	**83.247**

SD is the standard deviation and CV is the coefficient of variation. The major components and their values are indicated in bold font.

The lower amount of biomass allocated in heigher-order axes (roots and branches) support the visual analysis results that the branching topology of the root and shoot systems is herringbone; with the root system showing a tendency to a perfect herringbone branching, judging by the amout of biomass allocated in heigher-order roots when compared to the shoot system.

The altitude of the shoot system varied from 2 to 8, with an average of 4.6, and the magnitude varied from 2 to 13, with an average of 5.40. The TI for the shoot system was 0.70, consequentelly the hypotheses of being equal to 1 ($P < 0.0001$) or 0.53 ($P < 0.0001$) were rejected. The altitude of the root system varied from 3 to 5, with an average of 2.82, and the magnitude varied from 2 to 15, with an average of 7.29. The TI for the root system was 0.30, and the hypotheses of being equal to 1 ($P < 0.0001$) or 0.53 ($P = 0.0002$) were rejected.

The external path length (Pe) of the shoot system varied from 4 to 68, with an average of 21.40; the average TT value was 0.90; however, the hypotheses of being equal to 1 ($P < 0.0001$) or 0 ($P < 0.0001$) were rejected. Pe for the root system varied from 4 to 46, with an average of 17.80; the average TT was 0.37, and the hypotheses of being equal to 1 ($P < 0.0001$) or 0 ($P < 0.0001$) were rejected.

3.5.2 Branching parameters (p and q)

The average p values per node for the shoot system varied from 0.99 to 1.05, with an overall average of 1.03 (Table 29); none of the values were statistically different from 1 ($P \geq 0.05$). For the root system, the average p values per node varied from 1.02 to 2.65, with an overall average of 1.41, and only the average p value of the first node was not found to be statistically different from 1 ($P = 0.7185$). Therefore, the p values suggested that the area-preserving branching was confirmed for all stem nodes, thereby ensuring the self-similar branching pattern. For the root system, the area-preserving branching was only confirmed for the first node; for the second and third nodes, the CSA was found to decrease with branching, since the average p values were larger than 1.

Table 29. Summary of the basic statistics for the branching parameter *p*

| | Shoot system | | | | | | | Root system | | | |
	p1	*p2*	*p3*	*p4*	*p5*	*p6*	*p* for all nodes	*p1*	*p2*	*p3*	*p* for all nodes
Minimum	0.5025	0.6923	0.2549	0.4612	0.5104	0.5900	0.2549	0.4073	1.0544	0.7987	0.3352
Mean	0.9968	1.0541	1.0518	1.0245	1.0334	0.9925	1.0306	1.0169	2.6541	1.3887	1.4182
Maximum	1.5444	2.2669	1.7622	2.3607	2.3059	2.1202	2.3607	2.8412	7.4903	2.2368	7.4903
SD	0.1749	0.2481	0.3021	0.4621	0.3666	0.5786	0.3100	0.3994	1.6807	0.3448	1.2750
CV%	17.5461	23.5386	28.7237	37.1072	35.4722	58.2980	29.1482	39.2799	63.3242	24.8304	89.9028
Probability	0.8659	0.0546	0.1587	0.1035	0.6668	0.9759	0.0584	0.7185	0.0000	0.0001	0.0003

pi is the *p* statistic for the *ith* node

The average *q* values per node for the shoot system ranged from 0.46 to 0.60, with an overall average of 0.56; however, these values were not statistically different from 0.5 only for the last three nodes (Table 30). For the root system, where the average *q* values per node ranged from 0.45 to 0.53 with an overall average of 0.46, only the second and third nodes had average *q* values not different from 0.5.

Table 30. Summary of the basic statistics for the branching parameter *q*

| | Shoot system | | | | | | | Root system | | | |
	q1	*q2*	*q3*	*q4*	*q5*	*q6*	*q for all nodes*	*q1*	*q2*	*q3*	*q for all nodes*
Minimum	0.3846	0.4773	0.2941	0.2667	0.2759	0.2375	0.2375	0.1714	0.2000	0.4091	0.1714
Mean	0.6096	0.5902	0.5473	0.5062	0.5058	0.4554	0.5645	0.4483	0.4518	0.5334	0.4607
Maximum	0.8367	0.8158	0.7647	0.8387	0.7083	0.6000	0.8387	0.8478	0.6970	0.6316	0.8478
SD	0.0926	0.0781	0.1097	0.1297	0.1131	0.1455	0.1099	0.1870	0.1508	0.0735	0.1659
CV%	15.1835	13.2265	20.0488	25.6324	22.3619	31.9532	19.4659	41.7199	33.3873	13.7893	36.0118
Probability	0.0000	0.0000	0.0006	0.7538	0.8077	0.4867	0.0000	0.0208	0.0500	0.0634	0.0000

qi is the *q* statistic for the *ith* node

Since the diameters of the stems and taproots after branching were mostly larger than those of the laterals, the average *q* values were not statistically different from 0.5, suggesting that there is equity in terms of CSA between the stem or taproot after branching and the laterals. The average *q* values markedly larger than 0.5 for the first, second, and third and for all stem nodes suggested that the largest share of the CSA was for the stem after branching. Similarly, average *q* values markedly smaller than 0.5 for the first and all taproot nodes suggested that the largest share of CSA was in the laterals.

The linear regressions of *p* against the link diameter for each stem node and for all stem nodes together were not significant (Adjusted $R^2 < 0.015$ and $P > 0.05$), suggesting the independence of *p* values from link diameter (Table 31, Figure 13). The independence of *q* values from link diameter for each stem node and for all stem nodes together was also confirmed (Adjusted $R^2 < 0.018$ and $P > 0.05$) except for the fourth node (Adjusted $R^2 = 0.27$ and $P = 0.0002$). The independence of branching parameters (*p* and *q*) for all nodes to link diameter reconfirms the self-similar branching pattern of the shoot system (Salas et al. 2004; van Noordwijk and Purnomosidhi 1995).

For the root system, independence of *p* values to link diameters was verified only for the first and third nodes (Adjusted $R^2 < 0.039$ and $P > 0.05$), and independence of *q* values to link diameters was only confirmed for the first and second nodes (Adjusted $R^2 = 0.028$ and $P > 0.1$). The dependence of *p* and *q* to link diameter for all nodes suggested that there is no self-similar branching pattern for the root system. For the second taproot node, *p* values increased with the link diameter (Figure 13c).

58

Table 31. Regression of the branching parameters against the link diameter for the shoot and root systems

Shoot system								
Node sequence	$p = b_0 + b_1 d$				$q = b_0 + b_1 d$			
	b_0	b_1	Adjusted R^2	Probability	b_0	b_1	Adjusted R^2	Probability
First	0.9066	0.0056	0.0141	0.0530	0.6114	− 0.0001	− 0.0118	0.9380
Second	1.1189	− 0.0048	− 0.0018	0.3576	0.5607	0.0022	0.0102	0.1823
Third	1.0843	− 0.0028	− 0.0131	0.7275	0.4719	0.0064	0.0161	0.0523
Fourth	1.0287	0.0206	0.0108	0.2319	0.3303	0.0167	0.2662	0.0002
Fifth	1.0759	− 0.0047	− 0.0458	0.8493	0.5082	− 0.0003	− 0.0476	0.9716
Sixth	0.2681	0.0852	− 0.1605	0.6082	0.5219	− 0.0078	− 0.2381	0.8540
All nodes	1.0770	− 0.001	− 0.0029	0.7297	0.4971	0.0052	0.0176	0.0593
Root system								
Node sequence	$p = b_0 + b_1 d$				$q = b_0 + b_1 d$			
	b_0	b_1	Adjusted R^2	Probability	b_0	b_1	Adjusted R^2	Probability
First	1.4050	− 0.0147	0.0389	0.0580	0.5056	− 0.0022	0.0284	0.3954
Second	− 0.3843	0.1096	0.3514	0.0000	0.5555	− 0.0037	0.0284	0.1519
Third	1.1501	0.0174	− 0.0140	0.3980	0.6538	− 0.0088	0.1920	0.0346
All nodes	0.7324	0.0333	0.0625	0.0022	0.5487	− 0.0035	0.0348	0.0179

d is the link diameter; probability refers to the significance of the regression slope
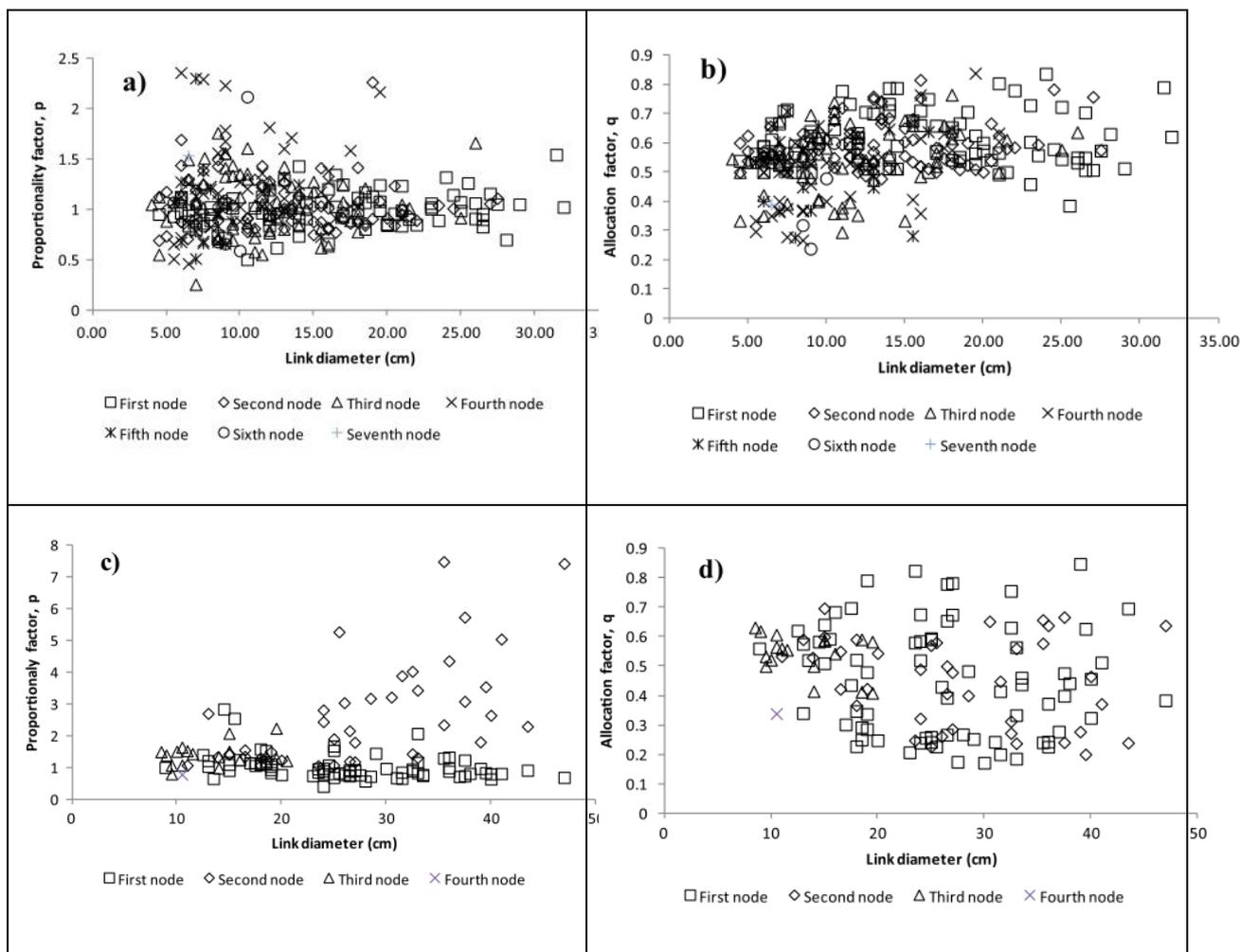
Figure 13. Regression of branching parameters (*p* and *q*) against link diameter for **(a, b)** shoot system and **(c, d)** root system

3.5.3 Diameter exponent (Δ)

For 25 of the 309 stem nodes and 34 of the 133 taproot nodes, there was no solution for Δ, i.e. the nonlinear optimisation of Equation 53 did not converge. The non-convergence was mainly because the diameters of these stem or taproot nodes after branching were larger than were those before branching.

For the shoot system, the average Δ per node ranged between 1.79 and 2.06, with an overall average of 1.99 (Table 32). The null hypothesis of average Δ to be equal to 2 was not rejected for any node or population of nodes ($P > 0.09$). This confirms the area-preserving branching for each stem node and the self-similar branching pattern.

For the root system, the average Δ per node ranged between 1.22 and 1.86, with an overall average of 1.54 (Table 32). The null hypothesis of average Δ to be equal to 2 was not rejected only for the first node ($P = 0.06$). Therefore, the area-preserving branching was only reconfirmed for the first taproot node. The average Δ values for the second, third, and all nodes were markedly smaller than 2, suggesting that the CSA increased with branching; contradicting the conclusion obtained by the proportionality factor (*p*).

60

Table 32. Summary of the basic statistics for the diameter exponent Δ

| | Shoot system | | | | | | | Root system | | | |
	$\Delta 1$	$\Delta 2$	$\Delta 3$	$\Delta 4$	$\Delta 5$	$\Delta 6$	Δ for all nodes	$\Delta 1$	$\Delta 2$	$\Delta 3$	Δ for all nodes
Minimum	0.9700	0.8914	1.0811	0.6879	0.9031	0.9325	0.6879	0.7828	0.4858	0.9524	0.4858
Mean	2.0588	1.9885	2.0319	1.7932	2.0807	2.2172	1.9968	1.8593	1.2177	1.5112	1.5407
Maximum	3.8018	4.3501	4.8206	4.7337	3.3546	2.8178	4.8206	2.6272	1.9390	2.9877	2.9877
SD	0.5360	0.5937	0.8064	0.7902	0.6564	0.8302	0.6723	0.4331	0.4169	0.4569	0.5242
CV%	26.0337	29.8564	39.6877	44.0660	31.5457	37.4408	33.6711	23.2927	34.2323	30.2350	34.0215
Probability	0.3328	0.8686	0.7567	0.0935	0.5796	0.5899	0.9363	0.0596	0.0000	0.0002	0.0000

Δi is the Δ statistic for the *ith* node

3.3.5.4 RTO of CSA before branching against CSA after branching

The slope α of RTO of CSA before branching against CSA after branching (Table 33) was not statistically different from 1 ($P > 0.07$) for any stem node or for the entire population of nodes. This result was expected since the average branching parameter *p* was not significantly different from 1. These results also suggest the area-preserving branching for each stem node and for the entire population of nodes and thus the self-similarity.

For the root system, the slope α was not found significantly different from 1 ($P > 0.05$) only for the first node (as expected) and for the entire population of nodes. Therefore, the area-preserving branching was not observed for any subsequent branching points (nodes), and thus, self-similarity was not confirmed for the root system.

Table 33. RTO of CSA before branching (CSA_b) against CSA after branching (CSA_a)

| Shoot system | | | |
| Node sequence | $CSA_b = b_1 CSA_a$ | | |
	b_1	Adjusted R^2	Probability
First	0.9785	0.9552	0.2750
Second	0.9791	0.9637	0.2259
Third	0.9443	0.9164	0.0781
Fourth	1.0120	0.9050	0.0830
Fifth	0.8962	0.9034	0.0688
Sixth	0.7116	0.6417	0.0909
All nodes	0.9775	0.9580	0.1002

| Root system | | | |
| Node sequence | $CSA_b = b_1 CSA_a$ | | |
	b_1	Adjusted R^2	Probability
First	0.8070	0.9355	0.0516
Second	2.1123	0.7322	0.0000
Third	1.3099	0.9009	0.0002
All nodes	0.9033	0.7591	0.3879

Probability refers to the significance of the regression slope

4. DISCUSSION

4.1 Biomass modelling and additivity (Article I)

4.1.1 Independent tree component and total tree models
Linear and nonlinear models were fitted for tree component and total tree biomass estimation. The difference between the performance of the selected linear and nonlinear tree component models are negligible. However, Ter-Mikaelian and Korzukhin (1997), Schroeder et al. (1997), and Salis et al. (2006) found nonlinear models to perform better than the linear ones.

   The crown models for both linear and nonlinear models in this study were found to be less accurate and precise than the other tree component models, as evaluated by its adjusted R^2 and CVs of the residuals, suggesting more variability. This confirms findings on other species for example by Seifert et al. 2006, Phiri et al. (2015). According to Pardé (1980), this is because of the variability of the internal crown structure, number of branches, and variation in wood density along the branches.

4.1.2 Additivity
Based on all of the results and analyses, the CON method was significantly superior to the SUR and NSUR methods and showed the best fit statistics for every tree component and total tree biomass models, including the largest adjusted R^2, smallest CV of the residuals, and no significant model bias or defects. However, although this model was found to be statistically superior, it should be noted that this method holds only under the assumption of independence among components (Parresol 1999), implying that the residuals are uncorrelated, therefore not taking into account contemporaneous correlations.

   Among the methods that consider contemporaneous correlations (i.e., SUR and NSUR), NSUR appeared superior to SUR. For all tree components, NSUR yielded higher adjusted R^2 values, smaller CV of the residuals, and less bias. However, the total tree model of the SUR method presented a higher adjusted R^2 when compared to the total tree model of the NSUR method.

   As shown in Figure 9, the regression lines for the CON and NSUR methods followed the same trend, and the CON method described the data slightly better than the NSUR method. Additionally, for all components, the SUR regression line had the poorest fit, especially for belowground, stem wood, stem bark, and total tree biomasses.

   As shown in Tables 6 and 7, the variance of the NSUR system was almost five times larger than that of the SUR system; however, the covariance errors for all tree components were almost two times smaller for the NSUR method; this last observation may explain the better fit of the NSUR method as all of the components in the NSUR method had larger R^2 values and smaller CVs of the residuals than those in the SUR method.

   Several authors, including Parresol (1999, 2001), Carvalho and Parresol (2003), Goicoa et al. (2011), Carvalho (2003), and Návar-Cháidez et al. (2004), have compared different methods of enforcing additivity. All these authors have concluded that either SUR or NSUR achieve more efficient estimates and should be

the choice for additivity. However, Parresol (1999) suggestted that the constraint of additivity (restriction of the parameters) may compromise the efficiency of the results, a conclusion supported by SAS Institute Inc. (1999), which states that restrictions should be consistent and not redundant, i.e., the data must be consistent with the restriction. In fact, the lower efficiency and precision of the SUR and NSUR estimates when compared to the CON method are associated with the imposed restriction as t-test results based on all the restrictions imposed on SUR and NSUR were highly significant, indicating that the data were not consistent with the restriction and that the models did not fit as well with the restriction imposed. For further details, please see Tables 8 and 9, which are SAS outputs that test the significance of the restrictions imposed for weighted SUR and weighted NSUR, respectively.

Carvalho (2003) compared methods of enforcing additivity and found that the bias (MR) for stem wood was slightly larger when the models were fit simultaneously using SUR than when tree components were fit separately using ordinary least squares (OLS), even though other fit statistics had improved with SUR. Similar findings were observed by Goicoa et al. (2011), who found that the SUR method was highly biased as it exhibited large MR and mean relative standard error (MRSE) values.

Parresol (1999, 2001), Carvalho and Parresol (2003), and Carvalho (2003) found that multivariate procedures (SUR and/or NSUR) produce more reliable estimates than when equations are estimated independently (ex.: the CON method or independent tree component models). However, Repola (2008) found no significant improvements in parameter estimates using SUR when compared to the case where the models are fitted independently.

Due to the large bias found using the SUR method in this study, this method cannot be suggested for biomass estimation of any tree component if not thouroughly evaluated on the data at hand. However, because the bias is far smaller than that of the SUR method, the NSUR method can be used for biomass estimation as long as the bias is considered. Moreover, while the NSUR method is not superior to the CON method in terms of bias, it does have the advantage of considering contemporaneous correlation, which the CON method does not. It might thus take into account changes between biomass component relations beyond the basic allometry.

The CV of the residuals for total tree biomass model obtained using the HAR procedure for the linear and nonlinear models were 72.4 and 69%, respectively, 83 and 216% larger than the CV for total tree model obtained using the SUR and NSUR procedures, respectively. This shows that, in this case, the model for total biomass obtained using SUR or NSUR procedure provide more precise results than what would be obtained by summing up the individual component models to the total (HAR procedure).

4.1.3. Upscaling to stand level

The models fitted in this research (separately or simultaneously) were based on a dataset of 93 trees with diameters varying from 5 to 32 cm. *A. johnsonii* trees can reach diameters at breast height (DBHs) larger than 35 cm. In a forest inventory of *A. johnsonii* stands where trees with a minimum DBH of 10 cm were measured, Magalhães and Soto (2005), unpublished data, found only 13 trees per ha with DBHs larger than

or equal to 30 cm, corresponding to only 5% of trees per ha. In this study, using 23 plots randomly distributed in the study area and a minimum DBH of 5 cm, only 19 trees per ha with diameters larger than or equal to 32.5 cm were found, corresponding to 1.54% of the total number of trees per ha. This implied that no serious bias would be added to the stand biomass estimation when extrapolating the models (independent tree component or NSUR models) outside the diameter range used to fit the models since very few trees were found outside the diameter range.

The newly established models can be applied with confidence over the whole range of areas where *A. johnsonii* occurs and outside the study area. This can be assumed because the study area covered the entire range of soil and climate variations where *A. johnsonii* occurs (despite the apparent lack of large variations). For example, besides the Chibuto, Mandlakaze, Panda, Funhalouro, and Mabote districts that comprised the study area, Mecrusse (*A. johnsonii*) is also found in Mabalane, Massangena, and Chicuacuala districts. However, in these latter districts, the soils are nearly identical to those of the study area, composed mainly of Ferralic Arenosols (Dinageca 1990; FAO 2003). Similarities were also found with regard to climate and hydrology, especially with regard to water shortage (Mae 2005a-e).

4.1.4 Effect of the measurement procedures on the estimates

In this study, wood density was obtained by dividing oven dry weight (at 105°C) of the discs (with and without bark) by the relevant saturated wood volume (de Gier 1992; Bunster 2006; Seifert and Seifert 2014) (air not included). It is noteworthy mentioning that different definitions of the weight and volume of the discs would potentially influence the estimates of density and therefore biomass. For example, Husch et al. (2003) defines density as the ratio of oven dry weight and green volume (air included). One could argue that compared to the definition adopted in this study, such a definition could potentially lead to large values of wood density and consequently wood biomass, as saturated volume is the maximum volume (Moura et al. 2007).

Moura et al. (2007) found no significant differences between those densities, as according to these authors, the densities must be quite the same because it is not expected volume variation above the fibre saturation point (FSP). FSP of a wood is here defined as the maximum possible amount of water that the composite polymers of the cell wall can hold at a particular temperature and pressure (Simpson and Barton 1991), excluding, therefore, free and adsorbed water. Differences in wood density and biomass estimates could also be found if the discs were dried to different moisture content (e.g. 12%) or if a different drying temperature was used (e.g. 65 °C) as found by Phiri et al. (2015), who found significant influence of the drying temperature.

Another crucial factor is the stem definition, which can impact on the distribution of biomass to stem and branch components. In this study, stem was defined as the length from the top of the stump to the height corresponding to 2.5 cm diameter. Differences among stem definitions (e.g. different stump height or different minimum top diameter, stump considered as part of the stem) would affect the biomass estimates, especially stem and root biomasses. Different estimates of root biomass could also be found if the root

64

system was partially removed, as performed by many authors (e.g. Levy et al. 2004; Soethe ey al. 2007; Kalliokoski et al. 2008; Ruiz-Peinado et al. 2011; Sanquetta et al. 2011), if the depths of excavation were predefined (Ruiz-Peinado et al. 2011; Sanquetta et al. 2011; Paul et al. 2014), if fine roots were excluded (Bolte et al. 2004; Ryan et al. 2011), and if root sampling procedures were applied, for example, where only a number of roots from each root system is fully excavated, and then the information from the excavated roots is used to estimate biomass for the roots not excavated (Niiyama et al. 2010; Kuyah et al. 2012; Mugasha et al. 2013). This was avoided by full excavation in this study.

4.2 Estimation of biomass, carbon stocks and error propagation (Article II)

4.2.1 Biomass and carbon stocks
The finding of this study that approximately half of total above and belowground tree biomass and carbon stocks were attributable to stem wood was consistent with the results of Paladinic et al. (2009) for fir-beech and oak forests and Wang et al. (2011) for *Abies nephrolepis* (Maxim). In Mozambique, *A. johnsonii* is classified as a first-class commercial species with minimum harvestable diameter of 30 cm (DNFFB 2002). Stakes of *A. johnsonii* used by local communities for construction purposes are generally from trees that are 10–15 cm in diameter (Mantilla and Timane 2005). This diameter class comprised <20% of the total biomass.

Biomass stock is a function of stem density and DBH, and thus of basal area (see Figures 10 and 11, where the diameter classes with the largest proportion of basal area are the same as those with the largest proportion of biomass stock). Biomass stock has been correlated with basal area by many authors (Rai 1981; Brunig 1983; Cannell 1984; Rai and Proctor 1986; Slik et al. 2009).

In Mozambique, most studies of tree biomass and carbon stocks focus on Miombo (Brachystegia spp.) woodlands, which represent 75% of the forest in this country (Sitoe and Ribeiro 1995). Existing estimates of biomass and carbon stocks for Miombo woodlands are much lower than the estimates obtained here for Mecrusse woodlands. Ribeiro et al. (2013) found that the tree biomass and carbon stocks in Miombo woodlands of Niassa National Reserve were approximately 59 and 30 Mg ha^{-1}, respectively. Miombo carbon stocks in Nhambita, Gorongoza District, in Mozambique were estimated as 21.2 Mg ha^{-1} for stems and 8.5 Mg ha^{-1} for coarse roots (Ryan et al. 2011).

Low stem density (380–400 ha^{-1}) and basal area (7–19 m^2·ha^{-1}) in Miombo (Ribeiro et al. 2002) can explain the lower estimates for biomass and carbon compared to the estimates for Mecrusse woodlands (1237 ha^{-1} and 22 m^2 ha^{-1}, respectively). Aboveground biomass estimates by Brown (1997) at the national scale indicated actual and potential biomass stock of 56 and 96 Mg ha^{-1}, respectively. However, Saatchi et al. (2011) estimated aboveground biomass densities from 51 to 75 Mg ha^{-1} for the region in which the current study is located. This lower estimate is presumably a result of consideration of other vegetation types (e.g. savannah and thicket) associated with Mecrusse woodlands by Saatchi et al. (2011). Lower values for biomass and carbon stock than those estimated here were also reported in neighbouring countries (Malimbwi et al. 1994; Munishi et al. 2010).

65

The default value for carbon content used by the Intergovernmental Panel on Climate Change is 50% (IPCC 2003). The measured values of this study were compared with those calculated with this default value and found only slight differences in the estimates (Table 34). However, although the differences were small, these errors would propagate as estimates are scaled up, for example to the stand or forest level.

Table 34. Comparison of carbon stock estimates using values estimated with TruSpec Micro analyser (this study) and the IPCC default value (carbon content = 50% of biomass) (IPCC 2003)

Tree component	Carbon stock (Mg ha^{-1})		Difference (%)
	This study	IPCC default	
Belowground	17.32	16.30	-6.28
Stem wood	41.58	42.39	1.92
Stem bark	4.41	4.88	9.70
Crown	19.42	19.95	2.66
Whole tree	82.73	83.52	0.95

4.2.2 Error propagation

The high level of precision in biomass estimates of this study was a result of the homogeneity of the forest type and site characteristics (*A. johnsonii* is the only canopy species in Mecrusse forest). Stellingwerf (1994) suggested that the 95% CI should not exceed ± 20% of the mean. Brown et al. (1995) reported a total error of 20% for aboveground biomass estimates for Amazonian forests, and this level of precision was considered acceptable. The 95% CI for estimates of whole tree biomass stock of this study was ± 9.6%, which was well within these accepted limits.

It was showed in this study that the relatively higher error for stem bark and crown biomass stocks was largely a result of the error in the allometric equations. These models showed less good fits presumably because of variation in crown weight among trees with the same DBH and height, which might have been caused by differences in stand density, crown shape, and density of branch wood (Pardé 1980; Carvalho & Parresol 2003), and by variation in stem bark density within and between trees.

Because the overall error was largely attributed to plot selection, the total error could be reduced by increasing the number of sampling plots.

In contrast to the findings of this study, it was expected the error due to allometric equations to be larger than that due to sample plot selection, because destructive measurement (phase two) is labour demanding and time consuming, typically done on smaller tree number and, therefore, more susceptible to errors. However, according to the definition of large sample size suggested by Husch et al. (2003), Stellingwerf (1994), Freese (1962, 1984) and Stauffer (1983), in which the number of replicates should be >30, the sample for the phase-two measurements of this study (*n* = 93) was large, which led to lower variance. In contrast, the phase-one sample size (*n* = 23) might be considered small, yielding relatively large variance values.

Field studies that estimate biomass generally perform destructive sampling on a relatively small number of trees (even in multi-species tropical forests), especially when the roots are included, which leads to higher variance (error) of the second sampling phase. Salis et al. (2006) destructively sampled 10 trees per species to estimate aboveground biomass and obtained wider confidence intervals than the suggested by Stellingwerf (1994). Wang (2006) and Dias et al. (2006) used sample sizes of 10 and 15 trees per species, respectively, which might not have been sufficient to represent all sources of variation. Malimbwi et al. (1994) performed destructive sampling of 17 trees from 15 species in 10 sample plots in Miombo woodland at Kitulangalo Forest Reserve, Tanzania, and obtained a total percent error of 36% for biomass stock. That study examined approximately one tree per species, which (combined with the small number of plots) might have contributed strongly to the large total error.

Samalca (2007) estimated aboveground biomass for a multi-species forest in Indonesia using 143 plots (0.05 ha each, first phase) and destructive sampling of 40 trees (second phase), and found that >60% of total error was attributed to allometric equations (second phase). The total variance was attributed to the second phase, where the sample size was relatively small considering the multi-species forest (Samalca 2007). Chave et al. (2004) and Molto et al. (2012), using Monte Carlo and Bayesian error propagation approaches, respectively, also found that the most important source of error in biomass estimates for tropical forest was related to allometric equations, in contrast to the findings of this study.

It was expected the contribution of DBH measurement error, in both the first and second phase, to be smaller than that of total tree height measurement/estimation as found by some authors (Schmid-Haas et al. 1981; Gertner and Köhl 1992; and Berger et al. 2014), since DBH is easily and directly measured and thus less susceptible to measurement error than tree height (Loetsch et al. 1973; Machado and Filho 2006; Sanquetta et al. 2006). The largest contribution of DBH measurement error to the total error of both phases is explained by the higher variability of DBHs compared to total tree height (Tables 3 and 4). Tables 3 and 4 showed that the variability (CV) of DBH was, approximately, twice as large as the variability of the total tree height in both phases. Moreover, the quadratic term for DBH in Eqs.9, 25, and 26 caused its error to propagate disproportionately (quadratically) to that of the height.

The larger error in height measurements for the first sampling phase compared to the second phase occurred because tree length was measured directly using a tape in the second phase, while height was estimated using a Vertex IV hypsometer in the first phase. In the first phase, the measurements were more susceptible to instrument error, error inherent to the trees, and error caused by the distance between the instrument and the tree.

The relatively higher total percent error for stem bark and crown biomass stock originating in the allometric equations might have been a result of variation in crown weight among trees with the same DBH and height. When the contribution of branches and foliage to error are removed (Table 18), variation in crown weight was seen to be influenced by error in fresh weight of branches, which in turn was a result of variation in branch weight within and between trees. This finding is consistent with findings of Pardé (1980). The higher error for stem bark in the allometric equations was caused by variations in density.

67

4.3 Biomass expansion factors and root-to-shoot ratio: measurement uncertainties (Article III)

4.3.1 Component biomass expansion factors and biomass stock

A wider range of DBH was measured during the first sampling phase than during the second phase. However, the DBH of *A. johnsonii* rarely exceeds 35 cm (here, <1% of trees during the first sampling phase). Although large variation in total tree-height was observed during both phases, <4% of the trees had tree-heights >16 m or <5 m, which indicated that phase-2 samples were representative of the phase-1 samples, and thus the values could be extrapolated.

BEF values are generally calculated from the ratio of tree biomass components or total tree biomass (W_h) to stem or merchantable timber volume (v) (Brown 2002; Lehtonen et al. 2004; Lehtonen et al. 2007; Dutca et al. 2010; Silva-Arredondo and Návar-Cháidez 2010; Marková and Pokorný 2011) or biomass (W_s) (FAO 2007; Levy et al. 2004; Segura and Kanninen 2005; Somogyi et al. 2007; Sanquetta et al. 2011). BEFs were calculated using the first option (here called BEF_1) with total stem volume since it is easier to apply from forest inventory data. The stem BEF value was 0.7334 Mg m^{-3}, which meant that stem biomass (in Mg) was 0.7334-fold larger than stem volume (in m^3). Therefore, BEF computed according to biomass (the second option, here called BEF_2) can be calculated as a function of BEF_1 as $BEF_2 = \dfrac{W_h}{0.7334 \times v} = \dfrac{1}{0.7334} \times BEF_1$.

Since BEF_2 is obtained by multiplying BEF_1 by a constant, the relationship between BEF_2 and tree size (DBH and tree-height) is the same as that between BEF_1 and tree size (both relationships will be either significant or insignificant). Therefore, trends in BEF values calculated here using the first option were compared indiscriminately to those calculated using either option.

The same principle holds for BEF values calculated using merchantable timber volume or biomass; because merchantable timber volume or biomass are obtained by multiplying stem biomass or volume by the merchantable fraction of the total stem (ratio of timber volume to stem volume) (Levy et al. 2004), which is a constant. For most trees, this fraction is very close to 1 (Levy et al. 2004), which makes BEF values calculated with merchantable volume or biomass very close to those calculated with stem volume or biomass.

BEF_1 was preferred to BEF_2 because stem volume is easily measured destructively than stem biomass, and volume is the main variable of interest in most forest inventories. In addition, stem volume was preferred to merchantable volume because merchantable height is sensitive to personal judgment and thus is more subjective than stem height, especially for standing trees. Merchantable tree height measurement (e.g. to 7 cm top diameter as defined by Edwards and Christie (1981), Lehtonen et al. (2004, Black et al. (2004), and Lehtonen et al. (2007)) in standing trees is subjective and more susceptible to measurement error than total tree height, because the 7 cm top diameter on the stem is more difficult to identify than the tip of the tree. Moreover, in most tropical tree species, and especially in broadleaf species (as opposed to monopodial conifers), taking a minimum top diameter of 7 cm to define merchantable tree height is somewhat

68

impractical because the merchantable height is limited by branching, irregular form or defects which causes inconsistence in the top diameter definition.

Because stem volume is the auxiliary variable for all tree components, estimation of biomass stock based on BEF achieves the property of additivity automatically for the major components (root system, shoot system, stem, and crown) and for total tree biomass, without additional efforts, which is an advantage.

The BEF values estimated in this study (1.0504 and 1.3072 Mg m^{-3} for above and total tree biomass, respectively) fall in the range of many estimates obtained worldwide (e.g. Lehtonen et al. 2004; Cháidez 2009; Dutca et al. 2010; Somogyi et al. 2007; Kamelarczyk 2009; Sanquetta et al. 2011; Marková and Pokorný 2011), especially with those of whole-tree BEF. For example, Kamelarczyk (2009) reported whole-tree BEF values from 0.06 to 2.90 for 17 Miombo tree species in Zambia. Estimates of aboveground and total tree BEF compiled for Africa by the FAO (2007) were 1.5 and 1.9, 43% and 45% larger than the current estimates, respectively; FAO values of eastern Africa were 2.3 for aboveground BEF and 2.9 for total BEF, which were more than two-fold higher than the estimates of this study. However, the FAO's global-scale estimates (1.0 for aboveground BEF and 1.3 for total tree BEF) were close to the current findings (FAO 2007).

Reports on the dependence of BEF values on DBH and total tree height vary, from strong reverse dependence (Brown et al. 1989; Lehtonen et al. 2004; Cháidez 2009; Dutca et al. 2010; Sanquetta et al. 2011) to weak reverse dependence or independence (Marková and Pokorný 2011). Here, tree component BEFs were found to be either independent or have a weak reverse dependence on DBH and total tree height, which indicated that small and large *A. johnsonii* trees contain approximately the same quantity of biomass per unit volume.

Dutca et al. (2010) stated that the reverse dependence of BEF on tree size is a result of an inverse relationship between wood density and tree size. In this study, no variation in stem wood and stem bark densities according to DBH and tree height for *A. johnsonii* were observed (adj. R^2 <0.0309, P >0.05), and a very weak positive relationship was found between total stem density and DBH (adj. R^2 =0.1342, P =0.0002) and tree height (adj. R^2 = 0.0661, P =0.0072). These results explained the independence or weak dependence of component BEF values on tree size.

The observation of this study of a slightly stronger relationship between BEF values and total tree height compared to DBH was consistent with the findings of other researchers (Lehtonen et al. 2004; Levy et al. 2004; Dutca et al. 2010; Silva-Arredondo and Návar-Cháidez 2010), but contradicted the report by Sanquetta et al. (2011).

The dependence of component BEFs (taproots, lateral roots, and foliage) on DBH detected by the linear regression test and Pearson´s correlation coefficient test of significance were also found by the dcov test of independence; suggesting that, the most pronounced dependence of these component BEFs on DBH is linear, since dcov test measures all types of dependence (linear and nonlinear). On the other hand, the absence of dependence of other 7 components and total tree BEFs on DBH by either method, suggests that there is not any type of dependence (linear, nonlinear or nonmonotone) of those component BEFs on DBH.

69

A linear dependence of crown and shoot system BEFs on tree height was detected by the linear regression test and Pearson´s correlation coefficient test of significance. However, this dependence was not detected by the dcov test of independence, which may suggest that this linear dependence is casual.

The finding of independence or weak dependence of the BEF on tree size might be related to the minimum DBH measured in the phase-2 (DBH $\geq$ 5 cm). It has been reported by Brown et al. (1989), Sanquetta et al. (2011), Marková and Pokorný (2011), and Soares and Tomé (2012) that the decrease of the BEF with tree size reaches an asymptote at a given tree size. This is presumably due to stabilization of growth rate (Sanquetta et al. 2011).

The finding of independence or weak dependence of the BEF on tree size suggests that, for *A. johnsonii*, constant component BEF values can be accurately used within the interval of harvested tree sizes ($5 \leq$ DBH $\leq$ 32, Table 3), in contrast to findings by Brown et al. (1989) and Sanquetta et al. (2011). Here, further research would be needed to reveal the relationship between tree component BEFs and tree´s DBH $\leq$ 5 cm.

In this study the stem was defined as the length from the top of the stump to the height corresponding to 2.5 cm diameter. Differences among stem definitions (e.g. different stump height or different minimum top diameter, stump considered as part of the stem) would affect the BEF estimates.

It was difficult to compare the 4 major and 6 minor component BEF and biomass stock values estimated in this study, because few similar studies have been performed in African and Mozambican woodlands. The majority of available studies provide estimates of BEF and biomass for shoot systems and occasionally for the whole tree. The estimated AGB stock (121 Mg ha^{-1}) of this study was within the range reported by Lewis et al. (2013) for tropical African forests (114–749 Mg ha^{-1}) and by Brown (2002) for hardwood forests (75–175 Mg ha^{-1}); and lower than estimates for closed tropical forests (144–513 Mg ha^{-1}) (Brown and Lugo 1982; Brown and Lugo 1984). AGB stock estimate of this study was higher than Brown and Lugo's estimate for open tropical forests (50 Mg ha^{-1}) (Brown and Lugo 1984).

Estimates of stem-wood biomass stock by Brown and Lugo (1984) for undisturbed, logged, and unproductive tropical African forests were 148.6, 41.2, and 36 Mg ha^{-1}, respectively, while that of this study was 75.75 Mg ha^{-1}. The current whole-tree biomass stock (approximately 150 Mg ha^{-1}) was similar to those for unproductive (129 Mg ha^{-1}) and logged (179 Mg ha^{-1}) tropical African forests, and smaller than Brown and Lugo's estimate for undisturbed forests (238 Mg ha^{-1}) (Brown and Lugo 1984). However, the estimates by Brown and Lugo (1982, 1984) were performed more than 4 decades ago, and thus, they might not fully reflect the current situation anymore.

The AGB stock of this study (121 Mg ha^{-1}) is in agreement with those estimated for Mozambique by Brown (1997) for dense forests in moist-dry season (120 Mg ha^{-1}) and in moist-short dry season (130 Mg ha^{-1}) but are higher compared to dense forests in dry season (70 Mg ha^{-1}). Yet, Mecrusse woodlands (*A. johnsonii* stands) are typically from dry season (Mae 2005a-e), implying that the biomass productivity of Mecrusse woodlands is, approximately, twice as larger than the average productivity of dense forests in dry season in Mozambique.

The estimated uncertainty in the current BEF values (2.9%–10.6%) was lower than that of Lehtonen et al. (2004, 2007) (3%–21%) and Jalkanen et al. (2005) (4%–13%). The component biomass and stem volume values used here to calculate BEF were obtained directly using destructive sampling, whereas those by Lehtonen et al. (2004, 2007) and Jalkanen et al. (2005) were based on values obtained indirectly using regression models. These different approaches might explain the differences among BEF estimates and the higher uncertainty reported by those authors, because they also incorporate uncertainty from the regression models.

The default IPCC aboveground BEF for tropical broadleaf species is 1.5 ± 0.2 (SE = 6.67%) (IPCC 2003). This BEF value is 43% larger and 200% more uncertain than the estimated aboveground BEF of this study (1.05 ± 0.07 Mg m^{-3}, SE = 3.23%). The default IPCC BEF-based AGB stock estimation was 173 ± 28 Mg ha^{-1} (SE = 8.10%), 43% larger and 107% more uncertain than the estimated AGB stock of this study (121 ± 6.47 Mg ha^{-1}, SE = 3.23%). The default IPCC BEF-based AGB stock is not in agreement with the estimated AGB stock for Mozambique by Brown (1997), which raises a flag of warning when applying general BEFs for tropical forests without caution.

4.3.2 Root-to-shoot ratio

The average root-to-shoot ratio found in this study (0.24 or approximately1:4) was larger than that observed by some authors, such as 1:5 (0.2) reported by Kramer and Kozlowski (1979), 1:6 (0.17) reported by Perry (1982), and 0.17 reported by Sanquetta et al. (2011). The findings of these authors suggest that AGB is 5- to 6-fold greater than BGB, but finding of this study that AGB is, on average, almost 4-fold higher than BGB was consistent with the default IPCC root-to-shoot ratio of 1:4 (0.25) (IPCC 2003). BGB was determined by complete removal of the root system, including the root collar and fine roots. Estimates of R/S may vary greatly if the root system is partially removed, as performed by many authors (e.g. Levy et al. 2004; Soethe et al. 2007; Kalliokoski et al. 2008; Kalliokoski 2011; Sanquetta et al. 2011; Ruiz-Peinado et al. 2011), if the depths of excavation are predefined (Sanquetta et al. 2011; Ruiz-Peinado et al. 2011; Paul et al. 2014), if fine roots are excluded (Bolte et al. 2004; Green et al. 2007; Ryan et al. 2011). R/S values may also vary if root sampling procedures are applied, for example, where only a number of roots from each root system is fully excavated, and then the information from the excavated roots is used to estimate biomass for the roots not excavated (Niiyama et al. 2010; Kuyah et al. 2012; Mugasha et al. 2013). Different estimates of R/S can also be obtained if the stump is considered as part of the stem, as in Segura and Kanninen (2005).

Wang et al. (2011) similarly observed little variation in the relationship between R/S and tree diameter. However, different results were obtained by Mokany et al. (2006) for root-to-shoot ratios in different terrestrial biomes (forests, woodland, shrublands and grasslands), where the ratios decreased significantly with increasing shoot biomass, tree height, and DBH. Findings of this study were also inconsistent with those by Sanquetta et al. (2011), who found that R/S decreased as DBH and total tree height increased. This might be presumably because *A. johnsonii*, as a tropical native species, has a very low and/or constant growth rate

71

within the interval of harvested DBH, as opposed to the planted *Pinus spp.* studied by Sanquetta et al. (2011).

As in the case of the BEF, the finding of independence of R/S on tree size might be related to the minimum DBH measured in the phase-2 (DBH $\geq$ 5 cm). Mokany et al. (2006), Sanquetta et al. (2011), Jenkins et al. (2003), and Zhou and Hemstrom (2009) have shown that decrease of R/S with tree size reaches an asymptote at a given tree size, presumably due to stabilization of growth rate (Sanquetta et al. 2011). Inclusion of trees with DBH $\leq$ 5 cm could cause variation of R/S with tree size. Therefore, researches are also needed here to reveal the relationship between R/S and tree´s DBH $\leq$ 5 cm.

4.4 Below- and aboveground architecture: topological analysis of the root and shoot systems (Article IV)

4.4.1 Topology

The TI values of the shoot and root systems were statistically different from 1 and 0.53, respectively, implying that their branching patterns could not be considered to be herringbone or to have a random growth, thereby contradicting the results of visual analysis. Nonetheless, the TI values were closer to 0.53 than to 1, suggesting a tendency to grow randomly. On the other hand, the TT values, although not statistically different from 1 and 0, were considerably closer to 1 for the shoot system (a tendency to assume the herringbone branching pattern) and to 0 for the root system (a tendency to assume the dichotomous branching pattern).

The TI might indicate a non-herringbone branching pattern since *A. johnsonii* has multiple laterals per stem or taproot node. However, the herringbone mathematical tree based on which TI is calculated, as described by Fitter (1987), Fitter and Stickland (1991), Spek and van Noordwijk (1994), Larkin (1995), van Noordwijk and Purnomosidhi (1995), Richardson and zu Dohna (2003), and Riccardo (2007), has only one lateral per node, and thus, a is equal to μ, as revealed by Fitter (1991), and TI is equal to 1 (Martínez-Sánchez et al. 2003). However, the maximum number of laterals per node of *A. johnsonii* was 4 for the shoot system and 11 for the root system, making μ considerably larger than a, and thus, TI was lesser than 1 and closer to 0.53. This was confirmed by the results of this study, where the average μ of the root system was 3 times the average a.

The same holds true for TT values, at least for the root system, since $P_{(max)}$ and $P_{(min)}$ are functions of μ, making the denominator of Equation 1 larger than the numerator and causing TT to be much lesser than 1 and closer to 0. The TT value for the shoot system was closer to 1 because the average a was closer to average μ, which in turn was due to the smaller number of laterals per node associated with the larger number of links, unlike in the root system.

This suggests that the TI and TT defined by Fitter et al. (1991) and Trencia (1995), respectively, might lead to biased conclusions with regards to the branching pattern when the main axis has multiple laterals per node, i.e. in these cases, a herringbone branching pattern might be regarded as a dichotomous one or as

72

having random branching according to the topological indexes (TI and TT), even if the branching pattern is clearly herringbone as is the case of the root system of *A. johnsonii*.

This situation can be overcome by using the modified TI (TIM) that addresses the situation of multiple laterals per node while conserving the value of TI for the cases of one lateral per node. TIM is computed as the slope of the regression between $\log_{10}(a)$ and $\log_{10}(N + 1)$, where N is the number of nodes in the root or shoot system. In the cases of single observation, TIM is computed as the ratio between $\log_{10}(a)$ and $\log_{10}(N + 1)$.

The index TI is computed based on μ and a; and the modified one (TIM) is computed based on $N+1$ and a. Therefore, whenever a mathematical tree has only one lateral per node, the equation for TIM yields the same value as that obtained using the equations for TI described by Fitter et al. (1991), since, in this case, $N + 1 = \mu$, regardless of exhibiting a herringbone or dichotomous branching, no distinguished main axis, higher-order branching, or lateral axes with more than one link. However, the TIM value is different from the TI value when there are multiple laterals per node ($N + 1 \neq \mu$), but, nonetheless, it is consistent with the visual analyses results, and thus more realistic.

Multiple branching per node is common in the shoot system; for example, multiple laterals per stem node are found in *Ceiba pentandra* (L.) Gaertn, *Araucaria columnaris* (G. Forst.) Hook, *Araucaria heterophylla* (Salisb.) Franco, *Pinus ponderosa* Douglas, and *Pinus cembra* L. (visual observation).

In Figure 14, the topological index TI described by Fitter et al. (1991) is compared with the modified one (TIM). In the herringbone branching with multiple laterals per node (Figure 14a), although the mathematical tree has perfectly herringbone branching pattern, the TI value is much closer to 0.53, suggesting that the tree tends to have a random growth of roots. However, the TIM indicates a perfect herringbone branching pattern consistent with the visual analysis results. For the herringbone branching with a single primary lateral per node (Figure 14b), dichotomous branching with no laterals (Figure 14c), when there is no distinguished main axis (Figure 14c), and when there is one primary lateral per node with secondary branching (or higher-order branching) (Figure 14d), the TIM yields the same results as TI, since $N + 1 = \mu$.
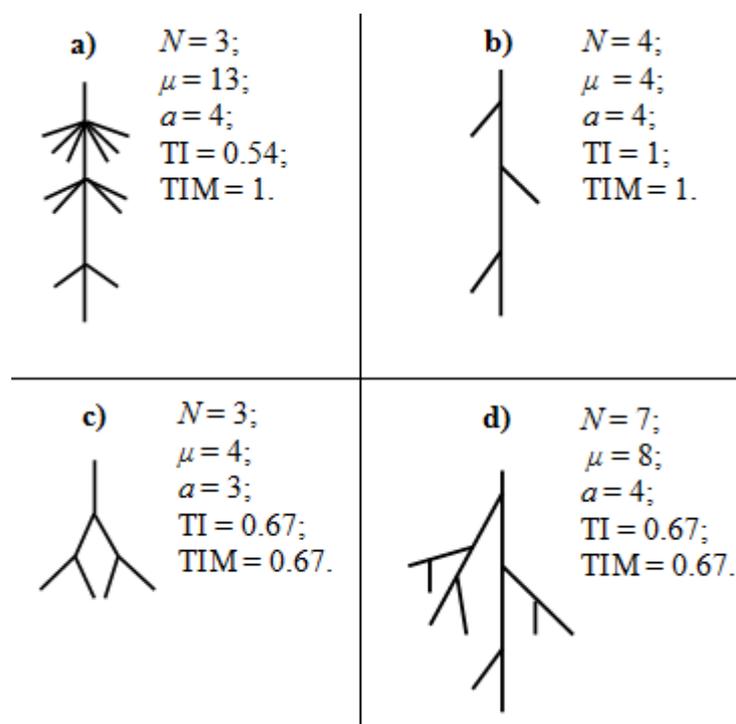
Figure 14. Comparison of the topological index by Fitter et al. (1991) and the modified topological index for **(a)** herringbone branching with multiple laterals per node **(b)** herringbone branching with a single lateral per node, **(c)** dichotomous branching , and **(d)** dichotomous with higher-order branching. TI and TIM are computed as log (a):log (μ) and log (a):log $(N + 1)$ ratios, respectively.

Further research is needed to develop a modified topological trend (TTM) that can cope with the situation of multiple laterals per node while conserving the TT values by Trencia (1995) in cases of one lateral per node.

The average value of TIM computed for *A. johnsonii* (for both the root and the shoot system) was 1, and thus consistent with the visual analysis results. The TIM was not expected to be exactly 1 for the shoot system not because the shoot system does not have a perfectly herringbone pattern since some laterals still branch, but because the secondary branches (those originating from the primary lateral branches) were not considered in this study and regarded as non-existing by the modified index.

A. johnsonii is a tree species found in regions with scanty rainfall and limited water resources (Mae 2005a, b, c, d, e; Dinageca 1997) and soil resources. This might be the reason why this tree species has a herringbone branching pattern of the root system (Fitter 1987; Fitter et al. 1991; Fitter and Stickland 1991; Malamy 2005; Echeverria et al. 2008).

4.4.2 Leonardo da Vinci rule

Van Noordwijk and Mulia (2002) suggested that a minimum of 50 but preferably 100 branching points (nodes) should be used for deriving the branching parameters. In this study, 309 and 133 branching points were used for deriving the branching parameters of the root and shoot systems, respectively.

The da Vinci rule was confirmed for each stem node and for the entire population of nodes by using four different methods: proportionality factor *p,* independence of *p* to link diameter, diameter exponent Δ, and the

regression of CSA before branching against CSA after branching. The assumption of self-similarity was confirmed by the repetition of the area preserving branching (by all methods) in all stem nodes and by the independence of p and q to the link diameter for the entire population of nodes (Noordwijk and Purnomosidhi 1995; Richardson and zu Dohna 2003).

For the root system, the area-preserving branching was only confirmed for the first node. However, the area-preserving branching was confirmed for the entire population of nodes by using the regression between CSA before branching and that after branching. Since the area-preserving branching was not confirmed for every node and there was a significant dependence of p and q to link diameter for the entire population of nodes, the self-similarity was not confirmed.

The area preservation that was analysed statistically here can be explained based on eco-physiologic principles. Variations might be attributed to the effect of different heartwood proportions of the root diameter. Nikolova et al. (2009) have reported different proportions of physiologically inactive heartwood in European species, which influences the remaining capacity of a root to conduct water. Area preservation in roots and stems is better interpreted as a derivate from the physiologically founded pipe model theory (Shinozaki et al. 1964a, b) that links the conductive sapwood area in the conductive elements of a tree to the foliage attached. Stem diameters are highly correlated with heartwood area (Seifert et al. 2006), even if Shinozaki's pipe model concept has to be extended to the real water flow in conductive elements (Nikolova et al. 2009) since doubling the size of conduits in the actively transporting sapwood increases water transport by the power of four (Schiller 1933). It has been observed for several tree species that conduits taper with increasing height in the tree, which seems to be a reason for a deviation of sapwood areas from a strict pipe-model based principle (Anfodillo et al. 2006) and might be affecting area preservation as a correlated variable as well. Here, further research would be needed to reveal the relationships between root dimension, sapwood and conduit anatomical traits to determine water conducting capacity in *A. johnsonii.*

The average proportionality factor p for each stem node and the overall average p for the entire population of stem nodes were in the range of those of the shoot system (Noordwijk and Purnomosidhi 1995). Similar results were obtained by using the average p of the root system to those reported by Noordwijk and Purnomosidhi (1995), except for the second node.

The diameter exponent Δ in this study for the root and shoot systems was in the range of those reported by Oppelt et al. (2001) and Richardson and zu Dohna (2003), although, in this case, the self-similarity was only confirmed for the shoot system. Further, the lack of dependence of p and q to link diameter of the shoot system and for the first taproot node was also in accordance with the finding by Noordwijk and Purnomosidhi (1995), Soethe et al. (2007), and Salas et al. (2004).

The average p for the second and third taproot nodes suggested that the CSA decreased with branching since the average p values were larger than 1. However, this contradicts the conclusion obtained using average Δ, since, for the second and third nodes, the average Δ values were markedly smaller than 2, suggesting that the CSA increased with branching. These contradictions are attributed to the fact that, for 34

of the 133 observed taproot nodes, there was no solution for Δ, which affected each node's average Δ and the overall average Δ.

5. CONCLUSIONS

This study showed that the CON method for biomass estimation was found to be unbiased and to fit the tree component and total tree biomass well; however, the CON method had the disadvantage of not considering contemporaneous correlations. Among methods that consider contemporaneous correlations, NSUR was far superior to SUR and fit the biomass reasonably well; however, both methods were significantly biased. The CON method can be used safely as long as its limitation is considered. The NSUR method can also be used as long as the bias is accepted and taken into account. Moreover, it is recommended that the SUR method should not be used due to its bias and poor description of biomass data. Since the data sets used to build the models (both independent and simultaneous) represented many variations (all diameters, soils, and climatic ranges), the selected models can be used for extrapolation.

The total tree biomass stock estimated using regression models was 167 Mg ha^{-1} of which, approximately, 134 Mg ha^{-1} was aboveground biomass. The measurements showed that more than half of the forest biomass and carbon stock in Mecrusse woodlands is contained in stem wood of trees that are 15–25 cm in diameter. The total error of the total tree biomass estimate of this study was very low (<5%), which indicated that the two-phase sampling approach and sample size were effective for capturing and predicting biomass of this forest type. Sources of measurement error included the sample plot selection (first phase) and the allometric models (second phase). Measurement errors of DBH and errors in estimates of total height and mean stem density contributed strongly to the total error.

The belowground, aboveground, and whole-tree BEFs were 0.26 ± 0.02 (SE = 3.89%), 1.05 ± 0.07 (SE = 3.23%), and 1.30 ± 0.09 Mg m^{-3} (SE = 3.27%), respectively; equivalent to, approximately, the following BEF-based biomass densities: 30 ± 2.31, 121 ± 7.84, and 151 ± 9.87 Mg ha^{-1}, respectively. Component BEFs in *Androstachys johnsonii* Prain were independent or only weakly dependent on tree size (DBH and total tree height), and that tree height was more important than DBH in explaining BEF. Therefore, it was suggested that constant component BEF values can be accurately used within the interval of harvested tree sizes. The root-to-shoot ratio (average = 0.24 ± 0.02; SE = 3.4%) was not dependent on tree height, DBH, AGB, or BGB.

The newly developed topological index TIM is an unbiased estimator of the branching tendency, since this index considers both the situations of single and multiple branching per node as opposed to the traditionally used topological index TI. The branching topology of the root and shoot systems of *A. johnsonii* trees was found to be perfectly to nearly herringbone, respectively. The area preserving branching was confirmed for each stem node, thereby confirming the self-similar branching. For the root system, the area preserving branching was only confirmed for the first node; therefore, the self-similarity was not confirmed.

6. REFERENCES

Anfodillo T, Carraro V, Carrer M, Fior C, Rossi S (2006) Convergent tapering of xylem conduits in different woody species. New Phytol 169(2): 279-290.

Antonio N, Tome M, Tome J, Soares P, Fontes L (2007) Effect of tree, stand and site variables on the allometry of Eucalyptus globulus tree biomass. Can J For Res 37: 895-906.

Berntson GM (1997) Topological scalling and plant root architecture: developmental and functional hierarchies. New Phytol 135: 621-634.

Bhattacharya D (2004) Seemingly unrelated regression with identical regressors: a note. Dartmouth College, New Hampshire.

Black K, Tobin B, Siaz G, Byrne KA, Osborne B (2004) Allometric regressions for an improved estimate of biomass expansion factors for Ireland based on a Sitka spruce chronosequence. Irish Forestry 61(1): 50–65.

Bolte A, Rahmann T, Kuhr M, Pogoda P, Murach D, Gadow Kv (2004) Relationships between tree dimension and coarse root biomass in mixed stands of European beech (*Fagus sylvatica* L.) and Norway spruce (*Picea abies* [L.] Karst.). Plant and Soil 264: 1–11.

Brandeis T, Matthew D, Royer L, Parresol B (2006) Allometric equations for predicting Puerto Rican dry forest biomass and volume, *In Proceedings of the Eighth Annual Forest Inventory and Analysis Symposium*, pp. 197–202.

Brasil MAM, Veiga RAA, Timoni JL (1994) Erros na determinação da densidade básica da madeira. CERNE 1(1): 55–57.

Brown IF, Martinelli LA, Thomas WW, Moreira MZ, Ferreira CAC, Victoria RA (1995) Uncertainty in the biomass of Amazonian forests: An example from Rondônia, Brazil. Forest Ecology and Management 75: 175–189.

Brown S (1997) Estimating biomass and biomass change of tropical forests: a primer. FAO Forest Paper 134.

Brown S (1999) Guidelines for inventorying and monitoring carbon offsets in forest-based projects. Winrock International Institute for Agricultural Development, Arlington.

Brown S (2002a) Measuring carbon in forests: current and future challenges. Environ Pollut 116:363–372.

Brown S (2002b) Measuring, monitoring, and verification of carbon benefits for forest-based projects. Phil. Trans. R. Soc. Lond. A 360: 1669-1683.

Brown S, Gillespie AJR, Lugo AE (1989) Biomass estimation methods for tropical forests with application to forest inventory data. Forest Sci 35(4): 881–902.

Brown S, Lugo AE (1982) The storage and production of organic matter in tropical forests and their role in the global carbon cycle. Biotropica 14:161–187.

Brown S, Lugo AE (1984) Biomass of tropical forests: a new estimate based on forest volumes. Science 223:1290–1293.

Brunig EF (1983) Structure and growth. In: Golley FB (ed) Ecosystems of the world 14A, tropical rain forest ecosystems: structure and function. Elsevier, New York. pp 49–75.

Bunster J (2006) Commercial timbers of Mozambique, Technological catalogue. Traforest Lda, Maputo.

Butnor JR, Doolittle JA, Johnsen KH, Samuelson L, Stokes T, Kress L (2003) Utility of ground-penetrating radar as a root biomass survey tool in forest systems. Soil Sci. Soc. Am. J. 67:1607–1615.

Butnor JR, Doolittle JA, Kress L, Cohen S, Johnsen KH (2001) Use of ground-penetrating radar to study tree roots in the southeastern United States. Tree Physiology 21: 1269–1278.

Cairns MA, Brown S, Helmer EH, Baumgardner GA (1997) Root biomass allocation in the world's upland forests. Oecologia 111: 1–11.

Cannell MGR (1984) Woody biomass of forest stands. Forest Ecology and Management 8: 299–312.

Cardoso GA (1963) Madeiras de Moçambique: *Androstachys* johnsonii. Serviços de agricultura e serviços de veterinária, Maputo.

Carreiras JMB, Melo JB, Vasconcelos M (2013) Estimating the above-ground biomass in Miombo savanna woodlands (Mozambique, East Africa) using L-band synthetic aperture radar data. Remote Sens.5: 1524-1548.

Carvalho JP (2003) Uso da propriedade da aditividade de componentes de biomassa individual de *Quercus pyrenaica* Willd. com recurso a um sistema de equações não linear. *Silva Lusitana* 11: 141–152.

Carvalho JP, Parresol BR (2003) Additivity of tree biomass components for Pyrenean oak (*Quercus pyrenaica* Willd.). Forest Ecology and Management 179: 269–276.

Cháidez JJN (2009) Allometric equations and expansion factors for tropical dry forest trees of Eastern Sinaloa, Mexico. Trop Subtrop Agroecosys 10:45–52.

Chave J, Condic R, Aguilar S, Hernandez A, Lao S, Perez R (2004) Error propagation and scaling for tropical forest biomass estimates. Phil. Trans. R. Soc. Lond. B 309: 409–420.

Chiatante D, Di Iorio A, Scippa GS, Schirone B (2004) Root architectural and morphological response of *Pinus Nigra* Arn. and *Quercus robur* L. to nutrient supply and root density in the soil. Annali di Botanica 4: 159-170.

Coll L, Potvin C, Messier C, Delagrange S (2008) Root architecture and allocation patterns of eight tropical native species with different successional status used in open-grown mixed plantations in Panama. Trees 22: 585-596.

Cortina J, Green JJ, Baddeley JA, Watson CA (2008) Root morphology and water transport of *Pistacia lentiscus* seedlings under contrasting water supply: a test of the pipe stem theory. Environmental and Experimental Botany 62: 343-350.

Cui X H, Chen J, Shen J S, et al. (2010) Modeling tree root diameter and biomass by ground-penetrating radar. Sci China Earth Sci 54: 711−719.

Cunia T (1965) Some theory on the reliability of volume estimates in a forest inventory sample. Forest Science 11: 115–128.

Cunia T (1979) On tree biomass tables and regression: some statistical comments, in *Forest resource inventory workshop proceedings*, W. E. Frawer, Ed., pp. 629–642, Colorado State University, Fort Collins.

Cunia T (1986a) Error of forest inventory estimates: its main components. In: Wharton EH, Cunia T (eds) Estimating tree biomass regressions and their error. NE-GTR-117. Broomall, PA, USDA, Forest Service, Northeastern Forest Experimental Station, USA. pp 1-13.

Cunia T (1986b) On the error of forest inventory estimates: double sampling with regression. In: Wharton EH, Cunia T (eds) Estimating tree biomass regressions and their error. NE-GTR-117. Broomall, PA, USDA, Forest Service, Northeaster Forest Experimental Station. pp 79-87.

Cunia T (1990) Forest inventory: on the structure of error of estimates. In: LaBau VJ, Cunia T (eds) State-of-the-art methodology of forest inventory: a symposium proceedings; Gen. Tech. Rep. PNW-GTR-263. Portland, USDA, Forest Service, Pacific Northwest Research Station. pp 169-176.

Cunia T, Briggs RD (1984) Forcing additivity of biomass tables: some empirical results. Can. J. For. Res.14: 376–385.

Cunia T, Briggs RD (1985) Forcing additivity of biomass tables: use of the generalized least squares method. Can. J. For. Res. 15: 23–28.

de Gier IA (1992) Forest mensuration (fundamentals). International Institute for Aerospace Survey and Earth Sciences (ITC), Enschede.

de Vries PG (1986) Sampling theory for forest inventory. Springer-Verlag, New York.

Dias ATC, Mattos EA, Vieira SA, Azevedo JV, Scarano FR (2006) Aboveground biomass stock of native woodland on a Brazilian sand coastal plain: Estimates based on the dominant tree species. Forest Ecology and Management 226: 364–367.

Dinageca (1997) Mapa Digital de Uso e Cobertura de Terra. CENACARTA, Maputo.

DNFFB (2002) Regulamento da lei de florestas e fauna bravia. Ministério de Agricultura e Desenvolvimento Rural (MADER). Maputo.

Dutca I, Abrudan IV, Stancioiu PT, Blujdea V (2010) Biomass conversion and expansion factors for young Norway spruce (*Picea abies* (L.) Karst.) trees planted on non-forest lands in Eastern Carpathians. Not Bot Hort Agrobot Cluj 38(3):286–292.

Echeverria M, Scambato AA, Sannazarro AI, Maiale S, Ruiz OA, Menéndez AB (2008) Phenotypic plasticity with respect to salt stress response by *Lotus glaber*: the role of its AM fungal and rhizobial symbionts. Mycorrhiza 18(6-7):317-329. doi: 10.1007/s00572-008-0184-3

Edwards PN, Christie JM (1981) Yield models for forest management. HMSO, London.

Eshete G, Ståhl G (1998) Functions for multi-pahase assessment of biomass in acacia woodlands of the Rift Valley of Ethiopia. Forest ecology and Management 105: 79–90.

ESRI (2009) ArcGis Desktop: Release 9.3. Redlands, CA: Environmental Systems Research Institute.

FAO (2003) FAO map of world soil resources. Rome: Food and Agriculture Organisation of the United Nations.

FAO (2007) State of the World´s forests 2007. FAO, Rome: Food and Agriculture Organisation of the United Nations.

FAO (2007) State of the World's forests 1997. FAO, Rome: Food and Agriculture Organisation of the United Nations.

Fitter AH (1987) An architectural approach to the comparative ecology of plant root system. New Phytol 106 (Suppl.):61-77.

Fitter AH (1991) Characteristics and function of root systems. In: Waissel Y, Eshel A, Kafkafi U (eds) Plant roots: the hidden half. Marcel Dekker, New York, pp 3-25.

Fitter AH, Stickland TR (1991) Architectural analysis of plant root system 2.Influence of nutrient supply on architecture in contrasting plant species. New Phytol 118: 383-389.

Fitter AH, Stickland TR, Harvey, GWW (1991) Architectural analysis of plant root system 3.Architectural correlates of exploitation efficiency. New Phytol 118: 375-382.

Freese F (1962) Elementary forest sampling. United States Department of Agriculture, Washington DC.

Freese F (1984) Statistics for land managers. Paeony Press, Edinburgh.

Gadow Kv., Hui GY (1999) Modelling forest development. Kluwer Academic Publishers, Dordrecht.

Gibbs HK, Brown S, Niles JO, Foley JA (2007) Monitoring and estimating tropical forest carbon stocks: Making REDD a reality. Environmental Research Letters 2: 1–13.

Glimskar A (2000) Estimates of root system topology of five plant species grown at steady-state nutrition. Plant Soil 227: 249-256.

Goicoa T, Militino AF, Ugarte MD (2011) Modelling aboveground tree biomass while achieving the additivity property. Environmental and Ecological Statistics 18: 367–384.

Green C, Tobin B, O´Shea M, Farrel E P, Byrne KA (2007) Above- and belowground biomass measurements in an unthinned stand of Sitka spruce (*Picea sitchensis* (Bong) Carr.). Eur J Forest Res 126: 179–188.

Greene WH (1989) Econometric analysis, 2nd edition. Macmillan Book Company, New York.

Grundy IM (1995) Wood biomass estimation in dry Miombo woodland in Zimbabwe. Forest ecology and Management 72: 109–117.

GTOS (2009) Assessment of the status of the development of the standards for the terrestrial essential climate variables.NRL, FAO, Rome.

Husch B, Beers TW, Kershaw Jr. JA (2003) Forest mensuration, 4th edition. John Wiley & Sons, Inc., Hoboken, New Jersey.

IPCC (2003) Intergovernmental Panel on Climate Change. Good Practice Guidance for Land Use, Land-Use Change and Forestry. [http:/www.ipcc.ch].

IPCC (2006) Intergovernmental Panel on Climate Change. Guidelines for National Greenhouse Gas Inventories. [http:/www.ipcc.ch].

Jacobs MW, Cunia T (1980) Use of dummy variables to harmonize tree biomass tables", Can. J. For. Res. 10: 483–490.

Jalkanen A, Mäkipää R, Stahl G, Lehtonen A, Petersson H (2005) Estimation of the biomass stock of trees in Sweden: comparison of biomass equations and age-dependent biomass expansion factors. Ann For Sci 62:845–851.

Jenkins JC, Chojnacky DC, Heath LS, Birdsey RA (2003) National-scale biomass estimators for United States tree species. For. Sci. 49(1):12–35.

Kalliokoski T (2011) Root system traits of Norway spruce, Scots pine, and silver birch in mixed boreal forests: an analysis of root architecture, morphology, and anatomy. PhD thesis. Department of Forest Sciences, University of Helsinki, Finland.

Kalliokoski T, Nygren P, Sievänen R (2008) Coarse root architecture of three boreal tree species growing in mixed stands. Silva Fennica 42 (2): 189-210.

Kamelarczyk KBF (2009) Carbon stock assessment and modelling in Zambia: a UN-REDD programme study. United Nations–Reducing Emissions from Deforestation and forest Degradation, Zambia.

Ketterings QM, Coe R, van Noordwijk M, Ambagau Y, Palm CA (2001) Reducing uncertainty in the use of allometric biomass equations for predicting above-ground tree biomass in mixed secondary forest. Forest Ecology and Management 146: 199–209.

Kitenge EM (2011) Harvesting of invasive woody vegetation (*Eucalyptus lehmanii*, *Leptospermum laevigatum*, *Acacia cyclops*) as energy feedstock in the Cape Agulhas Plain of South Africa. M.Sc. thesis, Department of Forest and Wood Science, Stellenbosch University, Stellenbosch.

Komiyama A, Poungparm S, Kato S (2005) Common allometric equations for estimating the tree weight of mangroves. J. Trop. Ecol. 21: 471–477.

Kozak A (1970) Methods of ensuring additivity of biomass components by regression analysis. For. Chron. 46: 402–404.

Kramer PJ, Kozlowski TT (1979) Physiology of Woody Plants, 2nd ed. Academic Press, San Diego.

Kunneke A, Aardt Jv, Roberts W, Seifert T (2014) Localisation of biomass potentials. In: Seifert T (ed) Bioenergy from wood: sustainable production in the tropics. Springer, Managing Forest Ecosystems 26: pp 11–41.

Kurz WA, Beukema SJ, Apps MJ (1996) Estimation of root biomass and dynamics for the carbon budget model of the Canadian forest sector. Can. J. For. Res. 26: 1973–1979.

Kuyah S, Dietz J, Muthuri C, Jamnadass R, Mwangi P, Coe R, Neufeldt H (2012) Allometric equations for estimating biomass in agricultural landscapes: II. Belowground biomass. Agriculture, Ecosystem and Environment 158: 225–234.

Körner, C (1994) Biomass fractionation in plants: a reconsideration of definitions based on plant functions. In *A whole plant perspective on carbon-nitrogen interactions* (ed. J. Roy & E.Garnier), pp. 173–185. The Hague: SPB Academic.

Lambert MC, Ung CH, Raulier F (2005) Canadian national tree aboveground biomass equations. Can. J. For. Res.35: 1996–2018.

Larkin RP, English JT, Mihail JD (1995) Effects of infection by *Pythium* spp. On root system morphology of alfalfa seedlings. Phyto-pathology 85: 430-435.

Leadley P, Pereira HM, Alkemade R, Fernandez-Manjarrés JF, Proença V, Scharlemann JPW, Walpole MJ (2010) Biodiversity scenarios: projections of 21st century change in biodiversity and associated ecosystem services. Secretariat of the Convention on Biological Diversity, Montreal. Technical Series no. 50.

Lehtonen A, Cienciala E, Tatarinov F, Mäkipää R (2007) Uncertainty estimation of biomass expansion factors for Norway spruce in the Czech Republic. Ann For Sci 64:133–140.

Lehtonen A, Mäkipää R, Heikkinen J, Sievänen R, Lisk J (2004) Biomass expansion factors (BEFs) for Scots pine, Norway spruce and birch according to stand age for boreal forests. Forest Ecol Manage 188:211–224.

Levy PE, Hale SE, Nicoll BC (2004) Biomass expansion factors and root: shoot ratios for coniferous tree species in Great Britain. Forestry 77(5): 421–430.

Lewis SL et al. (2013) Aboveground biomass and structure of 260 African tropical forests. Phil Trans R Soc B 368:1–14.

Litton CM, Ryan MG, Tinker DB, Knight DH (2003) Belowground and aboveground biomass in young postfire lodgepole pine forests of contrasting tree density. Can. J. For. Res. 33: 351–363.

Loetsch F, Zöhrer F, Haller KE (1973) Forest inventory, Volume II. BLV Verlagsgesellschaft. Muchen, Germany.

Lu D (2006) The potential and challenge of remote sensing-based biomass estimation. Int J Remote Sens 27: 1297–1328.

Lynch J (1995) Root achitecture and plant produtivity. Plant Physiol 109: 7-13.

Lynch JP, Ho MD (2005) Rhizoeconomics: carbon costs of phosphorus acquisition. Plant Soil 269: 45-56.

Machado SA, Filho AF (2006) Dendrometria. Editora unicentro. Paraná, Brasil.

Mae (2005a) Perfil do distrito de Chibuto, província de Gaza. Mae, Maputo.

Mae (2005b) Perfil do distrito de Funhalouro, província de Inhambane. Mae, Maputo.

Mae (2005c) Perfil do distrito de Mabote, província de Inhambane. Mae, Maputo.

Mae (2005d) Perfil do distrito de Mandhlakaze, província de Gaza. Mae, Maputo.

Mae (2005e) Perfil do distrito de Panda, província de Inhambane. Mae, Maputo.

Magalhães TM (2008) Calibration of commercial volume and form factor tables for *Androstachys johnsonii* for Madeiraarte concession in Changanine-Memo village. M.Sc thesis submitted to University of Copenhagen, Copenhagen.

Magalhães TM (2015) Allometric equation for estimating belowground biomass of *Androstachys jonhsonii* Prain. Carbon Balance and Management 10:16.

Magalhães TM, Seifert T (2015a) Estimation of tree biomass, carbon stocks, and error propagation in Mecrusse woodlands. Open Journal of Forestry 5: 471–488.

Magalhães TM, Seifert T (2015b) Biomass modelling of *Androstachys johnsonii* Prain – a comparison of three methods to enforce additivity. International Journal of Forestry Research 2015: 1–17.

Magalhães TM, Seifert T (2015c) Tree component biomass expansion factors and root-to-shoot ratio of Lebombo ironwood: measurement uncertainty. Carbon Balance and Management 10: 9.

Magalhães TM, Seifert T (2015d) Estimates of tree biomass, and its uncertainties through mean-of-ratios, ratio-of-eans, and regression estimators in double sampling: a comparative study of Mecrusse woodlands. American Journal of Agriculture and Forestry 3(5): 161–170.

Magalhães TM, Soto SJ (2005) Relatório de Inventário Florestal da Concessão Florestal de Madeiraarte: Bases para a elaboração do plano de maneio de conservação dos recursos naturais. Departamento de Engenharia Florestal (DEF), Universidade Eduardo Mondlane (UEM), Maputo.

Malamy JE (2005) Intrinsic and environmental response pathways that regulate root system architecture. Plant Cell Environ 28: 67-77.

Malimbwi RE, Solberg B, Luoga E (1994) Estimation of biomass and volume in Miombo woodland at Kitulangalo Forest Reserve, Tanzania. Journal of Tropical Forest Science 7(2): 230–242.

Mantilla J, Timane R (2005) Orientação para maneio de Mecrusse. SymfoDesign Lda, Maputo.

Marková I, Pokorný R (2011) Allometric relationships for the estimation of dry mass of aboveground organs in young highland Norway spruce stand. Acta Univ Agric Silvic Mendel Brun 59(6):217–224.

Martínez-Sánchez JJ, Ferrandis B, Trabaud L, Galindo R, Franco JA, Herranz JM (2003) Comparative root system structure of post-fire *Pinus halepensis* Mill. and *Cistus monspeliensis* L. saplings. Plant Ecology 168: 309-320.

Mason NWH, Beets PN, Payton I, Burrows L, Holdaway RJ, Carswell FE (2014) Individual-based allometric equations accurately measure carbon storage and sequestration in shrublands. Forest (5): 309–324.

Mate R, Johansson T, Sitoe A (2014) Biomass equations for tropical forest tree species in Mozambique. Forests 5: 535–556.

Meyer HA (1941) A correction for a systematic errors occurring in the application of the logarithmic volume equation. Forestry School Research: Pennsylvania.

Miranda SC, Bustamante M, Palace M, Hagen S, Keller M, Ferreira LG (2014) Regional Variations in Biomass Distribution in Brazilian Savanna Woodland. BIOTROPICA 46(2): 125–138.

Mokany K, Raison RJ, Prokushkin AS (2006) Critical analysis of root: shoot ratios in terrestrial biomes. Global Change Biol 12:84–96.

Molotja GM, Ligavha-Mbelengwa MH, Bhat RB (2011) Antifungal activity of root, bark, leaf and soil extracts of *Androstachys johnsonii* Prain. African Journal of Biotechnology 10(30): 5725–5727.

Molto Q, Rossi V, Blanc L (2012) Error propagation in biomass estimation in tropical forests. Methods in Ecology and Evolution 4: 175–183.

Moura S, Abella D, Anjos O (2007) Evaluation of wood basic density as an indirect measurement of the volume of wood raw material, *in proceeding of wood science and engineering in the third millennium,* pp. 72–78, ICWSE, Romania.

Mugasha WA, Eid T, Bollandsås OM, Malimbwi RE, Chamshama SAO, Zahabu E, Katani JZ (2013) Allometric models for prediction of above- and belowground biomass of trees in the Miombo woodlands of Tanzania. Forest Ecology and Management 310: 87–101.

Munishi PKT, Mringi S, Shirima DD, Linda SK (2010) The role of the Miombo woodlands of the southern highlands of Tanzania as carbon sinks. Journal of Ecology and the Natural Environment 2(12): 261–269.

Navár J (2009) Allometric equations for tree species and carbon stocks for forests of Northwestern Mexico. Forest Ecology and Management 257: 427–434.

Návar-Cháidez JJ (2010) Biomass allometry for tree species of Northwestern Mexico. Tropical and Subtropical Agroecosystems 12: 507–519.

Návar-Cháidez JJ, Barrientos NG, Luna JJG, Dale V, Parresol B (2004) Additive biomass equations for pine species of forest plantations of Durango, Mexico. Madera y Bosques 10: 17–28.

Nicotra AB, Babicka N, Westoby M (2002) Seedling root anatomy and morphology: an examination of ecological differentiation with rainfall using phylogenetically independent contrasts. Oecologia 130: 136-145.

Niiyama K, Kajimoto T, Matsuura Y, Yamashita T, Matsuo N, Yashiro Y, Ripin A, Kassim AR, Noor NS (2010) Estimation of root biomass based on excavation of individual root systems in a primary dipterocarp forest in Pasoh Forest Reserve, Peninsular Malaysia. Journal of Tropical Ecology 26: 271–284.

Nikolova P, Blaschke H, Matyssek R, Pretzsch H, Seifert T (2009) Combined application of computer tomography and light microscopy for analysis of conductive xylem area of beech and spruce coarse roots. European Journal of Forest Research 128(2): 145-153.

Ong CK, Deans JD, Wilson J, Mutua J, Khan AAH, Lawson EM (1999) Exploring below ground complementarity in agroforestry using sap flow and root fractal techniques. Agroforest. Syst. 44: 87–103.

Oppelt AL, Kurth W, Dzierzon H, Jentschke G, Godbold DL (2000) Structure and fractal dimensions of root systems of four co-occuring fruit tree species from Botswana. Ann. For. Sci. 57: 463-475.

Oppelt AL, Kurth W, Godbold DL (2001) Topology, scaling and Leonardo´s rule in root system from African tree species. Tree Physiology 21: 117-128.

Overman JPM, White HJL, and Saldarriaca JG (1994) Evaluation of regression models for above-ground biomass determination in Amazon rainforest. Journal of tropical Ecology 10: 207–218.

Ozier-Lafontaine H, Lecompte F, Sillon, JF (1999) Fractal analysis of the root architecture of *Gliricidia sepium* for the spatial prediction of root branching, size, and mass. Model development and evaluation in agroforestry. Plant Soil 209: 167–180.

Paladinic E, Vuletic D, Martinic I, Marjanovic H, Indir K, Benko M, Novotny V (2009) Forest biomass and sequestrated carbon estimation according to main tree components on the forest stand scale. Periodicum Biologorum 111(4), 459–466.

Pardé JD (1980) Forest biomass. Forest Abstracts 41(8), 343–362.

Parresol BR (1999) Assessing tree and stand biomass: a review with examples and critical comparisons. For. Sci. 45: 573–593.

Parresol BR (2001) Additivity of nonlinear biomass equations. Can. J. For. Res. 31: 865–878.

Parresol BR, Thomas CE (1991) Econometric modeling of sweetgum stem biomass using the IML and SYSLIN procedures, *In Proceedings of the Sixteenth Annual SAS User's Group International Conference*. pp. 694–699**,** Cary, NC: SAS Institute Inc.

Paul KI, Roxburgh S H, England JR, Brooksbank K, Larmour JS, Ritson P, Wildy D, Sudmeyer R, Raison RJ, Hobbs T, Murphy S, Sochacki S, McArthur G, Barton G, Jonson J, Theiveyanathan S, Carter J (2014) Root biomass of carbon plantings in agricultural landscapes of southern Australia: Development and testing of allometrics. Forest Ecology and Management 318: 216–227.

Pearson TRH, Brown SL, Birdsey RA (2007) Measurement guidelines for the sequestration of forest carbon. United States Department of Agriculture, Forest Science, General Technical Report NRS-18.

Perry TO (1982) The ecology of tree roots and the practical significance thereof. J Arboricult 8(8):197–211.

Petersson H, Holma S, Ståhl G, Algera D, Fridman J, Lehtonen A, Lundström A, Mäkipää R (2012) Individual tree biomass equations or biomass expansion factors for assessment of carbon stock changes in living biomass – A comparative study. Forest Ecology and Management, 270(15): 78–84.

Phiri D, Ackerman PA, Wessels B, Johansson M, Säll, H, Lundqvist S-O, du Toit B, Seifert T (2015) Biomass Equations for Selected Drought Tolerant Eucalypts in South Africa. Southern Forests, Southern Forests 1–8.

Pilli R, Anfodillo T, Carrer M (2006) Towards a functional and simplified allometry for estimating forest biomass. Forest ecology and Management 237: 583–593.

R Core Team (2013) A language and environment for statistical computing. R Foundation for Statistical Computing. Vienna, Austria.

R Core Team (2015) A language and environment for statistical computing. R Foundation for Statistical Computing. Vienna, Austria.

Rai SN (1981) Productivity of tropical rainforests of Karnataka. Dissertation, University of Bombay.

Rai SN, Proctor J (1986) Ecological studies on four forests in Karnataka, India. I. Environment, structure, floristics and Biomass. Journal of Ecology 74: 439–454.

Ravindranath NH, Ostwald M (2008) Methods for estimating above-ground biomass. In N. H. Ravindranath, and M. Ostwald, Carbon Inventory Methods: Handbook for greenhouse gas inventory, carbon mitigation and roundwood production projects. Springer Science + Business Media B.V 113-14.

Raz-Yaseef N, Kotten L, Baldocchi DD (2013) Coarse root distribution of a semi-arid oak savanna estimated with ground penetrating radar. Journal of Geophysical Research: Biogeosciences 118: 1–13.

Repola J (2008) Biomass equation for birch in Finland. Silva Fennica: 42: 605–624.

Repola J (2013) Modelling tree biomasses in Finland. P.hD Thesis, University of Helsinki, Finland.

Ribeiro N, Sitoe AA, Guedes BS, Staiss C (2002) Manual de silvicultura tropical. Food and Agriculture Organisation of the United Nations. Maputo, Mozambique.

Ribeiro NS, Matos CN, Moura IR, Washington-Allen RA, Ribeiro AI (2013) Monitoring vegetation dynamics and carbon stock density in Miombo woodlands. Carbon Balance and Management 8(11): 1–9.

Riccardo LB (2007) Root topology and allocation patterns of *Atriplex patula* seedlings supplied with different nutrient concentrations. Italian Journal of Agrometeorology 2: 35-39.

Richardson AD, zu Dohna H (2003) Predicting root biomass from branching patterns of Douglas-fir root systems. OIKOS 100: 96-104.

Rizzo ML, Székelly GJ (2015): Energy: E-statistics (energy statistics). R package version 1.6.2. R Foundation for Statistical Computing. Vienna, Austria.

Rötzer T, Seifert T, Gayler S, Priesack E, Pretzsch H (2012) Effects of stress and defence allocation defence on tree growth: Simulation results at the tree and stand level. In: Matyssek R, Schnyder H, Ernst D,

Munch J-C, Oßwald W, Pretzsch H (eds) Growth and Defence in Plants: Resource Allocation at Multiple Scales. Ecological Studies 220, Springer. 401-432.

Rötzer T, Seifert T, Pretzsch H (2009) Above and below ground carbon dynamics in a mixed beech and spruce stand influenced by environmental changes. European Journal of Forest Research 128(2): 171 – 182.

Ruiz-Peinado R, del Rio M, Montero G (2011) New models for estimating the carbon sink of Spanish softwood species. Forest Systems 20 (1): 176–188.

Ryan CM, Williams M, Grace J (2011) Above- and belowground carbon stocks in a Miombo woodland landscape in Mozambique. Biotropica 43(4): 423–432.

Saatchi SS, Harris NL, Brown S, Lefsky M, Mitchard ETA, Salas W, Zutta BR, Buermann W, Lewis SL, Hagen S, Petrova S, White L, Miles Silman M, Morel A (2011) Benchmark map of forest carbon stocks in tropical regions across three continents. Proceedings of the National Academy of Sciences 108 (24): 9899–9904.

Salas E, Ozier-Lafontaine H, Nygren P (2004) A fractal root model for estimating the root biomass and architecture in two tropical legume tree species. Ann. For. Sci. 61: 337-345.

Salis SM, Assis MA, Mattos PP, Pião ACS (2006) Estimating the aboveground biomass and wood volume of savanna woodlands in Brazil´s pantanal wetlands based on allometric correlations. Forest ecology and Management 228: 61–68.

Samalca KI (2007) Estimation of forest biomass and its error: A case in Kalimantan, Indonesia. Dissertation, International Institute for Geo-information Science and Earth Observation (ITC).

Sanquetta CR, Corte APD, Silva F (2011) Biomass expansion factors and root-to-shoot ratio for Pinus in Brazil. Carbon Bal Manage 6: 1–8.

Sanquetta CR, Watzlawick LF, Cortê APD, Fernandes LAV (2006) Inventários florestais: planejamento e execução. Multi-Graphic Gráfica e Editora, Curitiba.

SAS Institute Inc. (1999) SAS/ETS User's Guide, Version 8, Cary, NC: SAS Institute Inc.

Schiller L (1933) Ed. Drei Klassiker der Strömungslehre: Hagen, Poiseuille, Hagenbach. Akademische Verlagsgesellschaft, Leipzig.

Schroeder P, Brown S, Mo J, Birdsey R, Cieszewski C (1997) Biomass estimation for temperate broadleaf forest of the United States using inventory data. For.Sci. 43: 424–434.

Segura M, Kanninen M (2005) Allometric models for tree volume and total aboveground biomass in a tropical humid forest in Costa Rica. Biotropica 37(1):2–8.

Seifert T, Müller-Starck G (2009) Impacts of fructification on biomass production and correlated genetic effects on Norway spruce (*Picea abbies* L [Karst.]). Eur J For Res 128 (2): 155–169.

Seifert T, Schuck J, Block J, Pretzsch H (2006) Simulation von Biomasse- und Nährstoffgehalt von Waldbäumen mit dem Waldwachstumssimulator SILVA. Tagungsband der Jahrestagung der Sektion Ertragskunde im Deutschen Verband Forstlicher Forschungsanstalten, 208-223.

Seifert T, Seifert S (2014) Modelling and simulation of tree biomass. In: Seifert T (ed) Bioenergy from wood: sustainable production in the tropics. Springer, Managing Forest Ecosystems 26: pp 42–65.

Shinozaki K, Yoda K, Hozumi K, Kira T (1964a) A quantitative analysis of plant form-the pipe model theory. I. Basic analyses. Jpn. Ecol. 14: 97-105.

Shinozaki K, Yoda K, Hozumi K, Kira T (1964b) A quantitative analysis of plant form- the pipe model theory: II. Further evidence of the theory and its application in forest ecology. Jpn. Ecol. 14: 133-139.

Silva-Arredondo FM, Návar-Cháidez JJN (2010) Factores de expansión de biomasa en comunidades florestales templadas del Norte de Durango, México. Rev Mex Cien For 1(1):55–62.

Simpson DG (2014) General physics I: classical mechanics. Department of Physical Sciences and Engineering, Prince George's Community College, Largo, Maryland.

Simpson L, Barton AFM (1991) Determination of the fibre saturation point in whole wood using differential scanning calorimetry. Wood Sci Technol 25: 301–308.

Sitoe AA, Mondlate LJC, Guedes BS (2014) Biomass and carbon stocks of Sofala bay mangrove forests. Forests 5: 1967–1981.

Sitoe AA, Ribeiro NS (1995) Miombo book project (Case study of Mozambique). Universidade Eduardo Mondlane (UEM), Maputo.

Slik JWF, Aiba SI, Brearley FQ, Cannon CH, Forshed O, Kitayama K, Nagamasu H, Nilus R, Payne J, Paoli G, Poulsen AD, Raes N, Sheil D, Sidiyasa K, Suzuki E, Valkenburg JLCH (2010) Environmental correlates of tree biomass, basal area, wood specific gravity and stem density gradients in Borneo's tropical forests. Global Ecology and Biogeography 19: 50–60.

Snedecor GW, Cochran WG (1989) Statistical methods, 8th edition. Iowa State University Press, Iowa.

Soares P, Tome M (2012) Biomass expansion factores for Eucalyptus globulus stands in Portugal. Forest system 21(1): 141–152.

Soethe N, Lehmann J, Engels C (2007) Root tapering between branching points should be included in fractal root system analysis. Ecol Model 207: 363–366.

Somogyi Z, Cienciala E, Mäkipää R, Muukkonen P, Lehtonen A, Weiss P (2007) Indirect methods of large-scale forest biomass estimation. Eur J Forest Res 126:197–207.

Spanos I, Ganatsas P, Raftoyannis Y (2008) The root system architecture of young Greek fir (*Abies cephalonica* Loudon) trees. Plant Biosystem 142(2): 414-419.

Spek LY, van Noordwijk M (1994) Proximal root diameter as predictor of total root size for fractal branching. II. Numerical model. Plant and Soil 164: 119-127.

Spiess AN (2013) Propagate: propagation of uncertainty. R package version 1.0-1. R Foundation for Statistical Computing. Vienna, Austria.

Srivastava VK, Giles DED (1987) Seemingly unrelated regression equations models: estimation and inference. Marcell Dekker Inc., New York.

Stauffer HB (1983) Some sample size tables for forest sampling. Ministry of Forests. British Columbia, Canada.

Stellingwerf DA (1994) Forest inventory and remote sensing. International Training Centre for Aerial Survey (ITC), Enschede.

Suganuma HS, Kawada K, Smaout A, Suzuki K, Isoda H, Kojima T, and Abe Y (2012) Allometric equations and biomass amount of representative Tunisian arid land shrubs for estimating baseline. Journal of Arid Land Studies 22 (1): 219–222.

Székelly GJ, Rizzo ML (2009) Brownian distance covariance. The Annals of Applied Statistics 3(2): 1236–1265.

Székelly GJ, Rizzo ML, Bakirov NK (2007) Measuring and testing independence by correlation of distances. The Annals of Statistics 35(6): 2769–2794.

Ter-Mikaelian MT, Korzukhin MD (1997) Biomass equation for sixty five North American tree species", Forest Ecology and Management 97: 1–27.

Tobin B, Nieuwenhuis M (2007) Biomass expansion factors for Sitka spruce (*Picea sitchensis* (Bong.) Carr.) in Ireland. Eur J Forest Res 126: 189–196.

Trencia J (1995) Identification de descripteurs morphomètriques sensibles aux conditions gènèrales croissance des semis de chêne rouge (*Quercus rubra*) en milieu naturale. Can J Forest Res 25: 157-165.

Trubat R, Cortina J, Vilagrosa A (2012) Root architecture and hydraulic conductance in nutrient deprived *Pistacia lentiscus* L. seedlings. Oecologia 170(4): 899-908. doi: 10.1007/s00442-012-2380-2

Tworkoski T, Scorza R (2001) Root and shoot characteristics of peach trees with different growth habitats. J. Amer. Soc. Hort. Sci. 126(6): 785-790.

Valladares F, Pearcy RW (2000) The role of crown architecture for light harvesting and carbon gain in extreme light environments assessed with a structurally realistic 3-D model. Anales Jard. Bot. Madrid 58(1): 3-16.

Valladares, F (1999) Architecture, ecology and evolution of plant crowns. In: Pugnaire FI, Valladares F (eds) Handbook of functional plant ecology. New York, pp 121-194.

van Noordwijk M, Spek LY, de Willigen P (1994) Proximal root diameters as predictors of total root system size for fractal branching models. I. Theory. Plant Soil 164: 107–118.

van Noordwijk M, Mulia R (2002) Functional branch analysis as tool for fractal scaling above- and belowground trees for their additive and non-additive properties. Ecological Modeling 149: 41-51.

van Noordwijk M, Purnomosidhi P (1995) Root architecture in relation to tree-soil-crop interactions and shoot pruning in agroforestry. Agroforestry Systems 30: 161-173.

Vashum TK, Jayakumar S (2012) Methods to estimate aboveground biomass and carbons stock in natural forests – a review. J Ecossyst Ecogr 2(4): 2–7.

Wang C (2006) Biomass allometric equations for 10 co-occurring tree species in Chinese temperate forests. Forest Ecology and Management 222: 9–16.

Wang J, Zhang C, Xia F, Zhao X, Wu L, von Gadow K (2011) Biomass structure and allometry of *Abies nephrolepis* (Maxim) in Northeast China. Silva Fennica 45(2): 211–226.

Wiese L, Ros I, Rozanov A, Boshoff A, de Clercq W, Seifert T (2015) An approach to soil carbon accounting and mapping using vertical distribution functions for known soil types. Geoderma (*http://dx.doi.org/10.1016/j.geoderma.2015.07.012*).

Yanai RD, Battles JJ, Richardson AD, Blodgett AC, Wood DM, Rastetter EB (2010) Estimating uncertainty in ecosystem budget calculations. Ecosystems 13: 239–248.

Yanai RD, Vadeboncoeur MA, Park BB, Hamburg, SP (2007). Estimating root biomass in rocky soils using pits, cores, and allometric equations. Soil Sci. Soc. Am. J. 71 (1): 206–213.

Zhou X, Hemstrom MA (2009) Estimating aboveground tree biomass on forest land in the Pacific Northwest: a comparison of approaches. Res. Rap. PNW-RP-584. Portland, OR: U. S Department of Agriculture, Forest Service, Pacific Northwest Research Station.

Zhu S, Huang C, Su Y, Sato M (2013) 3D ground penetrating radar to detect tree roots and estimate root biomass in the field. Remote Sensing 6: 5754−5773.

Zianis D, Muukkonen P, Makipaa R, Mencuccini M (2005) Biomass and stem volume equations for tree species in Europe. Silva Fennica, Monographs 4.

APPENDICES

Appendix 1. Coefficients of regression of SUR using the system of the best linear models

Tree component	Weight function	b_0 (± SE)	b_1 (± SE)	b_2 (± SE)
Roots	$1/D^2H$	0.1404 (± 0.5950)	0.0046 (± 0.0002)*	
Stem wood	$1/D^2H$	0.1025 (± 0.4193)	0.0070 (± 0.0001)*	
Stem bark	$1/D^2H$	0.1076 (± 0.3150)	0.0001 (± 0.0001)	
Crown	$1/D^2H$	− 1.8559 (± 1.5017)	0.1124 (± 0.0044)*	
Total tree	$1/D^2H$	− 1.5053 (± 1.8765)	0.0117 (± 0.0002)*	0.1124 (± 0.0044)*

"*" = significant at $\alpha \geq 5\%$; " " = not significant at any probability level.

Appendix 2. Fit statistics of SUR using the system of the best linear models

Tree component	Weight function	Adj.R^2(%)	S$_{y.x}$(kg)	CV(%)	MRSE (kg)	MR (kg)	$\hat{\sigma}_{ii}$	$\hat{\sigma}^2_{SUR}$
Roots	1/D^{2}H	56.00	34.9040	73.1758	0.2750	0.3227*	0.1503	
Stem wood	1/D^{2}H	22.17	116.6327	94.0069	0.5181	1.1685*	1.7454	
Stem bark	1/D^{2}H	− 29.22	18.1996	128.1809	0.8488	0.1751*	0.0432	1.0028
Crown	1/D^{2}H	81.50	28.5040	48.8144	1.4814	− 0.1298*	0.1087	
Total tree	1/D^{2}H	63.19	249.5561	102.1272	0.2332	1.5366*	14.4049	

"*" = significant at α ≥ 5%; " " = not significant at any probability level.

The table above shows the results of SUR using the system of the best linear model forms. However, as 3 of the 5 equations in the system use the same independent variables the SUR is not effective: it has lower adjusted R^2, sometimes negative, larger CV of the residuals, larger system variance ($\hat{\sigma}^2_{SUR}$) and larger component covariance errors ($\hat{\sigma}_{ii}$) when compared to the results in Tables 6 and 7. The most jeopardized equations are those sharing the same independent variables.